Environmental Measurements in the Beaufort Sea, Spring 1991

by T. Wen, F. Karig, W. Felton, and P. Keller

Applied Physics Laboratory   University of Washington
1013 NE 40th Street   Seattle, Washington 98105-6698

Acknowledgments

The purpose of this report is simply to present the environmental data obtained during the camp. The data analysis is very limited. All the data presented here are stored in digital format and are available for further analysis. Requests for data should be forwarded to

> Director
> Applied Physics Laboratory
> 1013 N.E. 40th Street
> Seattle, WA 98105-6698.

TABLE OF CONTENTS

LIST OF FIGURES

LIST OF TABLES

Executive Summary

This report presents environmental and ambient noise data obtained by the Applied Physics Laboratory of the University of Washington (APL-UW) and the Naval Surface Warfare Center (NSWC) at APLIS 91, an ice camp established in the Beaufort Sea in spring 1991 to support Navy-sponsored tests and research during ICEX-91.

The purpose of this report is to provide field data to ice camp participants, so data analysis is limited here. The data were collected to document the meteorological and oceanographic conditions that existed during camp activities. The main data sets are weather, floe drift, STD profiles, current, ice properties, and ambient noise.

I. INTRODUCTION

This report presents environmental data taken in the spring of 1991 at Ice Camp APLIS 91 in the Beaufort Sea. The camp was established and maintained by personnel from the Applied Physics Laboratory, University of Washington, to support the Navy-sponsored research and test activities conducted by the many organizations participating in ICEX 1-91. The environmental data — weather, floe drift, STD profiles, ice properties, and underwater noise — were gathered primarily by APL-UW personnel to support the analysis of experimental data obtained by ICEX 1-91 participants. Additional water current data were contributed by NSWC.

The camp was established on a multiyear floe approximately 360 km north of Prudhoe Bay, Alaska (see Figure 1). The floe was selected on 18 March after a two-day search. Camp buildup ensued. Environmental data were collected from 27 March to 9 April, during which period the floe remained stationary most of the time. Upon the completion of test and research objectives, the camp was evacuated on 13 April.

The camp was located at the edge of the floe, next to a refrozen lead. Level ice, in this case the refrozen lead, was essential for building a runway for aircraft, the only means of transportation to and from APLIS 91. Snow cover averaged 50 cm on the multiyear ice and 8 cm on the refrozen lead. On 9 April, a crack opened up on the far side of the refrozen lead. The crack extended for several hundred yards and then cut across the lead. When another crack cut across the middle of the floe, many cables to the remote sites were stretched, and over half broke.
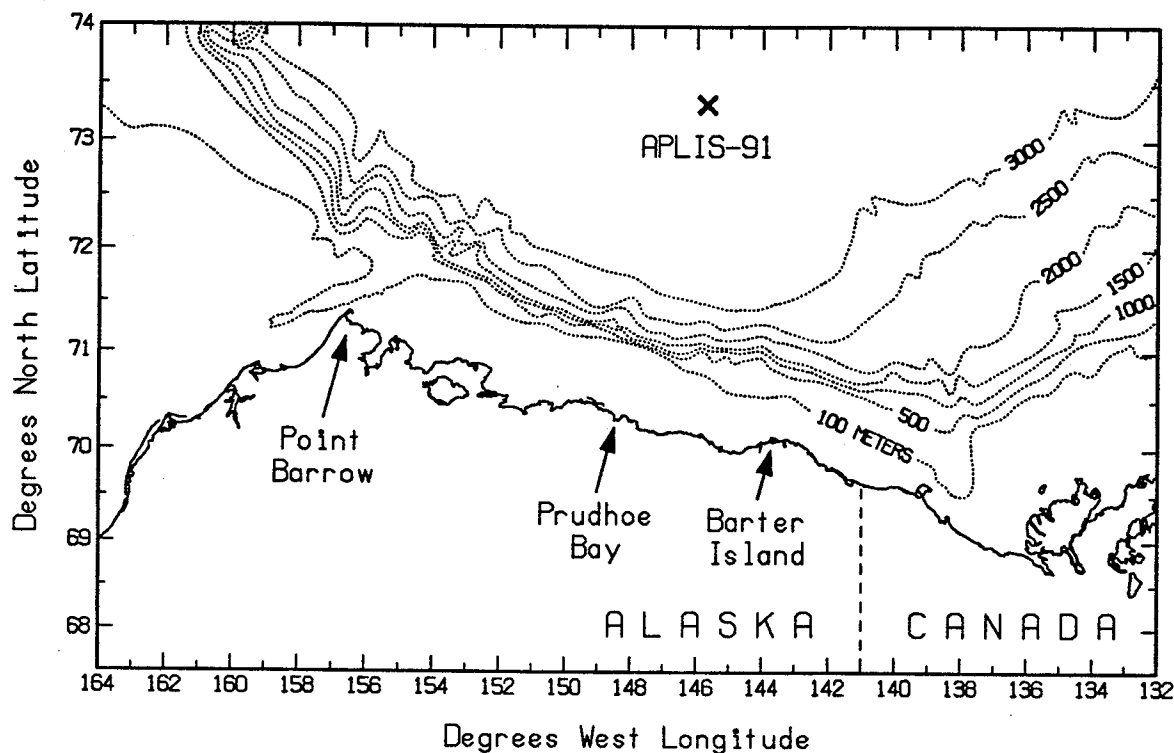

Figure 1.   Position of APLIS 91.

Air temperature and pressure and wind direction and speed were recorded automatically at 10-minute intervals. In general, the weather was benign, with low winds and temperatures typically hovering at about −25°C.

CTD casts were made often to determine the properties of the water column down to 400 m. Sound speed profiles were then derived from the measured temperature and salinity. Predictions of the real-time performance of acoustic equipment were based on the profiles.

Underwater ambient noise affected the quality of the acoustic data. Sources of the noise included thermal cracking of the ice, ridging, wind-generated waves at open leads, and organisms. Some ambient noise was recorded coincident with certain acoustic tests; the noise data are useful in interpretating the acoustic test data.

Some data presented here are tagged with local time, while others are tagged with UTC (Universal Coordinated Time). The relationship is local time = UTC − 9 hours up to and including 7 April, and −8 hours afterwards.

Since the purpose of this report is simply to present environmental data from the camp, the analysis is very limited. All the data presented here are stored in digital format and are available for further analysis.

II. THE CAMP

Selection of an ice floe suitable for a camp was based on several requirements. First, the long axis of the floe needed to be a minimum of 2.5 km long and parallel to the magnetic north-south axis. Second, it needed a refrozen lead long enough and thick enough (at least 1.2 m) to serve as a runway, since transportation to and from the camp depended entirely on aircraft. Third, the floe needed to be over water with good acoustic propagation characteristics, i.e., minimal shadow zone and longest possible propagation range. The third stipulation required the camp to be located north of 72° latitude where the warm subsurface intrusion layer (a remnant of the summer Alaskan Coastal Current that produces complex sound speed structure) is less pronounced and the deeper water helps reduce bottom acoustic interference. The fourth criterion was that the initial site had to be far enough to the east to allow for the westerly drift that historically would occur during the period of camp occupancy. A floe fulfilling the above requirements was found at latitude 73.5°N and longitude 143.5°W on the second day of search (see Figure 1).

The camp was established near the edge of the floe, next to a refrozen lead (see Figure 2). Average snow cover was 50 cm on the multiyear ice, which is deeper than typical, and 8 cm on the refrozen lead. A layout and corresponding picture of the camp are shown in Figure 3.

An underwater tracking range with an XY coordinate system was set up as shown in Figure 4. The origin of the system was a hydrohole in the control building where an acoustic scanner was deployed. The Y axis was nominally aligned with the magnetic north-south using a compass and extended approximately parallel to the long axis of the floe.

The magnetic variation at the general locale was 34.3°, calculated using "GEOMAG," a PC program based on WMM-90 (World Magnetic Model for Epoch 1990.0).[1] This would have been the angle between the +Y axis and true north since the direction of the +Y axis was established with a compass. When sun sights were made later, however, the +Y axis of the coordinate system was found to be 37.6 ° True, with negligible changes during the camp period. Details on celestial sightings are described in section III.
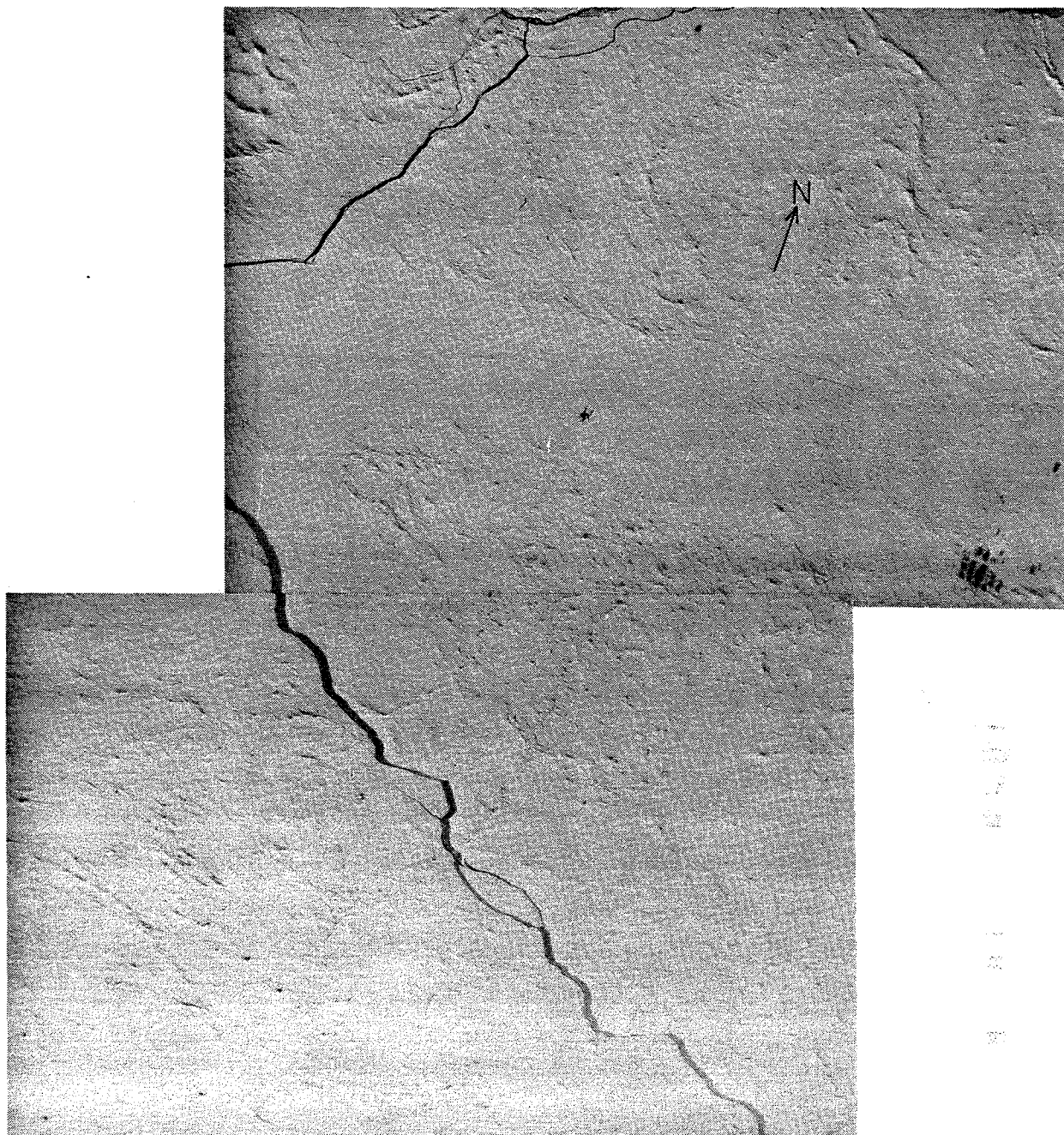
Figure 2. Aerial view of the floe. Cracks in the floe did not form until 8 April.

GENERATORS

MAINT.

$\mathcal{N}$ TRUE

MESS HALL

CONTROL

LOGISTICS
&
DIVING

RADIO

SLEEPING QUARTERS

Figure 3. Layout of the camp.

N1: noise hyd
RS: NRL hydrohole
ADCP: NSWC current profiler
S4/F: NSWC fixed S4
S4/V: NSWC variable S4
(0,0): APL hydrohole & transit
A1-A4: tracking transducers

Figure 4. Tracking coordinate system and location of holes and instruments.

III. FLOE MOVEMENT

During the test period, the camp position was determined using a GPS receiver (Kinemetrics/Truetime GPS-DC) and displayed and logged on an HP85 computer via GPIB bus. GPS fixes were read from the receiver every 10 minutes and stored on a tape cartridge. The logging interval was changed to 30 minutes after it was determined that the floe was not moving much. The system was dismantled at the en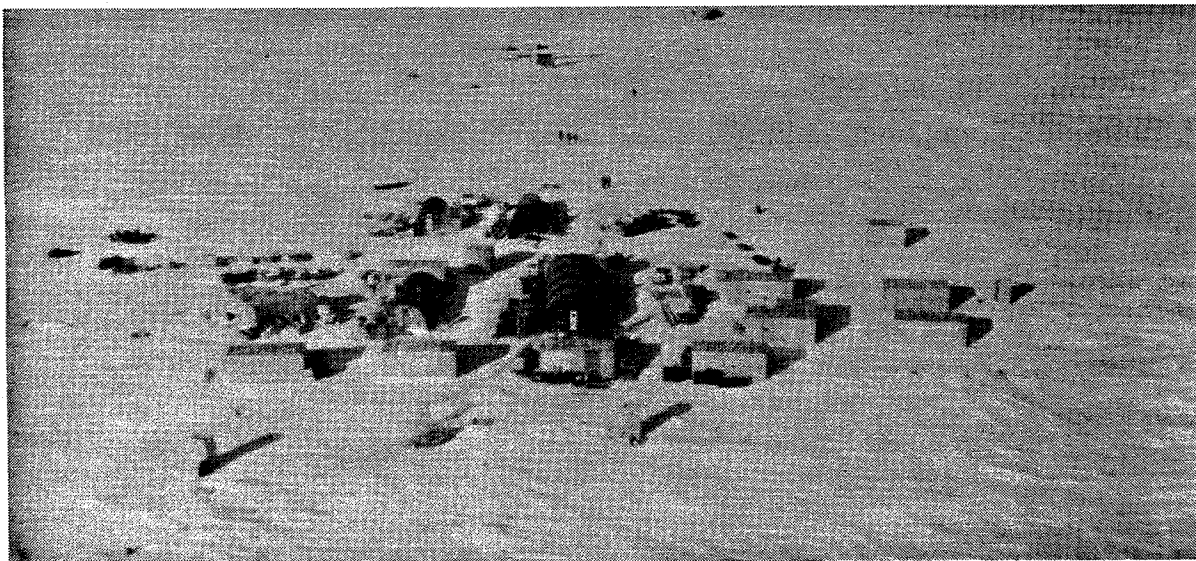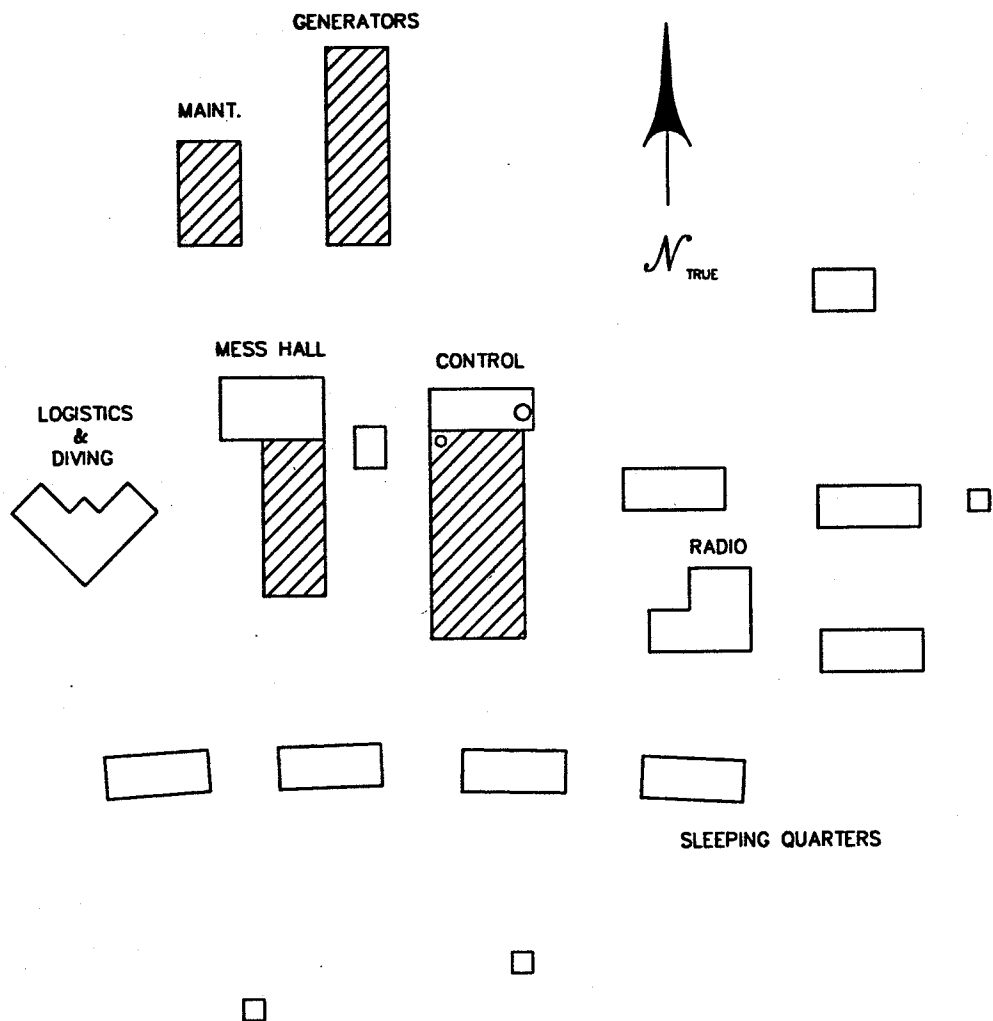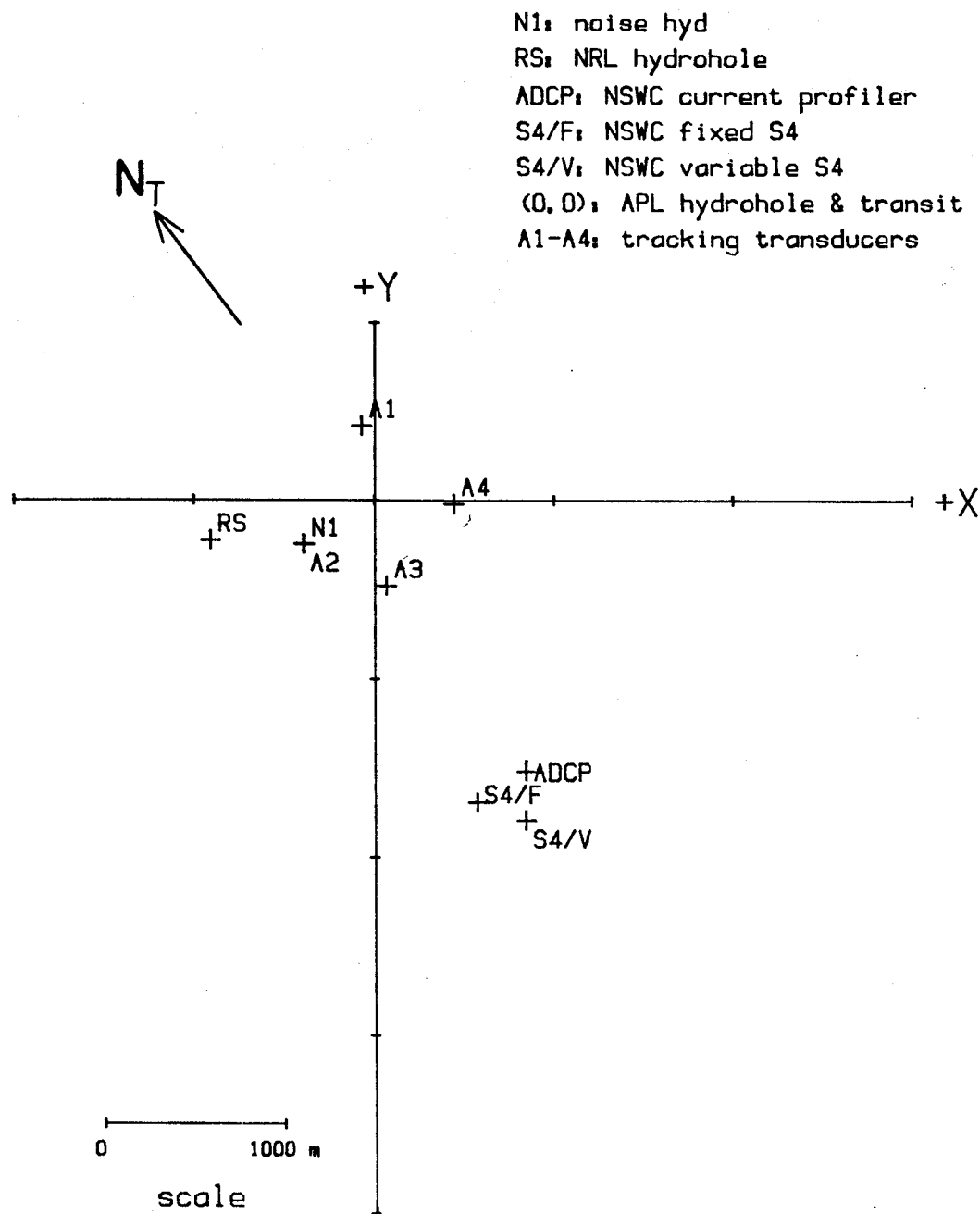d of the 10-day test period, and occasional fixes were obtained with a portable GPS receiver after 10 April. Since the floe motion is mainly wind driven, the low wind conditions typically meant a very low drift rate. Figure 5 shows the position of the floe, which remained practically stationary during most of the camp duration, and the subsequent drift after breakup.

The rotation of the floe was determined by daily measurements of the true bearing of the +Y axis of the XY coordinate system. To obtain the true bearing of the +Y axis, the bearing of the sun relative to one of the tracking hydrophones (marked with a flag) was first read with a transit positioned atop the control building over the (0,0) hydrohole. Then the true bearing of the sun at the time of the transit sighting was calculated using a PC program "ICE" (Interactive Computer Ephemeris).[2] The difference between the relative and true bearings of the sun was the true bearing of the tracking hydrophone. The true bearing of the +Y axis was then simply obtained by adding the offset, 9.14° computed from its (X,Y) coordinates, of the hydrophone from the +Y axis. Our sun sights throughout the camp period showed that very little rotation occurred. The +Y axis of the system remained at 37.6° ± 0.3° True for the camp duration, as shown in Table 1.

IV. WEATHER

A Weatherpak 100 weather station, manufactured by Coastal Climate Co. in Seattle, Washington, was mounted on a telescoping mast at a height of 10 m. The mast was guy-wired so it would not sway in high winds and cause erroneous wind speed readings. Air temperature, atmospheric pressure, and wind speed and direction were recorded at regular intervals. The accuracy of the meteorological measurements is 0.5 m/s for wind speed, 2° for wind direction, 0.5 mbar for atmospheric pressure, and 0.2°C for temperature.

A laptop PC in the control building was used to control the weather station and to display meteorological data. Commands and data were sent over an RS232C link. The Weatherpak was programmed to average the weather parameters for 5 seconds at 10-minute sample intervals. The sampled data were stored in the Weatherpak's internal memory and also downloaded to the PC for display. The weather parameters could also be read at any time by pressing a programmed menu key on the PC. Once a day the data collected in the previous 24 hours were downloaded to the PC and stored on a floppy disk. These data are presented in Figure 6.

The weather was fairly monotonous, with stable average daily temperatures and predominantly weak southwesterly winds. Variation in the atmospheric pressure was also minor. Wind chill factor typically ranged around −40°C.
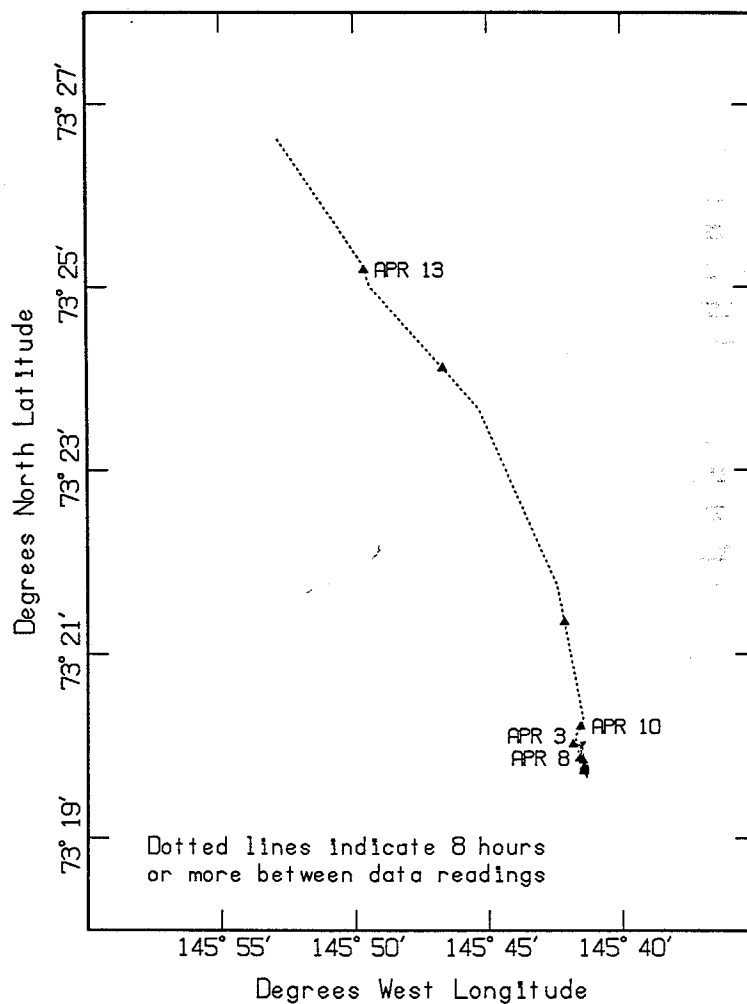
Figure 5. Drift track of APLIS 91.

Table 1. Bearing of +Y axis.

| Time-of-Day (UTC)	True Bearing of Sun	Grid Bearing of Sun	True Bearing of Hyd #1	True Bearing of +Y Axis
4/1 20:41:38	162.7	134.2	28.5	37.6
20:43:53	162.3	134.8	28.5	37.6
4/3 18:29:24	128.4	99.88	28.52	37.66
18:31:24	128.9	100.38	28.52	37.66
4/4 03:37:00	269.4	240.93	28.47	37.61
03:41:00	270.4	241.90	28.5	37.60
4/5 19:46:18	179.6	151.07	28.53	37.63
4/6 18:22:28	126.6	98.1	28.5	37.6
18:33:28	129.4	100.9	28.5	37.6
4/7 19:38:43	146.2	117.68	28.52	37.66
4/8 01:06:45	233.3	205.13	28.17	37.31
4/9 16:59:16	105.9	77.52	28.38	37.52
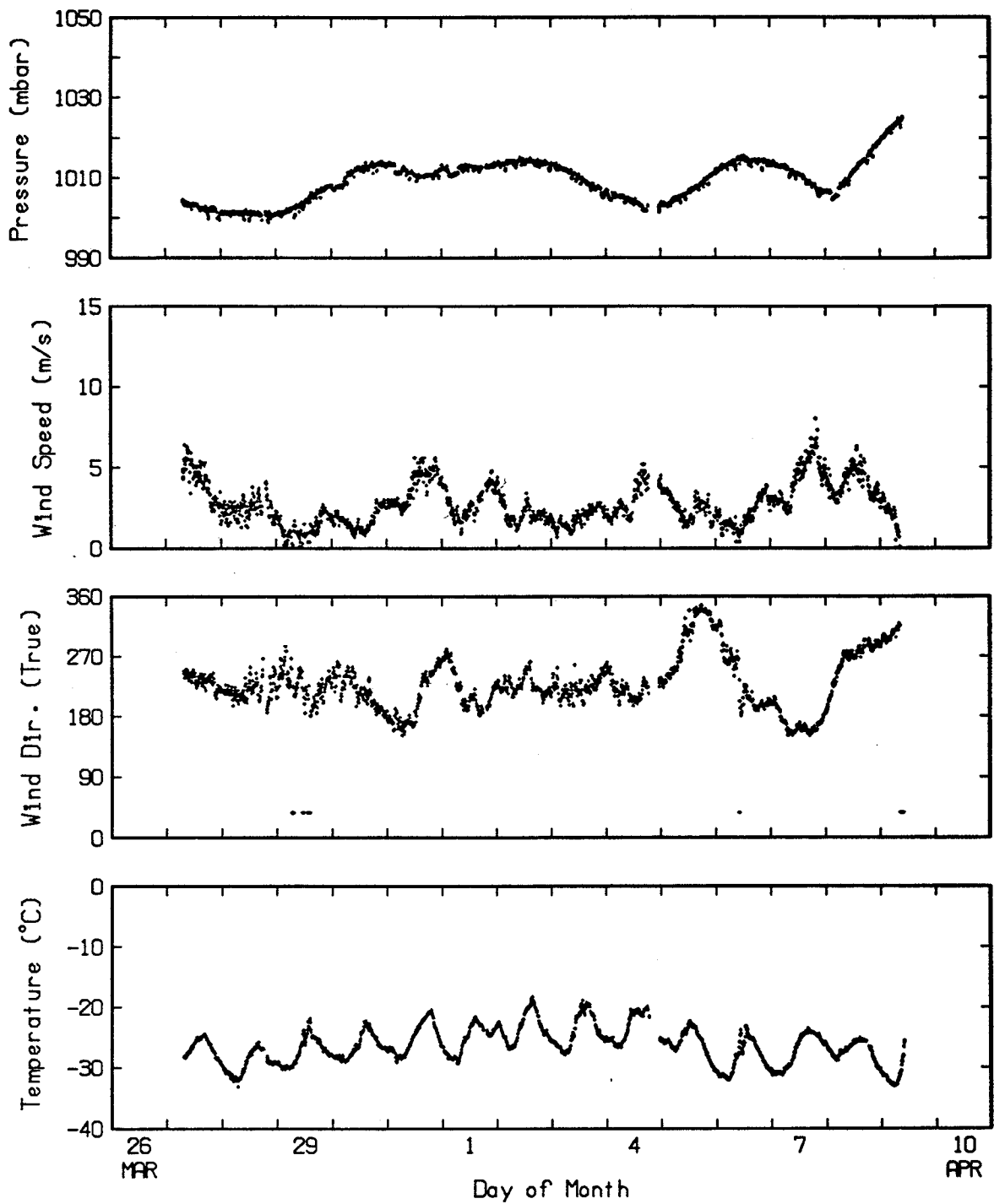
Figure 6. Weather.

V. CTD MEASUREMENTS

CTD casts were made several times daily to obtain the temperature and salinity properties of the water column. The components of the CTD profiler were a solid state data logger (Sea-Bird), a thermistor (Sea-Bird), a conductivity cell (Sea-Bird), and a pressure sensor (Paroscientific Digiquartz). The profiler was attached to the end of a 6.4 mm diameter nylon line and deployed with an ac-powered winch. The winch was mounted on the wall next to a hydrohole in the control building. To ensure adequate flushing of the seawater through the conductivity cell, the profiler was lowered at a rate of ~1.3 m/s, the maximum speed of the winch motor. Since the sampling rate of the logger is 8 Hz, the water column was sampled at ~16 cm intervals, resulting in high resolution temperature and salinity profiles. Casts generally reached only ~400 m because water properties at greater depths do not vary significantly from day to day. On one occasion, the conductivity cell was replaced with a thermistor, and a temperature time series at the bottom of the mixed layer (~30 m) was taken. After each cast, the raw data were read out of the logger via an RS232C link to an HP Integral Personal Computer for processing and plotting. The raw data were first converted to temperature, conductivity, and depth using sensor calibration constants. UNESCO '83 algorithms[3] were then used to compute salinity, sound speed, and σ_t (the density of the in-situ water with the pressure reduced to atmospheric). Before the trip, the sensors were calibrated at the Northwest Regional Calibration Center in Bellevue, Washington. The accuracy of the measurements is 0.002°C for temperature, 0.002 mS/cm for conductivity, and 0.1 m for depth, and that of the computed properties is 0.002 ppt for salinity, 0.005 m/s for sound speed, and 0.002 kg/m^3 for σ_t.

Table 2 lists the casts made at the camp. The STD plots from all the casts are given in Appendix A. Many earlier casts show a negative salinity gradient in the upper mixed layer. This was due to improper casting procedure: not letting the sensors soak in water long enough to bring their temperatures down to that of the water. As a result, the slight residual heat in the conductivity sensor caused a higher reading in conductivity, and ultimately salinity. After this error was corrected by longer soaking time, the subsequent casts yielded the right salinity gradient in the layer.

Figure 7 shows an example of the STD profiles. Its corresponding temperature-salinity (T-S) diagram is shown in Figure 8. The well-mixed upper layer was only 30 m thick, although it had been observed to extend to depths as great as 60 m in other seasons. A warmer intrusion layer from the Bering Sea lies under the mixed layer, creating a thermocline and a halocline (and therefore a pycnocline) between the two layers. The intrusion layer extends to a depth of 80 m, and below that lies colder Chukchi Sea bottom water. Below ~200 m is the Atlantic water with a temperature maximum of 0.5°C. A temperature staircase is evident between 200 and 250 m. Figures 9a and 9b show some historical STD profiles taken at APLIS in the Beaufort Sea in the spring seasons of 1986 to 1990.[4-7] These show the variation in the thickness of the mixed layer. The Bering Sea intrusion layer is the most pronounced for the 1987 profile because of its more southerly location (71° 50') relative to the other years.

Table 2. CTD casts at ice camp APLIS 91.

Date	Time-of-Day (L)	Cast #	Position Latitude	Longitude
03-28-91	1355	CAST# 1	73-19.7N	145-41.5W
03-28-91	2254	CAST# 2	73-19.7N	145-41.4W
03-29-91	0650	CAST# 3	73-19.7N	145-41.4W
03-29-91	2032	CAST# 4	73-19.7N	145-41.4W
03-30-91	0707	CAST# 5	73-19.7N	145-41.4W
03-30-91	2059	CAST# 6	73-19.7N	145-41.5W
03-31-91	0611	CAST# 7	73-19.7N	145-41.5W
03-31-91	0633	CAST# 8	73-19.8N	145-41.3W
03-31-91	2100	CAST# 9	73-19.7N	145-41.3W
04-01-91	0755	CAST# 10	73-19.7N	145-41.4W
04-01-91	2132	CAST# 11	73-19.7N	145-41.4W
04-02-91	0721	CAST# 12	73-20.1N	145-41.5W
04-02-91	1624	CAST# 13	73-20.2N	145-41.6W
04-02-91	2159	CAST# 14	73-19.7N	145-40.5W
04-03-91	0017	CAST# 15	73-19.7N	145-40.5W
04-03-91	0719	CAST# 16	73-19.7N	145-40.5W
04-03-91	1023	CAST# 17	73-19.7N	145-40.5W
04-03-91	1437	CAST# 19	73-19.7N	145-40.5W
04-03-91	2124	CAST# 20	73-19.7N	145-41.4W
04-04-91	0005	CAST# 21	73-19.7N	145-41.5W
04-04-91	0619	CAST# 22	73-19.8N	145-41.5W
04-04-91	1058	CAST# 23	73-19.8N	145-41.5W
04-04-91	1358	CAST# 24	73-19.8N	145-41.4W
04-04-91	1440	CAST# 25	73-19.8N	145-41.4W
04-04-91	1842	CAST# 26	73-19.8N	145-41.4W
04-04-91	2159	CAST# 27	73-19.8N	145-41.4W
04-05-91	0731	CAST# 28	73-19.7N	145-41.5W
04-05-91	1201	CAST# 29	73-19.7N	145-41.5W
04-05-91	2139	CAST# 30	73-19.7N	145-41.4W
04-06-91	0847	CAST# 31	73-19.7N	145-41.5W
04-06-91	1245	CAST# 32	73-19.7N	145-41.5W
04-06-91	1934	CAST# 33	73-19.8N	145-41.5W
04-07-91	0933	CAST# 34	73-19.8N	145-41.6W
04-07-91	2118	CAST# 35	73-19.8N	145-41.6W
04-08-91	0920	CAST# 36	73-19.8N	145-41.5W

03-30-91 0707   CAST# 5   73-19.7N   145-41.4W

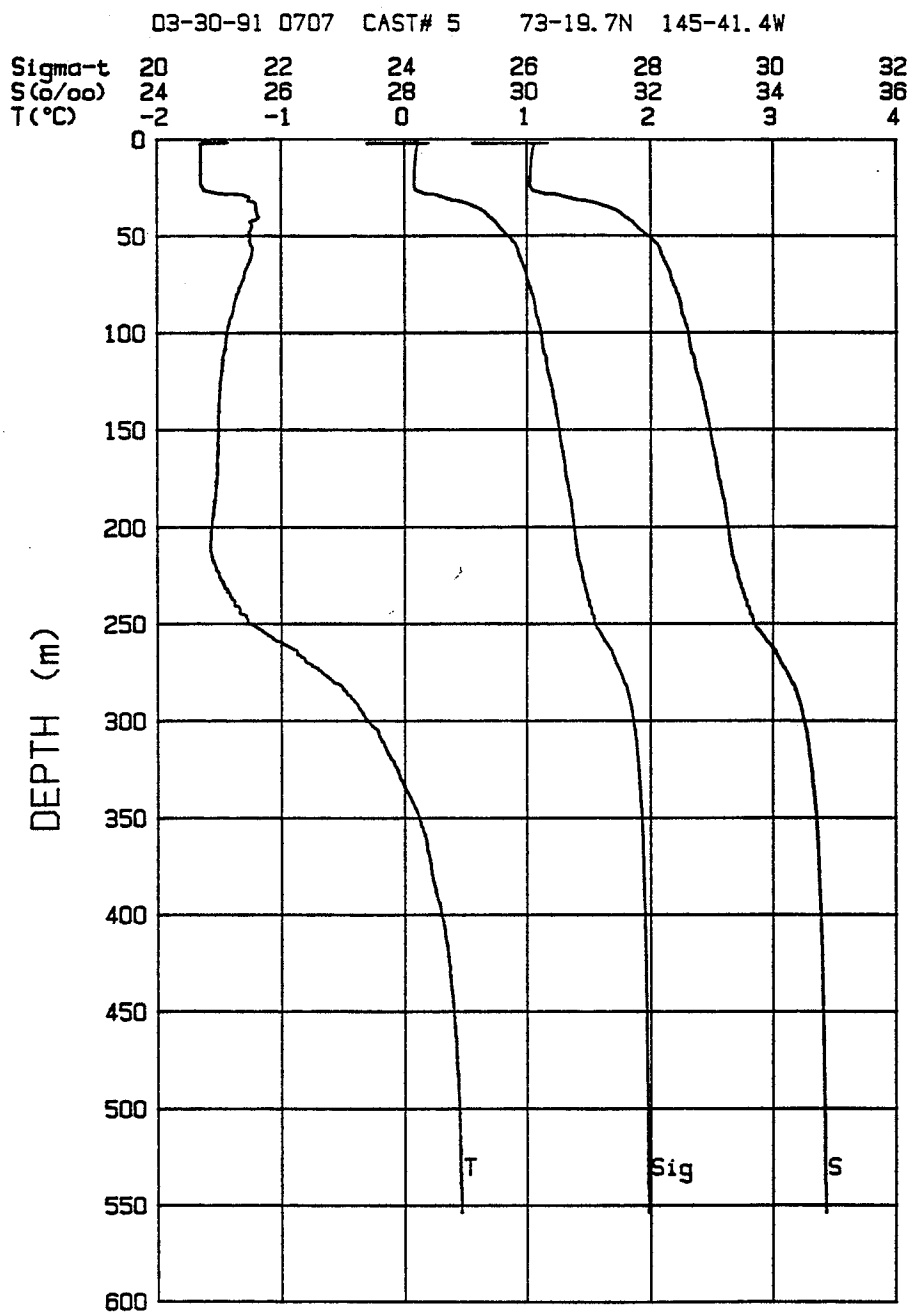| Sigma-t | 20 | 22 | 24 | 26 | 28 | 30 | 32 |
| S(o/oo) | 24 | 26 | 28 | 30 | 32 | 34 | 36 |
| T(°C) | -2 | -1 | 0 | 1 | 2 | 3 | 4 |

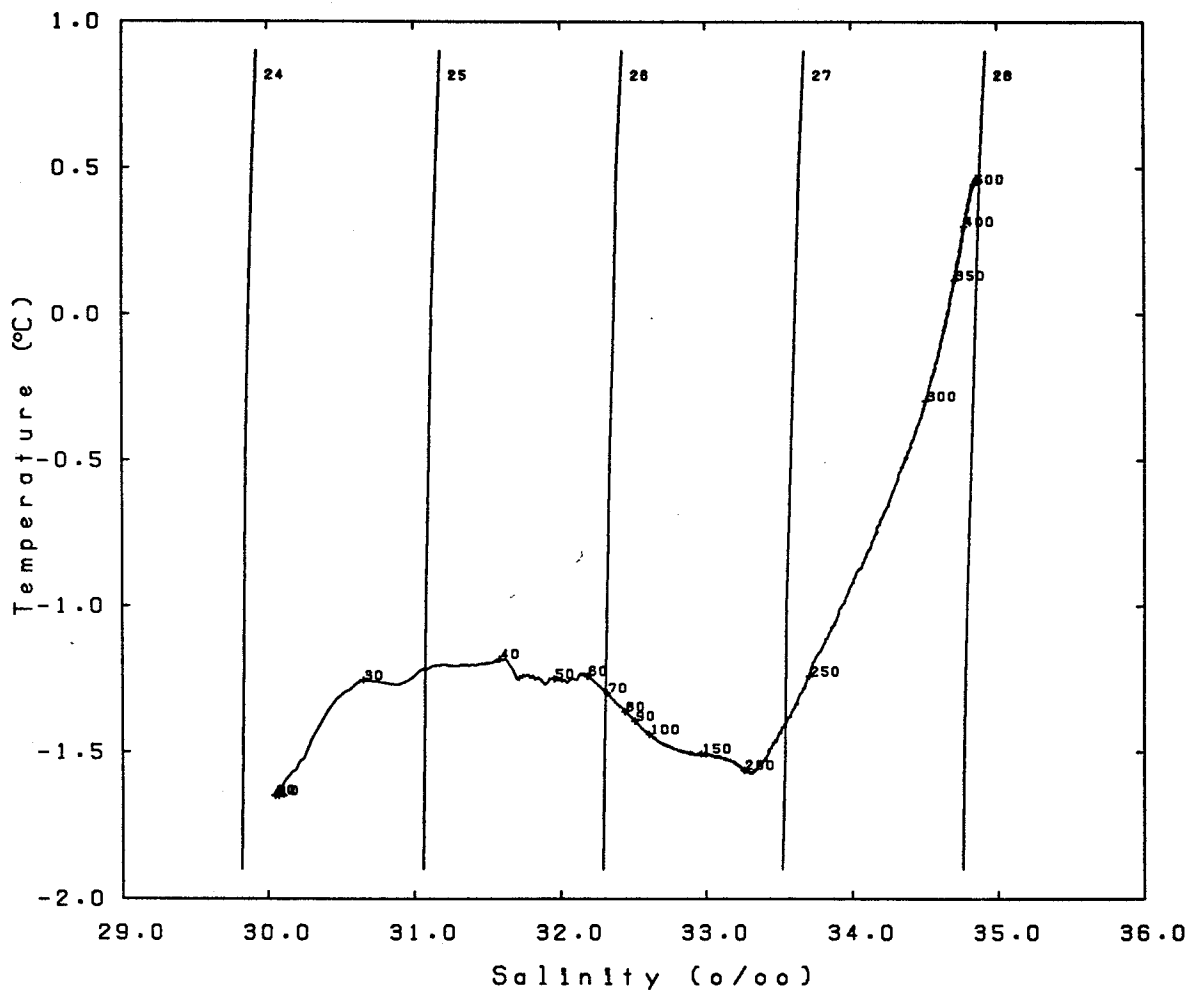*Figure 7.   STD profile.*

-11-

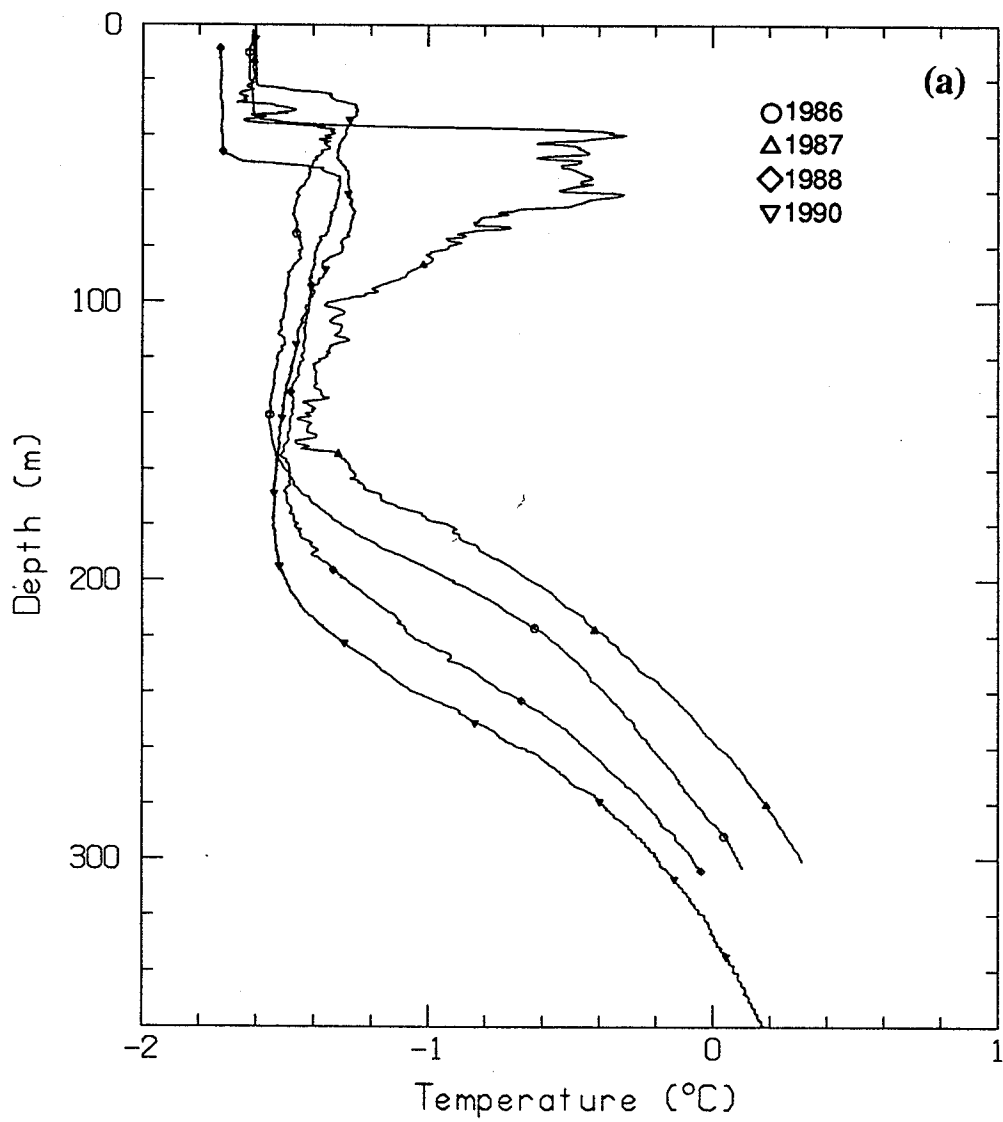*Figure 8. Temperature-salinity diagram. Depths are given along the T-S curve.*

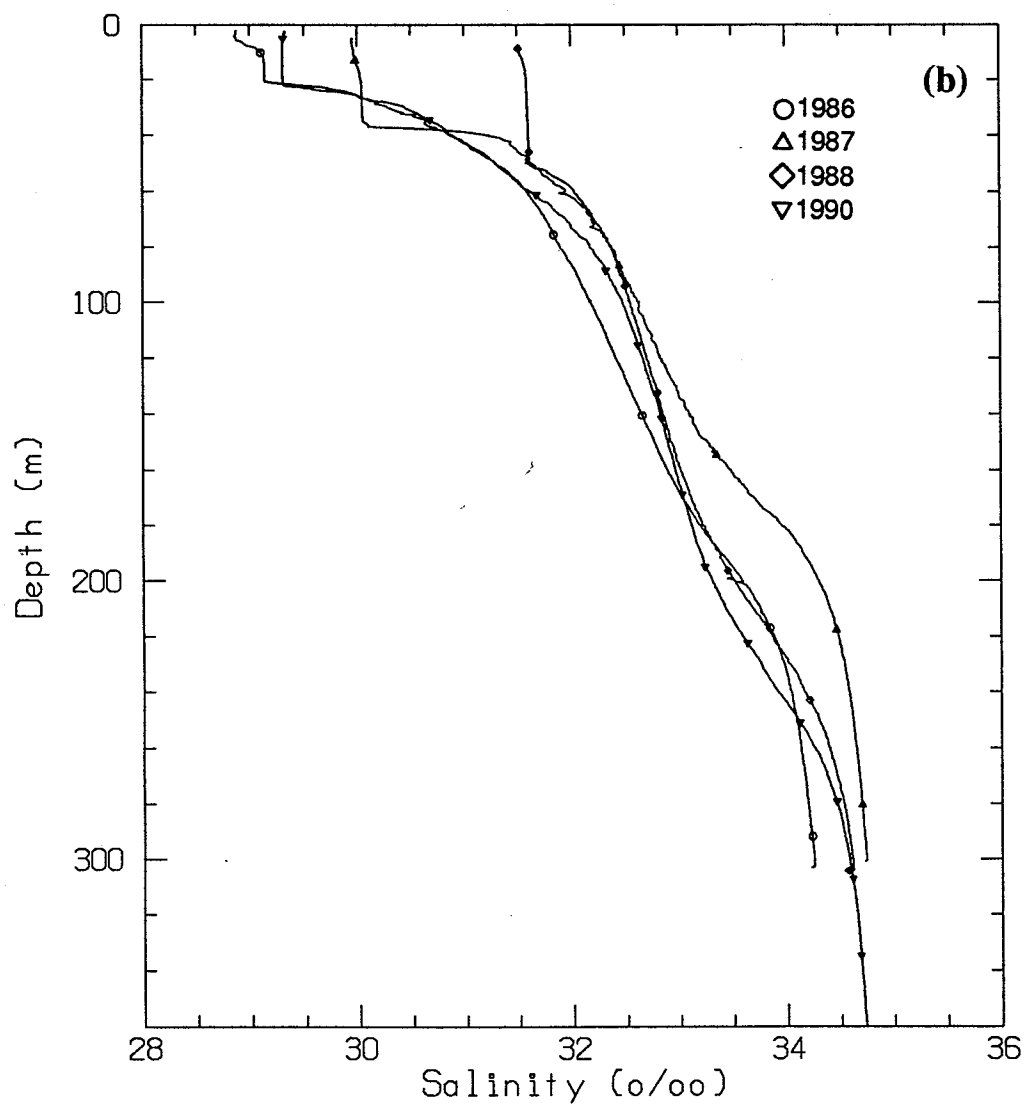*Figure 9. Comparison of historical STD profiles.*

Figure 9.   (Cont.)

Figure 10 shows the Brunt-Vaisala frequency of the water column, computed using cast #5. At the interface of the mixed layer and the intrusion layer, a frequency of over 15 cycles/h was obtained. To investigate any possible internal wave phenomenon, a time series cast (#18) was made with a thermistor at a depth of 28.5 m and another at 30 m. Samples were averaged over 1-second intervals and recorded. The time series lasted only ~1.6 hours. The recorded temperatures are shown in Figure 11 and can be seen to be highly variable. The frequency components of the two temperature time series were estimated using spectral analysis and are shown in Figure 12. Since the temperature time series do not show a major spectral component at about 15 cycles/h, as predicted by the Brunt-Vaisala formula, the variations can be attributed mainly to minor changes in the properties of the intrusion water and are not caused by vertical oscillation in the water column.
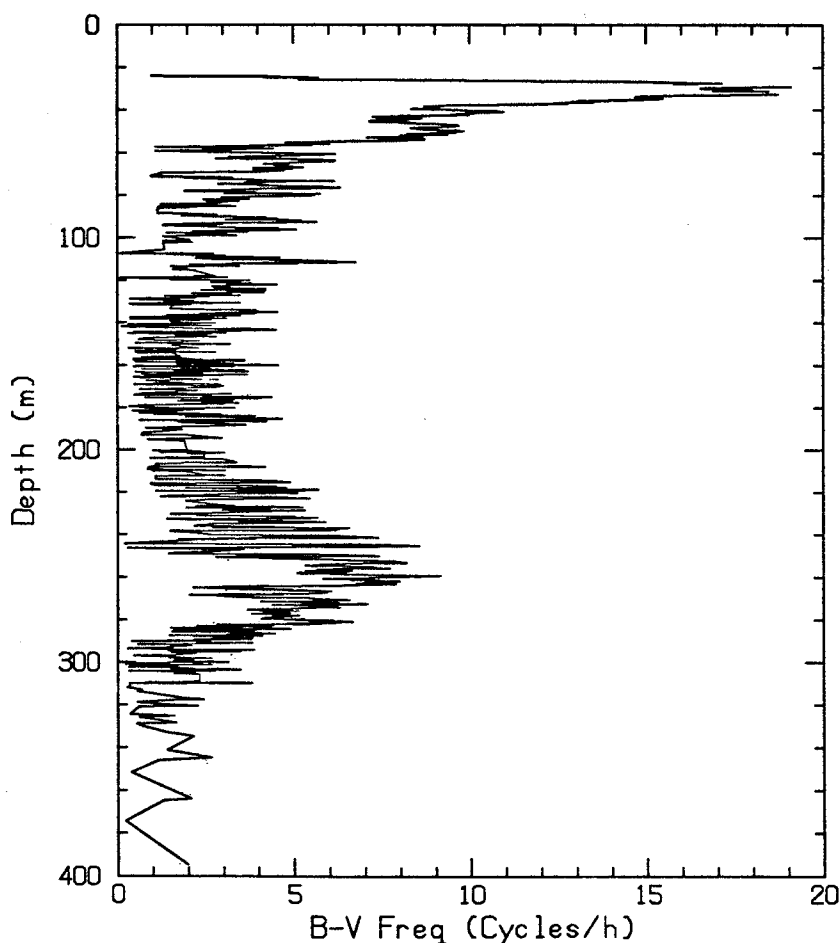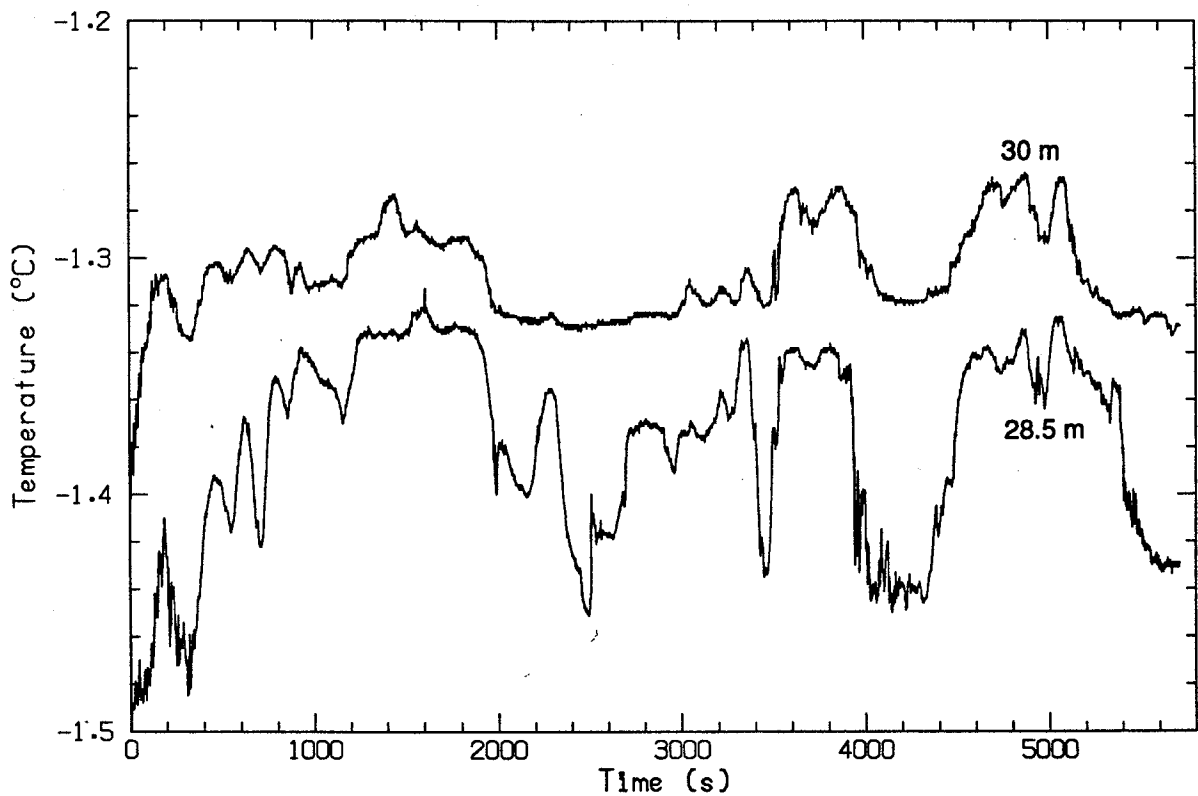

Figure 10.   Brunt-Vaisala frequency of cast 5.

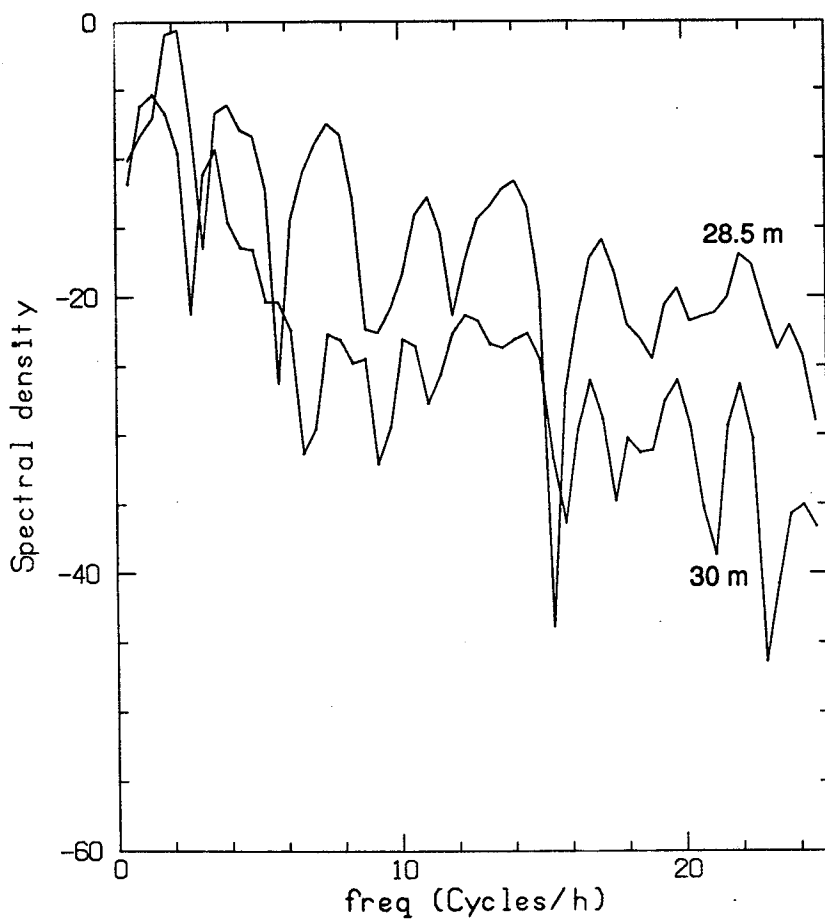*Figure 11. Time series temperature at depths of 28.5 m and 30 m.*

Figure 12. Spectral components of the two temperature time series at depths of 28.5 m and 30 m, respectively.

VI. CURRENTS

Because major tests required knowledge of the water current for optimum test geometry, currents at discrete depths down to 150 m were measured by APL personnel. In addition, NSWC personnel deployed two arrays of current meters and an acoustic Doppler current profiler (ADCP) for time series measurements. Because of limited resources, data obtained by the ADCP are not presented here.

APL current casts

To make a current cast, the CTD logger was replaced with an InterOcean S4 current meter, which was kept in a vertical attitude by a 4.5 kg lead weight attached 1 m below the instrument. The default sampling rate of the current meter was 2 Hz, but it could be programmed to record the average of samples. In our casts, we arbitrarily used the average of two points. In addition to magnetic north and east components of the current, depth was also recorded internally. To obtain stable current measurements, the meter was lowered at depth increments of ~5 m and stopped for approximately 1 minute at each depth. When the current meter was brought back to the surface, data were uploaded to a computer for processing. Only 11 data points, corresponding to 11 seconds, were used to compute the mean and standard deviation at each of those depths. These 11 points were taken from the data series where the current meter had settled down, as indicated by a stable depth reading. Table 3 lists the casts made. Plots of the vertical profiles of the current are shown in Appendix B. Bars plotted at each depth represent plus or minus one standard deviation about the averages. Because the floe was virtually motionless during the camp period, these currents can be considered absolute as well. An offset of 34.3° was added to the magnetic direction to obtain the true direction for the current.

Most profiles are characterized by a very low-speed upper layer that corresponds to the mixed layer (see the example in Figure 13), and below it by a shear layer from < 2 cm/s at 30 m depth to 30 cm/s at 80 m. The direction of the current within the mixed layer was erratic and has a large standard deviation due to very low or nonexistent currents. Below the mixed layer, the current was mostly westerly or southwesterly and began to decrease in magnitude below 180 m. Typically the maximum current was about 35 cm/s. Cast #15, however, shows a magnitude of 40 cm/s at the bottom of the cast (168 m), and it probably was even higher at greater depths, judging from the gradient.

NSWC time series

The locations of the two vertical arrays are given in Figure 4. Each array had four S4 current meters, and each S4 had a platinum-resistance temperature sensor and an inductive conductivity sensor, in addition to the standard current sensors. The S4's on one array were spaced 20 m apart and deployed to depths of 85 m, 105 m, 125 m, and 145 m, respectively, with a lead weight at 146 m. Other than one recovery for the retrieval of data, this array remained stationary in the water for most of the test period and was designated the "fixed" array. The S4's on the other array were spaced 8 m apart and were either deployed to depths of 45 m, 53 m, 61 m, and 69 m, respectively, or

Table 3. Current meter casts at APLIS 91.

Date	Time-of-Day (L)	Cast #
04-01-91	1644	Cast #01
04-02-91	1407	Cast #02
04-02-91	2328	Cast #03
04-03-91	0743	Cast #04
04-03-91	1106	Cast #05
04-03-91	1458	Cast #06
04-03-91	2053	Cast #07
04-04-91	0638	Cast #08
04-04-91	1536	Cast #09
04-04-91	1952	Cast #10
04-05-91	0914	Cast #11
04-05-91	1100	Cast #12
04-05-91	2155	Cast #13
04-06-91	0638	Cast #14
04-06-91	1118	Cast #15
04-06-91	2250	Cast #16
04-07-91	0749	Cast #17
04-07-91	1412	Cast #18
04-08-91	0959	Cast #19

stowed at shallower depths of 1 m, 9 m, 17 m, and 25 m. This second array was designated the "variable" array and was lowered or raised as the testing schedule allowed. All the S4 meters were programmed to average the temperature, conductivity, and current component vectors over 10-second intervals in continuous mode, resulting in very large data sets. In addition, the orientation of each S4 was recorded at 60-second intervals.

Some STD values measured by the S4's were in error due to sensor drift. Table 4 shows the offsets used to bring the readings into agreement with CTD Cast #31. Time series plots of the measured parameters are given in Appendix C. Note that the time of day is in UTC. Figure 14 shows some sample current data from an S4 of each of the fixed and variable arrays. In Figure 14a, the orientation of the S4 changed suddenly at about 04/04 0400Z and then began to oscillate. Current direction simultaneously took a sudden jump. Whatever caused the oscillation in the S4's internal compass also produced higher noise in the current direction signal. In Figure 14b, a similar phenomenon concerning the orientation of the meter occurred at 04/05 1700, 04/06 0500, 04/07 0000, and 04/07 1800, but did not affect the current direction. We believe this was caused by interference generated by artificial sources nearby. Furthermore, these interference fields were fairly localized, affecting only S4's on the same array.

In Figures 15a, b, and c APL's current profiles are compared with the NSWC time series measurements. Eight NSWC measurements were available for each selected APL profile at the corresponding time and different depths. The figures show that the current speed measured by APL's S4 meter was often higher than that measured by NSWC by up
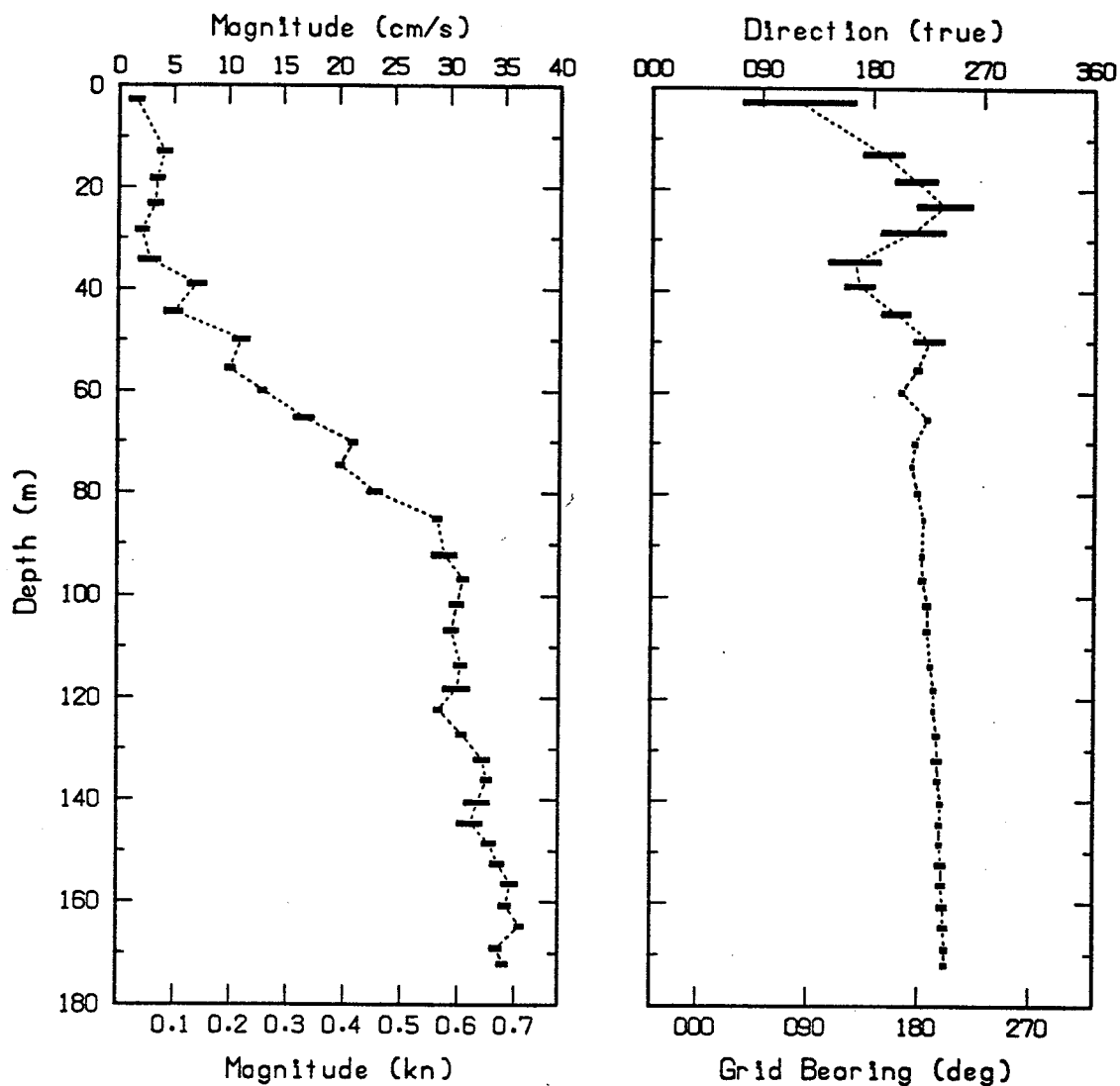
Magnetic bearing + 34.3 degrees = True bearing
True bearing of +Y axis = 37.6 degrees

Figure 13.   Sample current profile.

Table 4. Offsets added to S4 depth, temperature, and salinity values. Letter prefix indicates the array (fixed or variable), and two digit numbers are the last two digits of serial numbers.

S4 #	Depth	Temperature	Salinity
f19	0	-0.06	-0.02
f20	0	-0.05	-0.8
f25	0	-0.07	-0.07
f26	-3	-0.05	-0.4
v21	30	-0.04	17.14
v22	-1.7	-0.57	0.55
v23	-5	0	0
v24	-3.8	0	0

to 10 cm/s, a fairly significant difference. We believe the discrepancy is due to the sensitivity and the calibration of the S4's. The APL S4 meter has a measurement range of 0-350 cm/s, compared with the 0-100 cm/s range of the NSWC instrument, and was therefore not as accurate. Nevertheless, the discrepancy is larger than expected, even though all the S4's had been calibrated prior to the field trip. There is also an approximately 20° discrepancy in the measured current direction. This could have been caused by the high inclination in the earth's magnetic field at the camp locale. Since the APL S4 does not have compensation for tilt, it could not register direction as well as the NSWC S4, which does have the tilt compensation capability.

VII. ICE CORE SAMPLES

Two ice cores were taken in the vicinity of the NRL test hut on 6 April to determine the electrical conductivity of the sea ice. The cores were removed from undisturbed first-year ice with 7.6 cm of snow cover at locations approximately 40 m apart from each other and from the hut. Ice was 172 cm thick at the first core location and 182 cm at the second.

For each core, short segments of ice were removed one at a time, using a 7.6 cm (inside diameter) SIPRE corer. The short segments reduced the length of time the core was exposed to the colder ambient air during handling and therefore limited temperature changes. Each segment was placed in a miter box designed for cutting 7.5 cm- and 10 cm-long sections. For each sawed-off section, a 0.32 cm diameter hole was drilled to a depth of 3.8 cm at the mid-point. A digital thermometer was inserted to read the temperature of the ice. The section was then sealed in a jar and tagged. The depth of the section and the corresponding temperature were recorded. This procedure was repeated until the whole segment, and subsequently the whole ice column, was sampled. The lowest few centimeters of core #1 were pushed beneath the neighboring ice and could not be recovered. The bottom of the second hole was observed to be partially filled with brine/seawater.

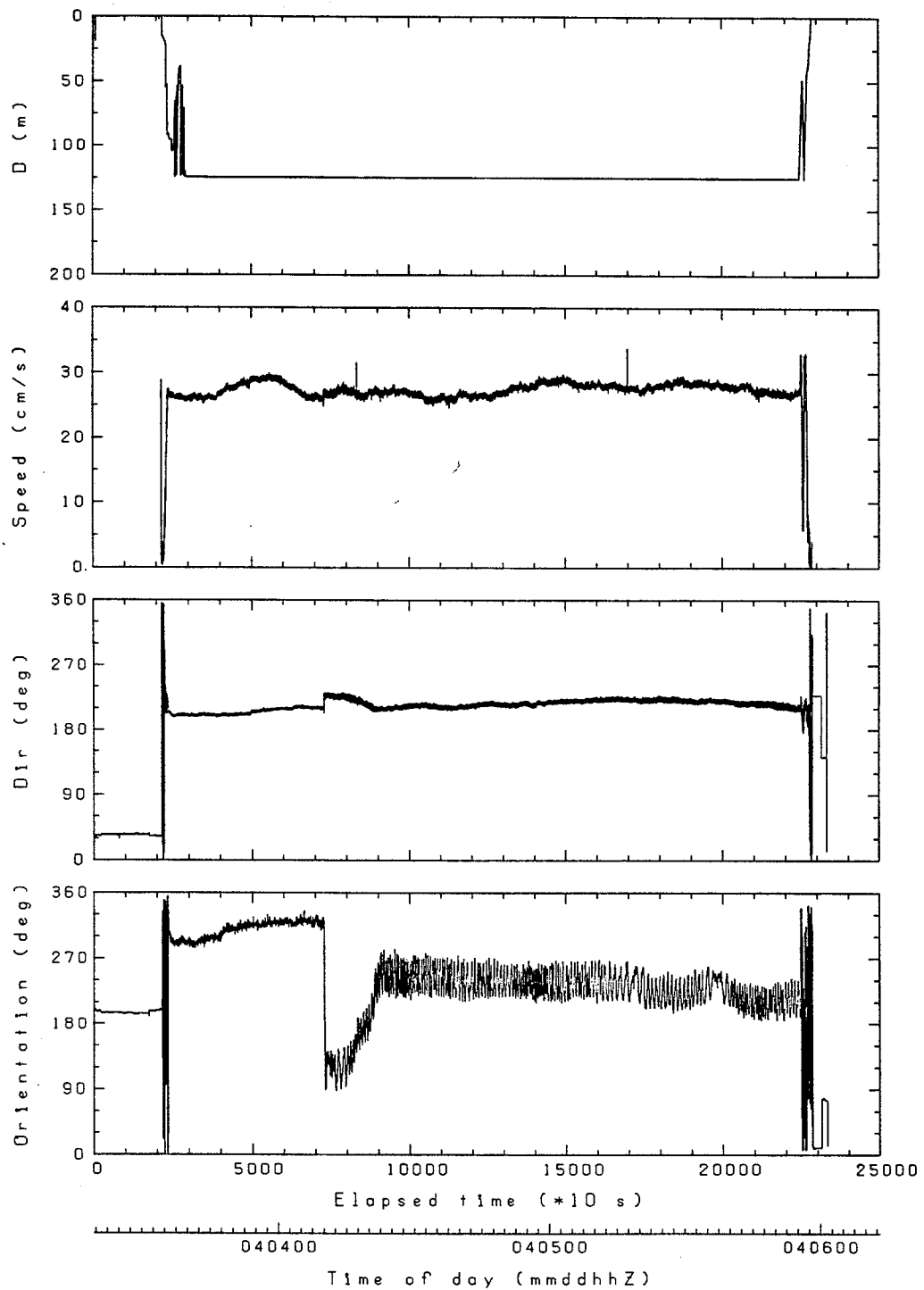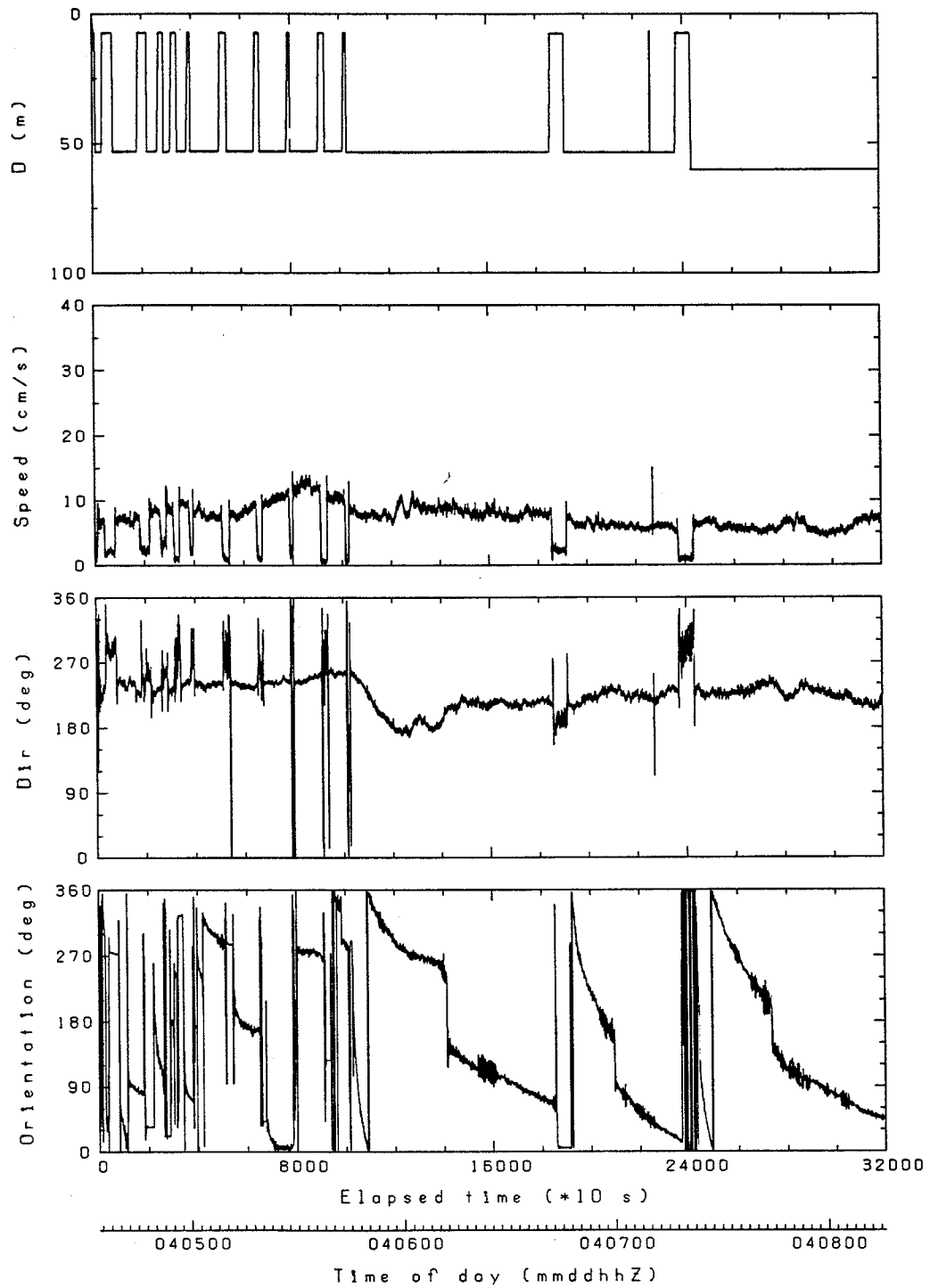*Figure 14.   Sample time-series S4 current meter data.*

(b)
variable-depth S4

Figure 14. (Cont.)

-22-
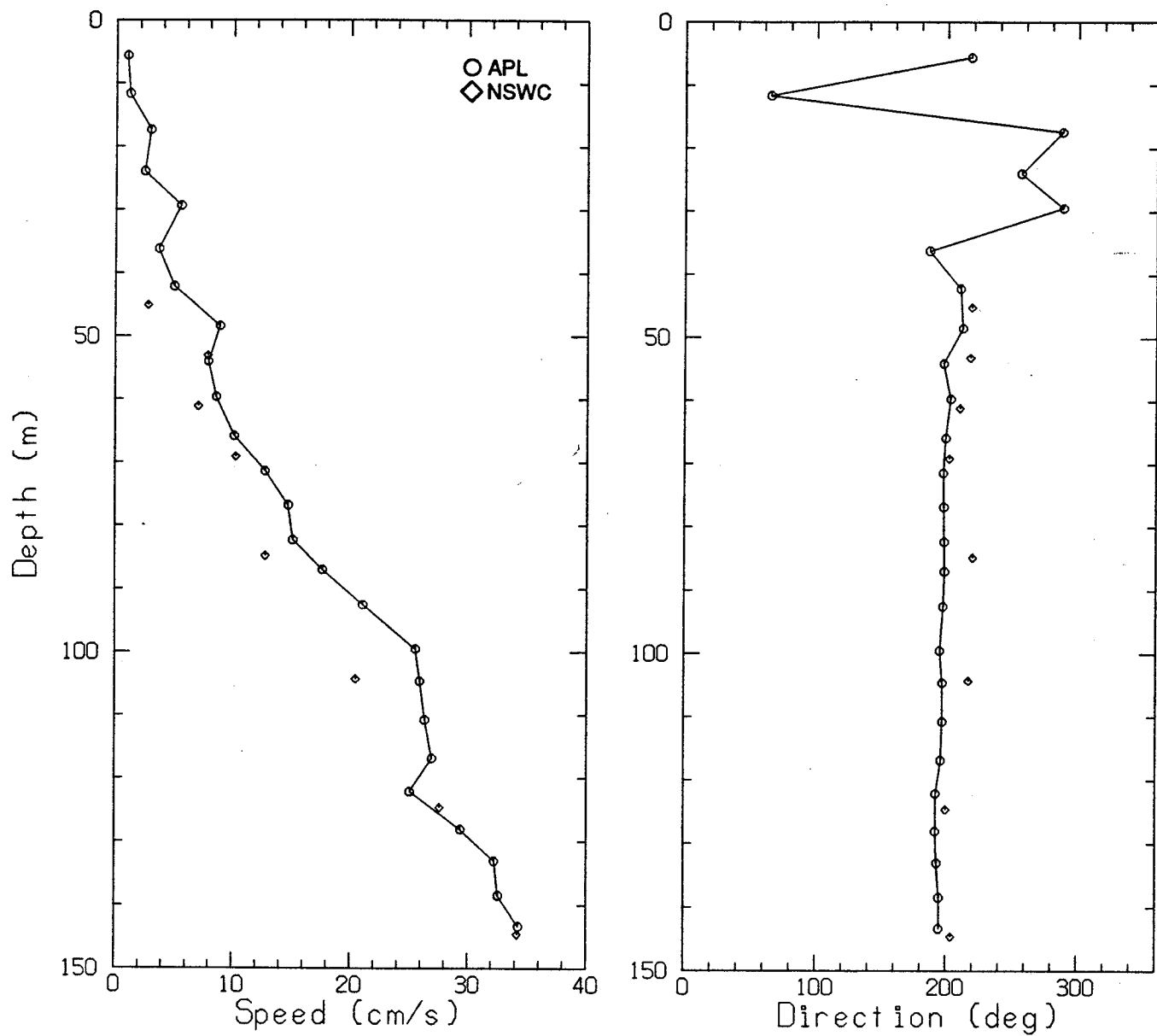
Figure 15.   Comparison of APL and NSWC current measurements.

(b)
04-05-91 1100 cast #12
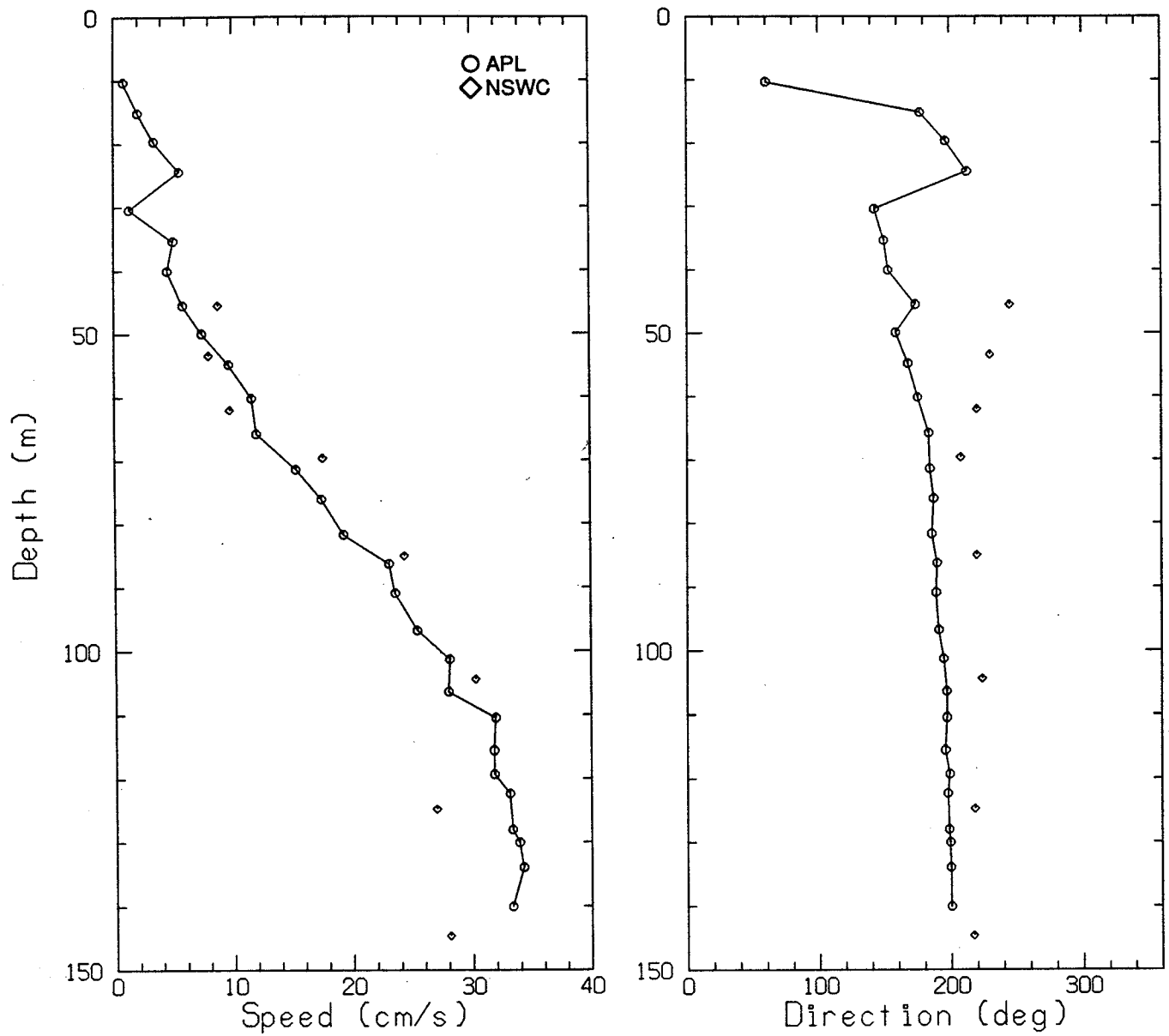

Figure 15. (Cont.)
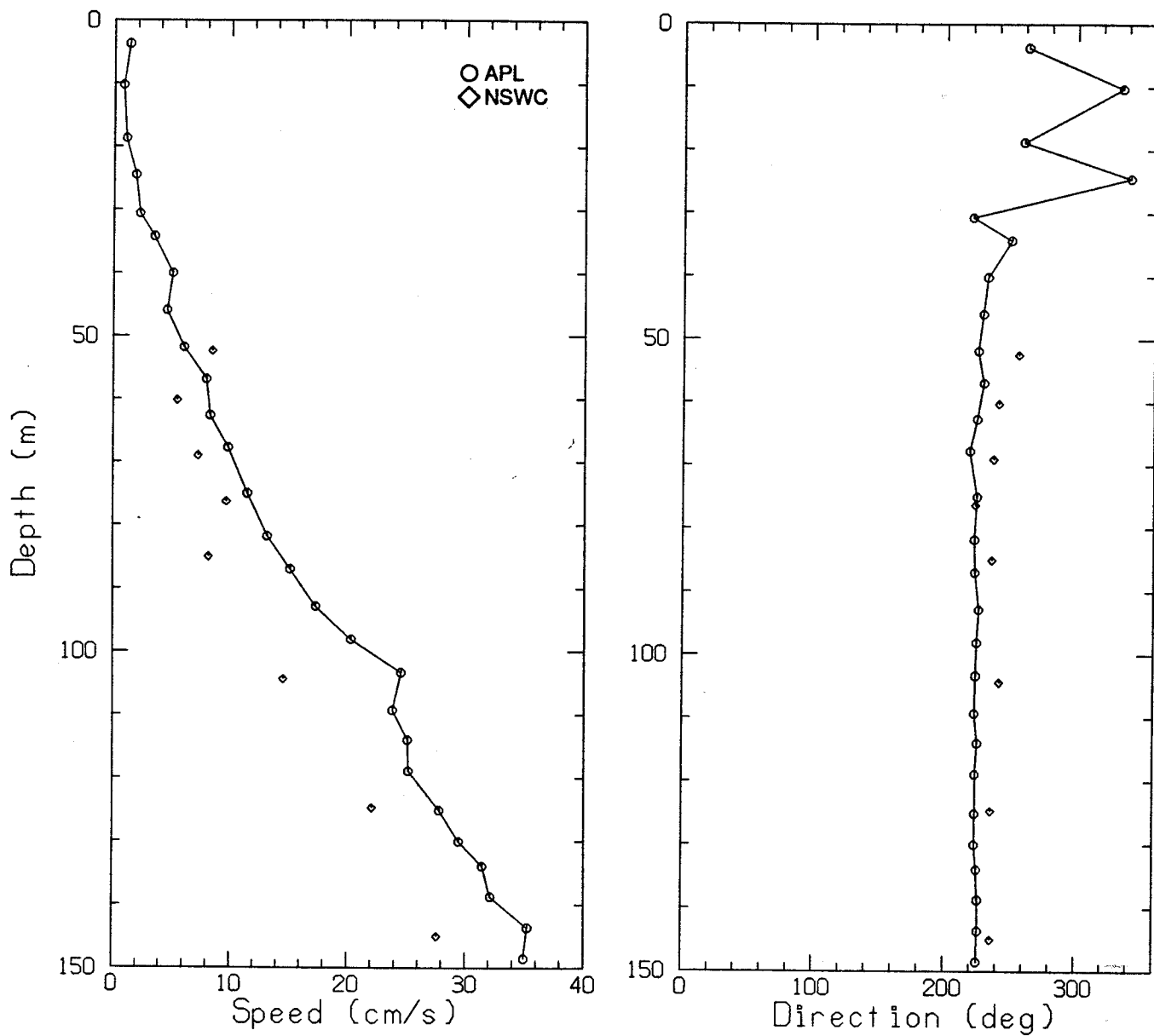
(c)
04-07-91 0749 cast #17

Figure 15.   (Cont.)

Air temperature at the time of core sampling was -23.1°C. Seawater was at a temperature of -1.66°C and a salinity of 30.2 ppt, with an electrical conductivity of 24 mS/cm.

Figure 16 shows the segments and sections for each core. The cores are designated NRL-1 and NRL-2. Note that, for core NRL-2, some sections in the mid-column were not saved after temperature measurement due to a shortage of storage jars. This did not compromise our knowledge of the salinity profile because the profile is monotonic in the mid-column of the first-year ice.

The samples were taken back to the camp and allowed to melt at room temperature. We rigged up a "salinometer" with the thermistor and the conductivity cell of APL's CTD profiler to determine the salinity; this configuration allowed us to use the standard data acquisition and reduction system. The sensors were mounted in a jig with the cell tilted to avoid trapping air bubbles. Tygon tubing was attached to both ends of the 1 cm × 18 cm cylindrical conductivity cell, and the thermistor was inserted into the tubing close to the cell. When the melted sample was shaken and poured into the tubings and the cell, both the conductivity and the temperature were measured simultaneously, and the salinity was computed. Prior to the analysis, the samples and the sensors were placed on the bench top for several hours to bring them to the same temperature. This was necessary because any large temperature differential would have affected the conductivity results. To further reduce the temperature differential, the water sample was mixed within the cell by raising and lowering the pinched-off Tygon tubing at one end to slosh the water sample back and forth.

Figures 17a and b show the measured and computed properties of the ice cores. To obtain the electrical conductivity, brine volume had to be determined first.[8] To compute the brine volume, density was required. Because of irregular diameters of the cores and brine drainage, it was not appropriate to measure the ice density by dividing the core weight by its volume. To obtain more precise results, density and brine volume were calculated using relationships derived by Cox and Weeks[9] from measured temperature and salinity. The properties shown in the figures are also listed in Appendix D.

In general, the temperature profiles were fairly linear. Since the temperature profile of the ice column in spring is practically linear, we believe that any deviation from linearity was caused by measurement errors and by the exposure of core sections to colder ambient air. The estimated theoretical temperature profiles are shown as solid lines in the figures, with the value at the bottom approaching that of the seawater. It can be seen that more cooling took place for the lower core sections, resulting in a temperature offset of up to 2.5°C. For the last segment of NRL-2, all the sections registered higher temperatures compared with the theoretical profile. This was caused by the hole flooding with seawater, which warmed the segments.

The salinity profiles of the cores are typical of first-year ice. The salinity is high near the surface due to a faster freezing rate, decreasing as the ice grows thicker and more slowly, thus allowing a longer time for brine expulsion. Although the salinity should increase again near the bottom because the brine has not had enough time to drain out, the measurements show relatively low salinities there. This could be explained in terms of brine drainage during core retrieval and seawater dilution or displacement of
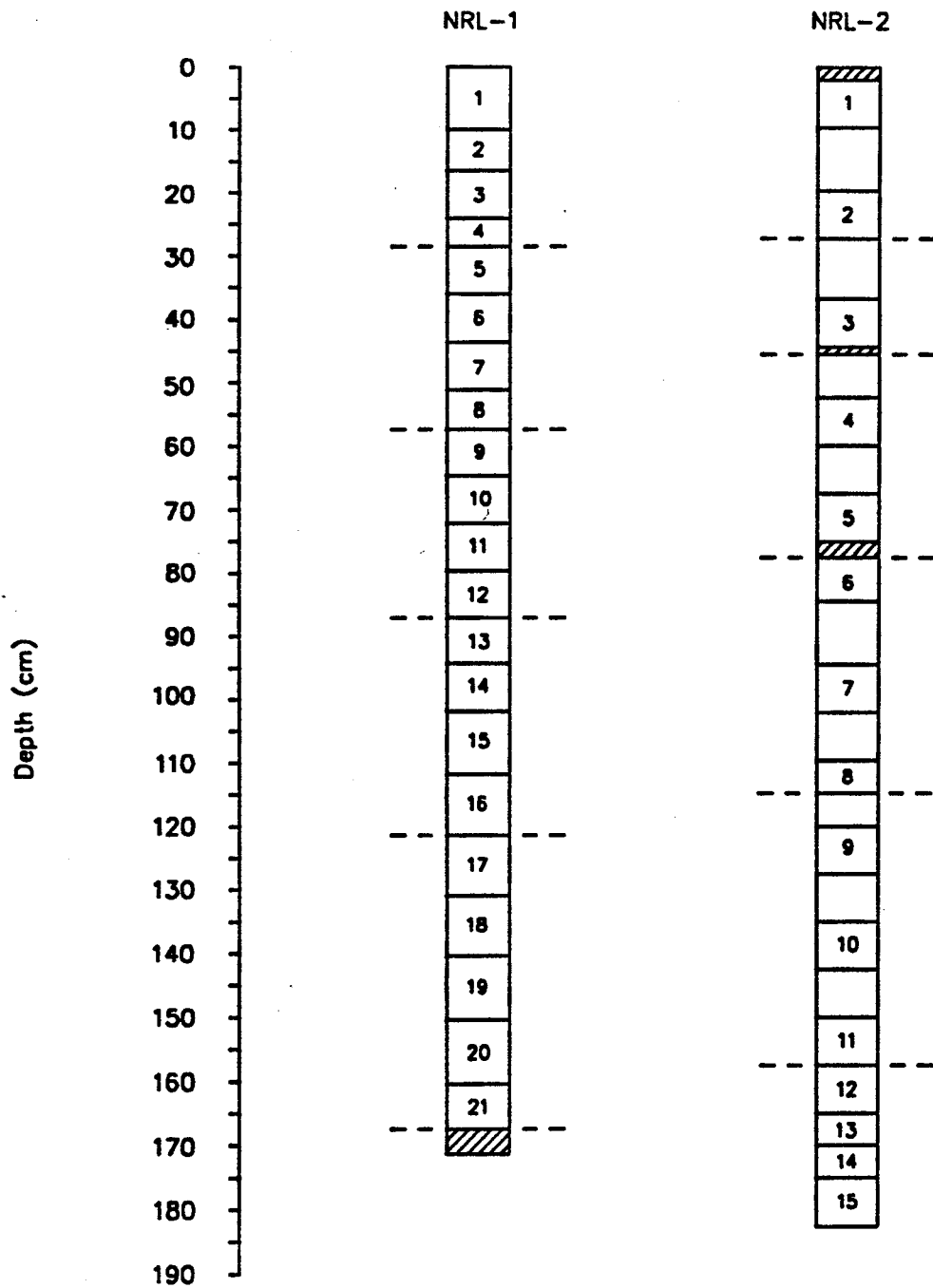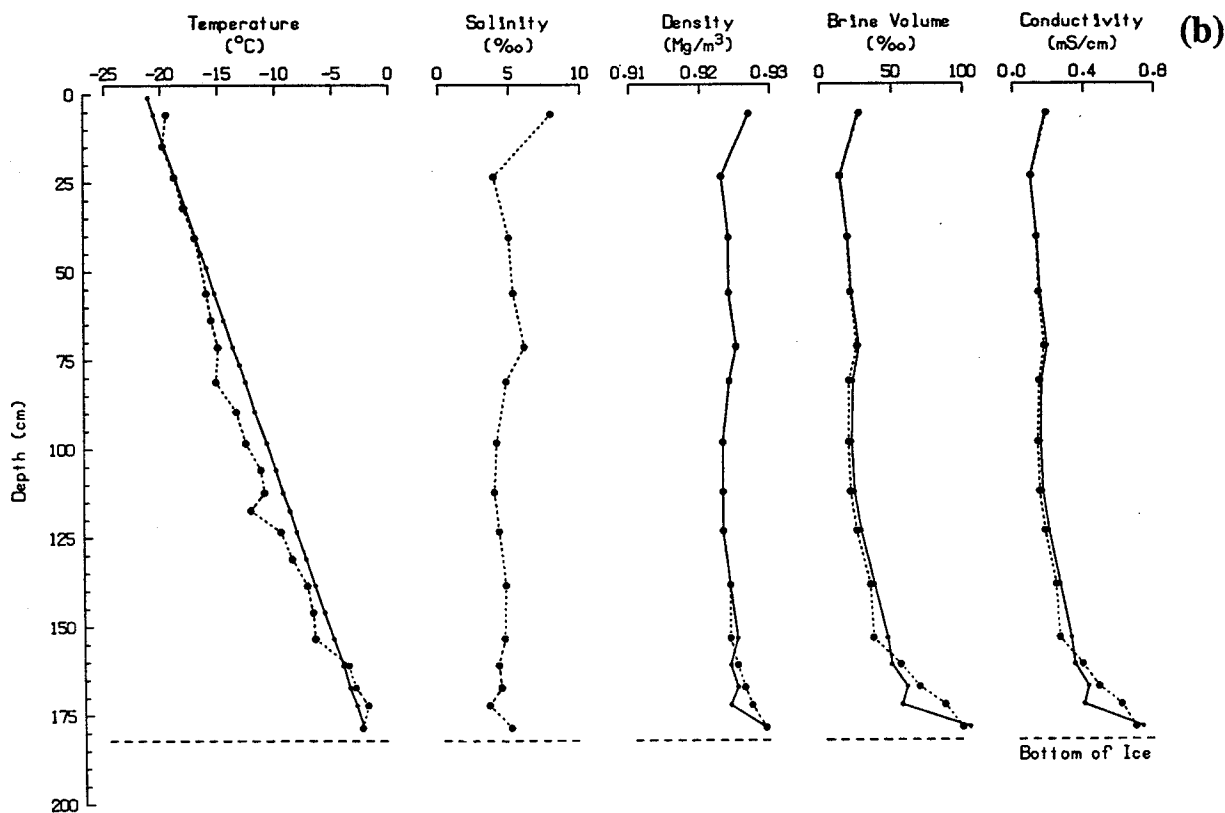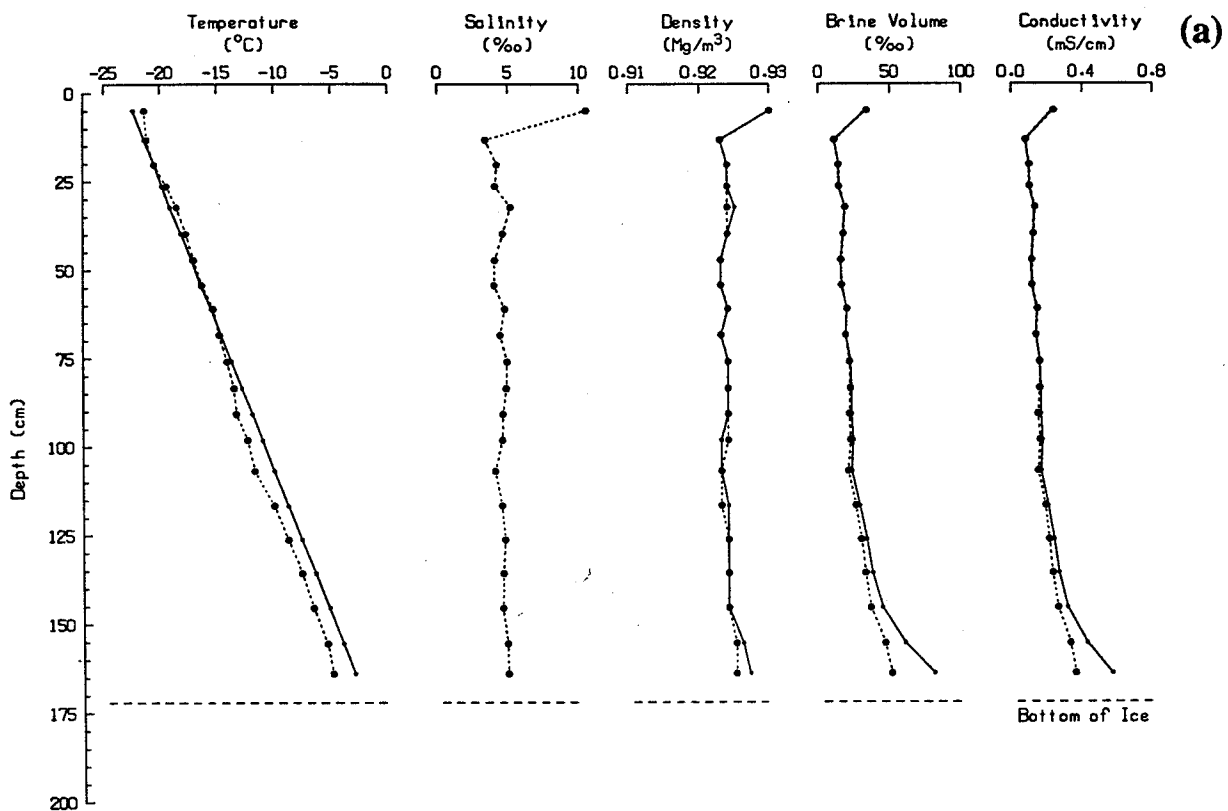
Figure 16.   Ice core segments.

Figure 17. Measured and theoretical (solid line) properties of ice cores.

brine, which has a higher salinity (for example: 37.6 ppt at -2°C and 70.6 ppt at -4°C) than that of seawater (~30 ppt).

The estimated theoretical temperature profile and the measured salinity profile were used to recompute the ice properties. The new results are given in Appendix D and shown as solid lines in Figures 17a and 17b.

VIII. UNDER-ICE AMBIENT NOISE

An omnidirectional hydrophone (B&K 8101) with a self-noise level of 30 dB//μPa/Hz at 20 kHz was deployed ~400 m from camp to minimize interference from noise generated by activities at the camp. The ambient noise signals were cabled back to camp, boosted by 40 dB with a battery-powered amplifier, and recorded on a VCR system with 88 dB dynamic range and 20 kHz bandwidth. IRIG-B time code was also recorded for time-stamping.

During processing at APL-UW, the data tapes were played back, and the signal from the hydrophone was fed into an HP3561 spectrum analyzer operating in narrow band mode with a Hanning data window and into an amplifier/speaker for audio monitoring. Figure 18 shows a typical ensemble-averaged noise spectrum. Note the unusual hump centered at ~1.6 kHz. Further investigation using smaller analysis bandwidth revealed many line components, both within and outside the region. Because of the 60 Hz power and larger bandwidth (375 Hz) used at first, these line components, most likely caused by RF interferences, were not resolved. These interferences are found on all of the ambient noise data.

To resolve these line components and obtain the actual ambient noise level, we reprocessed the data by digitizing the signals at 50 kHz on a digital scope. For each arbitrarily selected time period, twenty near-consecutive traces 317.4 ms in length were digitized. The data were then uploaded to a computer and spectral analysis was performed on each. The length of the time series translates to a bandwidth of 3.15 Hz. Finally, an average spectrum was obtained by power-summing the twenty spectra and averaging the sum. Figure 19 shows an average ambient noise spectrum of the same period as in Figure 18. The actual noise level can now be estimated by reading near the bottom of the spurious lines. Note that self-noise of the system dominated at higher frequencies. More ambient noise level plots are given in Appendix E. In some of those noise spectra, a broad peak is present at a distance of about 10 kHz from the artificial source.

When the ambient noise was very low, the level of noise at high frequencies was masked by the self-noise limit of the hydrophones. It should be noted that the measured level is the incoherent sum of the ambient noise and the hydrophone self-noise. If the actual ambient level had been the same as the self-noise of 30 dB the measured level would have been 33 dB//μPa/Hz. Therefore, the measured level is always higher than the actual level. The difference between the two is significant only when the measured noise level is a few decibels above the self-noise limit of the hydrophone. When the measured level is 30 dB//μPa/Hz, the actual ambient noise is lower but cannot be determined. Because of that, no attempts were made to correct for the incoherent noise summing effect in the results presented.
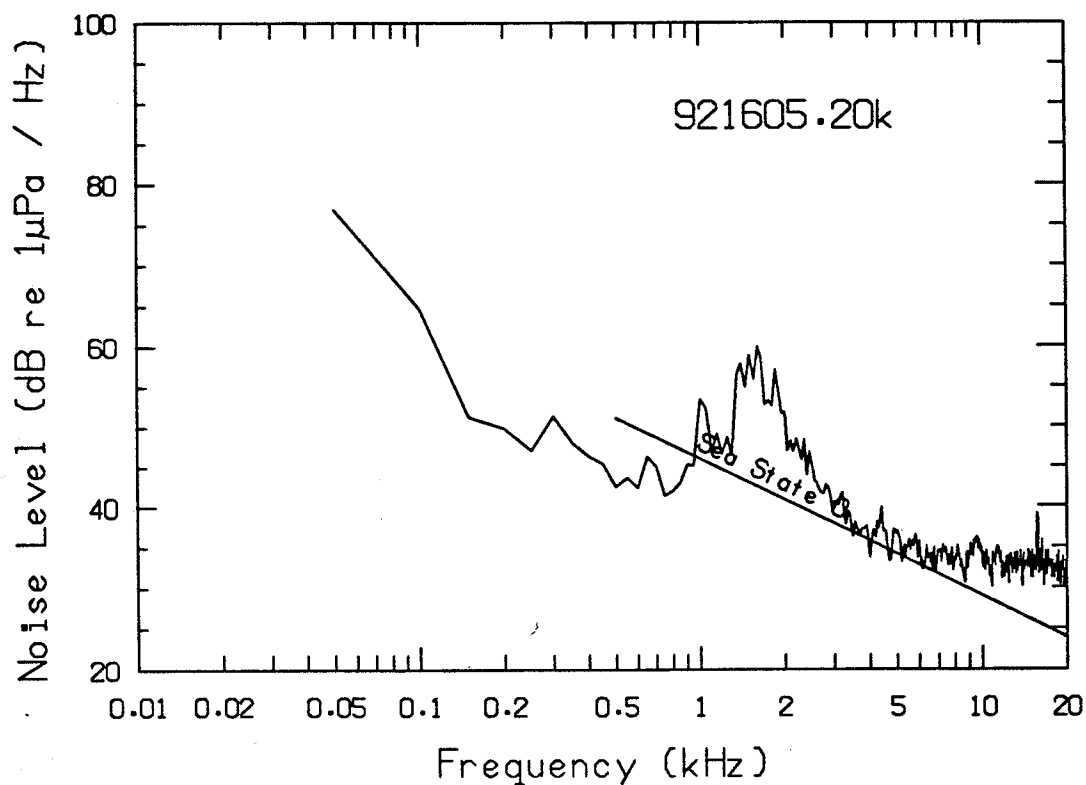
Figure 18. Ambient noise spectrum resulting from usage of a wide analysis bandwidth of 375 Hz.
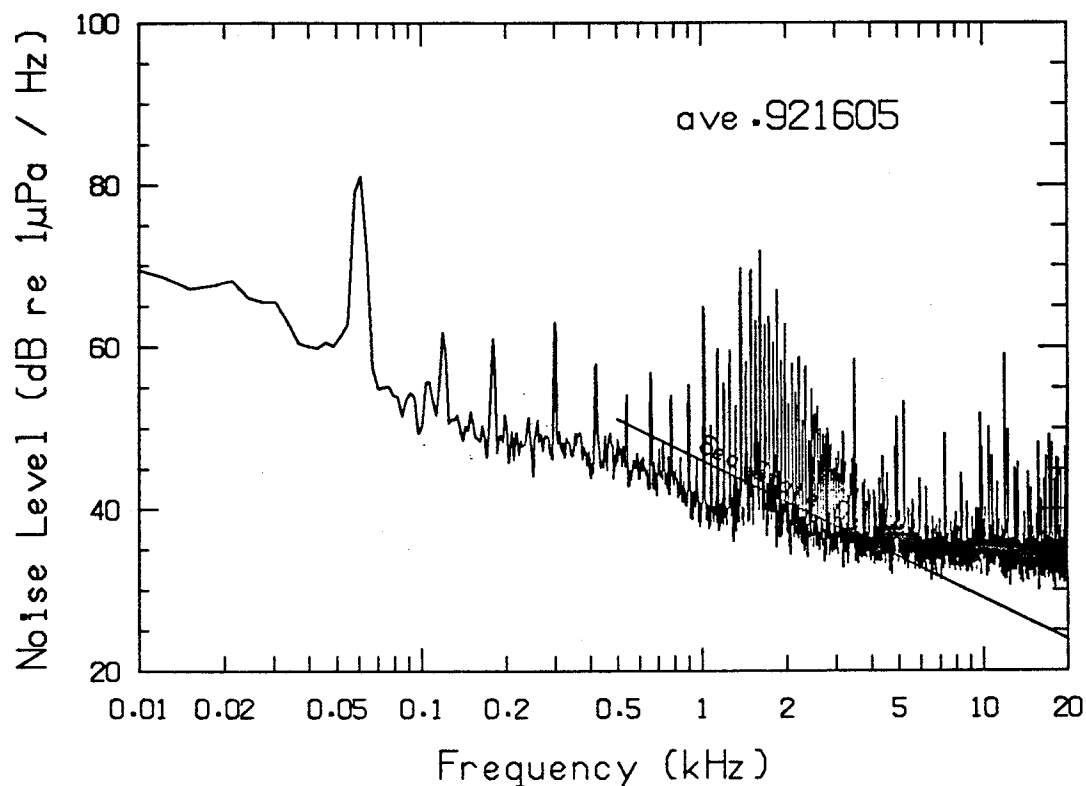

Figure 19. Better esimate of ambient noise level using a narrow analysis bandwidth of 3.15 Hz.

-30-

IX. REFERENCES

1. Naval Oceanographic Office, Stennis Space Center, MS.

2. Naval Observatory, Washington, D. C.

3. N. P. Fofonoff and R. C. Millard, Jr., "Algorithms for computation of fundamental properties of seawater," UNESCO Technical Papers in Marine Science, #44, Paris, 1983.

4. G. R. Garrison, T. Wen, R. E. Francois, W. J. Felton, and M. L. Welch, "Environmental measurements in the Beaufort Sea, spring 1986," APL-UW 4-86, Applied Physics Laboratory, University of Washington, Seattle, WA, 1987.

5. T. Wen, R. P. Stein, F. W. Karig, R. T. Miyamoto, and W. J. Felton, "Environmental measurements in the Beaufort Sea, spring 1987," APL-UW 1-87, Applied Physics Laboratory, University of Washington, Seattle, WA, 1988.

6. T. Wen, W. J. Felton, J. C. Luby, W. L. J. Fox, and K. L. Kientz, "Environmental measurements in the Beaufort Sea, spring 1988," APL-UW TR 8822, Applied Physics Laboratory, University of Washington, Seattle, WA, 1989.

7. T. Wen, F. W. Karig, W. J. Felton, J. C. Luby, and K.L. Williams, "Environmental measurements in the Beaufort Sea, spring 1990," APL-UW TR9105, Applied Physics Laboratory, University of Washington, Seattle, WA, 1990.

8. R. M. Morey, A. Kovacs, and G. F. N. Cox, "Electromagnetic properties of sea ice," CRREL report 84-2, Cold Regions Research and Engineering Laboratory, Hanover, NH, 1984.

9. G. F. N. Cox and W. F. Weeks, "Equations for determining the gas and brine volumes in sea-ice samples," *J. Glaciol.*, *29*, 306- 316, 1983.

APPENDIX A

STD Plots

Table 2. CTD casts at ice camp APLIS 91.

Date	Time-of-Day (L)	Cast #	Position Latitude	Longitude	
03-28-91	1355	CAST# 1	73-19.7N	145-41.5W	
03-28-91	2254	CAST# 2	73-19.7N	145-41.4W	
03-29-91	0650	CAST# 3	73-19.7N	145-41.4W	
03-29-91	2032	CAST# 4	73-19.7N	145-41.4W	
03-30-91	0707	CAST# 5	73-19.7N	145-41.4W	
03-30-91	2059	CAST# 6	73-19.7N	145-41.5W	
03-31-91	0611	CAST# 7	73-19.7N	145-41.5W	* plot not included
03-31-91	0633	CAST# 8	73-19.8N	145-41.3W	
03-31-91	2100	CAST# 9	73-19.7N	145-41.3W	
04-01-91	0755	CAST# 10	73-19.7N	145-41.4W	
04-01-91	2132	CAST# 11	73-19.7N	145-41.4W	
04-02-91	0721	CAST# 12	73-20.1N	145-41.5W	
04-02-91	1624	CAST# 13	73-20.2N	145-41.6W	
04-02-91	2159	CAST# 14	73-19.7N	145-40.5W	
04-03-91	0017	CAST# 15	73-19.7N	145-40.5W	
04-03-91	0719	CAST# 16	73-19.7N	145-40.5W	
04-03-91	1023	CAST# 17	73-19.7N	145-40.5W	
04-03-91	1437	CAST# 19	73-19.7N	145-40.5W	
04-03-91	2124	CAST# 20	73-19.7N	145-41.4W	
04-04-91	0005	CAST# 21	73-19.7N	145-41.5W	
04-04-91	0619	CAST# 22	73-19.8N	145-41.5W	
04-04-91	1058	CAST# 23	73-19.8N	145-41.5W	
04-04-91	1358	CAST# 24	73-19.8N	145-41.4W	
04-04-91	1440	CAST# 25	73-19.8N	145-41.4W	
04-04-91	1842	CAST# 26	73-19.8N	145-41.4W	
04-04-91	2159	CAST# 27	73-19.8N	145-41.4W	
04-05-91	0731	CAST# 28	73-19.7N	145-41.5W	
04-05-91	1201	CAST# 29	73-19.7N	145-41.5W	
04-05-91	2139	CAST# 30	73-19.7N	145-41.4W	
04-06-91	0847	CAST# 31	73-19.7N	145-41.5W	
04-06-91	1245	CAST# 32	73-19.7N	145-41.5W	
04-06-91	1934	CAST# 33	73-19.8N	145-41.5W	
04-07-91	0933	CAST# 34	73-19.8N	145-41.6W	
04-07-91	2118	CAST# 35	73-19.8N	145-41.6W	
04-08-91	0920	CAST# 36	73-19.8N	145-41.5W	

T = Temperature

S = Salinity

V = Sound Speed

Sig = Sigma–T
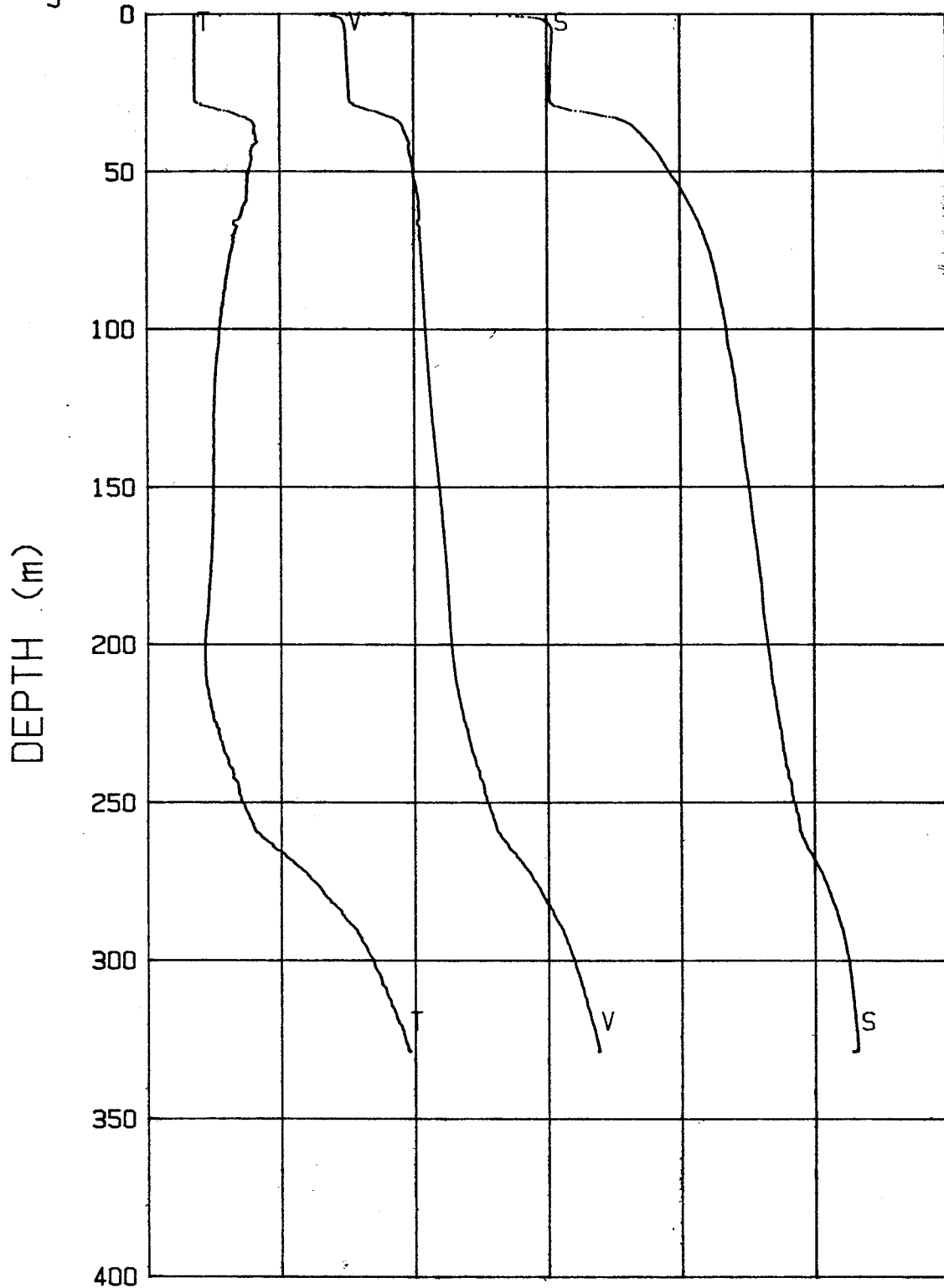
03-28-91 1355   CAST# 1   73-19.7N   145-41.5W

V(m/s) 1420   1430   1440   1450   1460   1470   1480
S(o/oo) 24   26   28   30   32   34   36
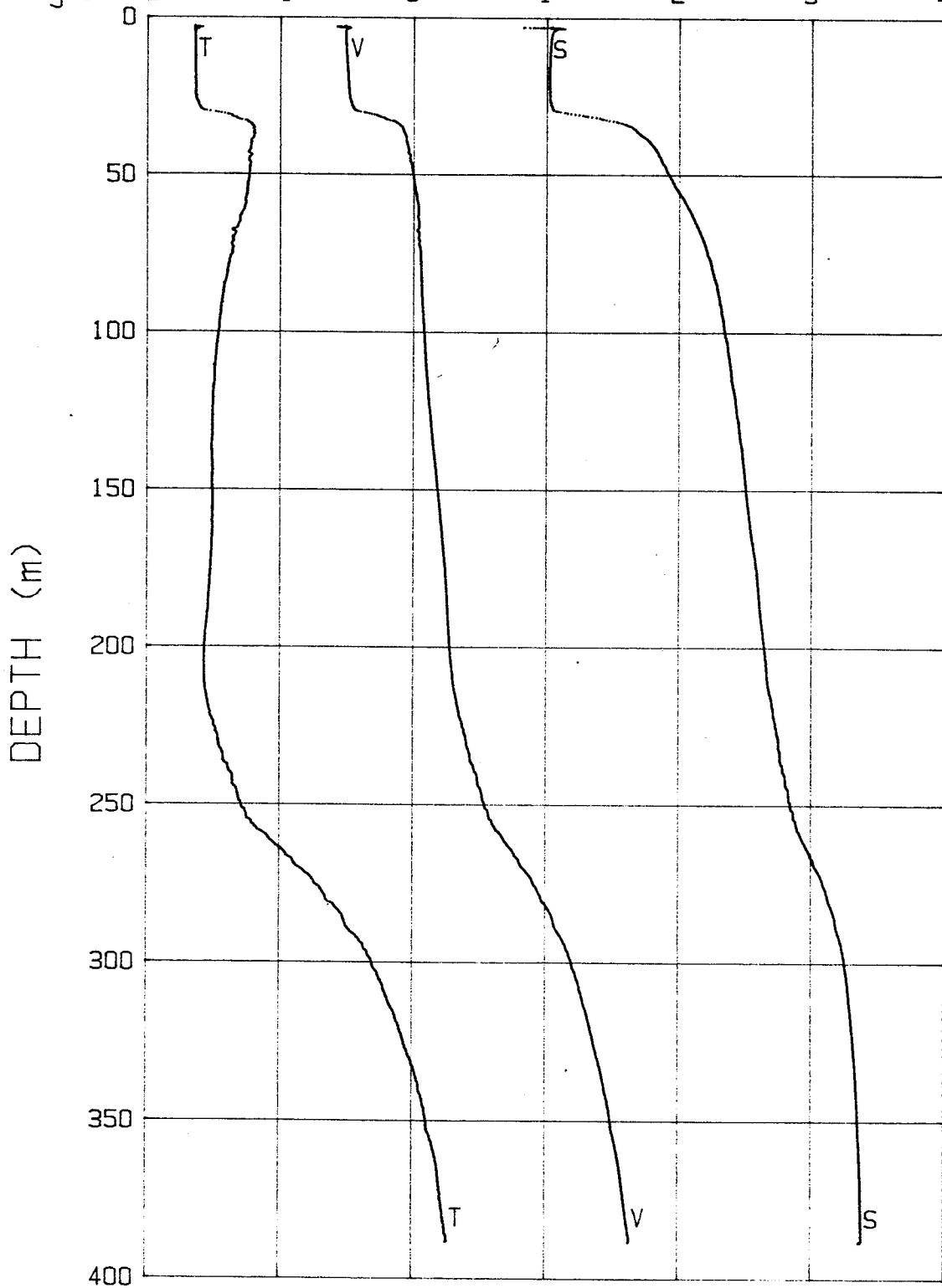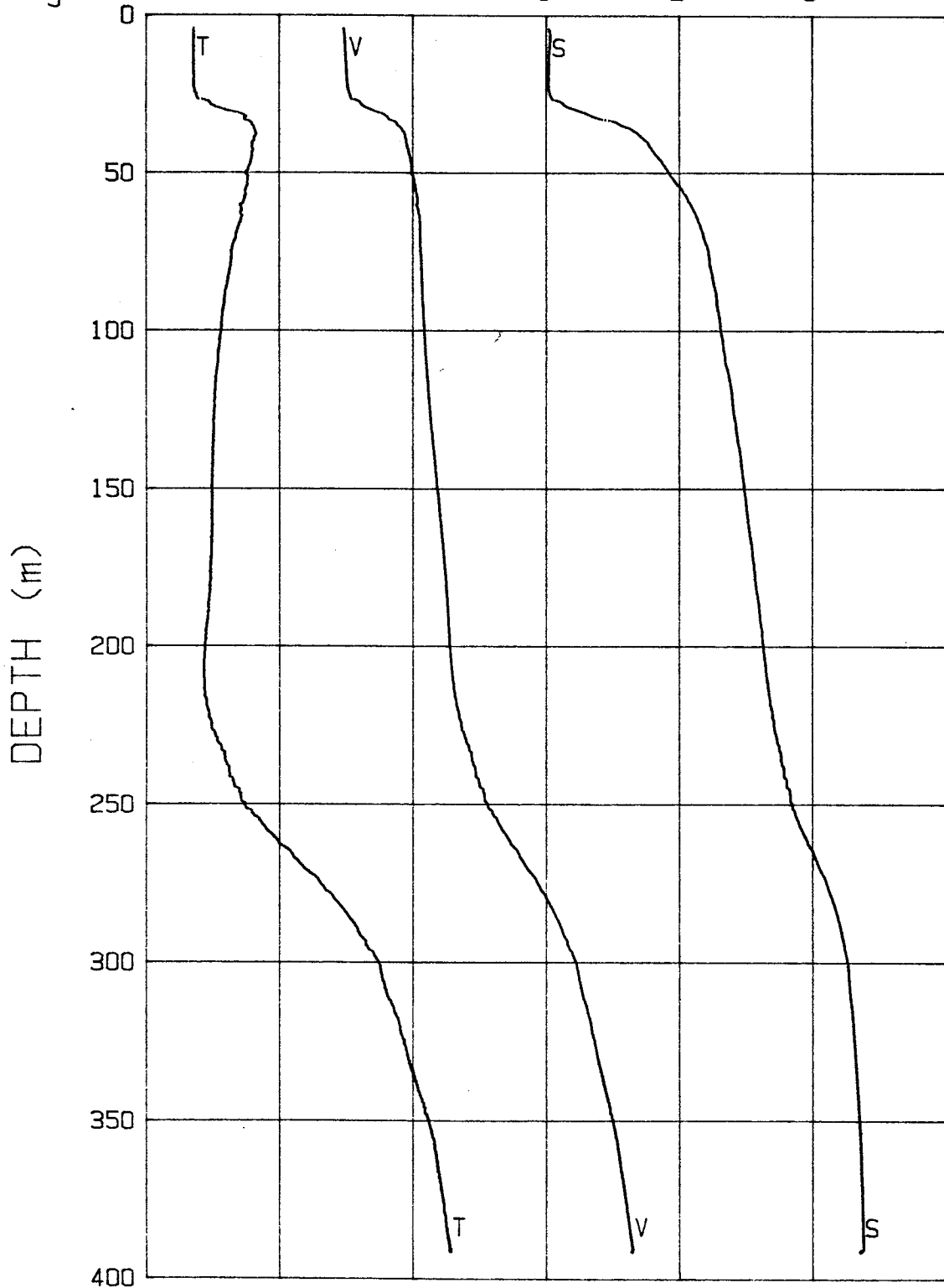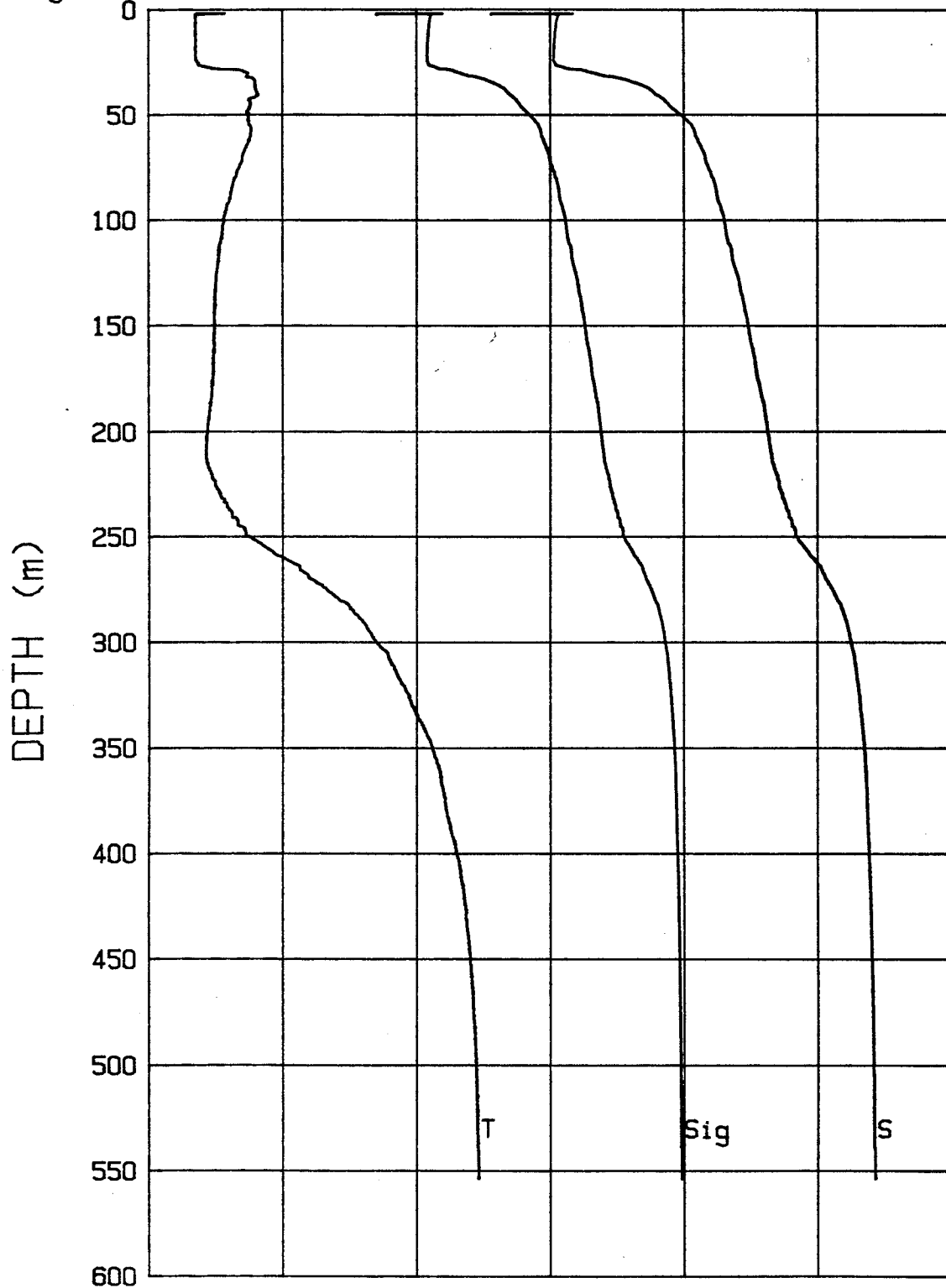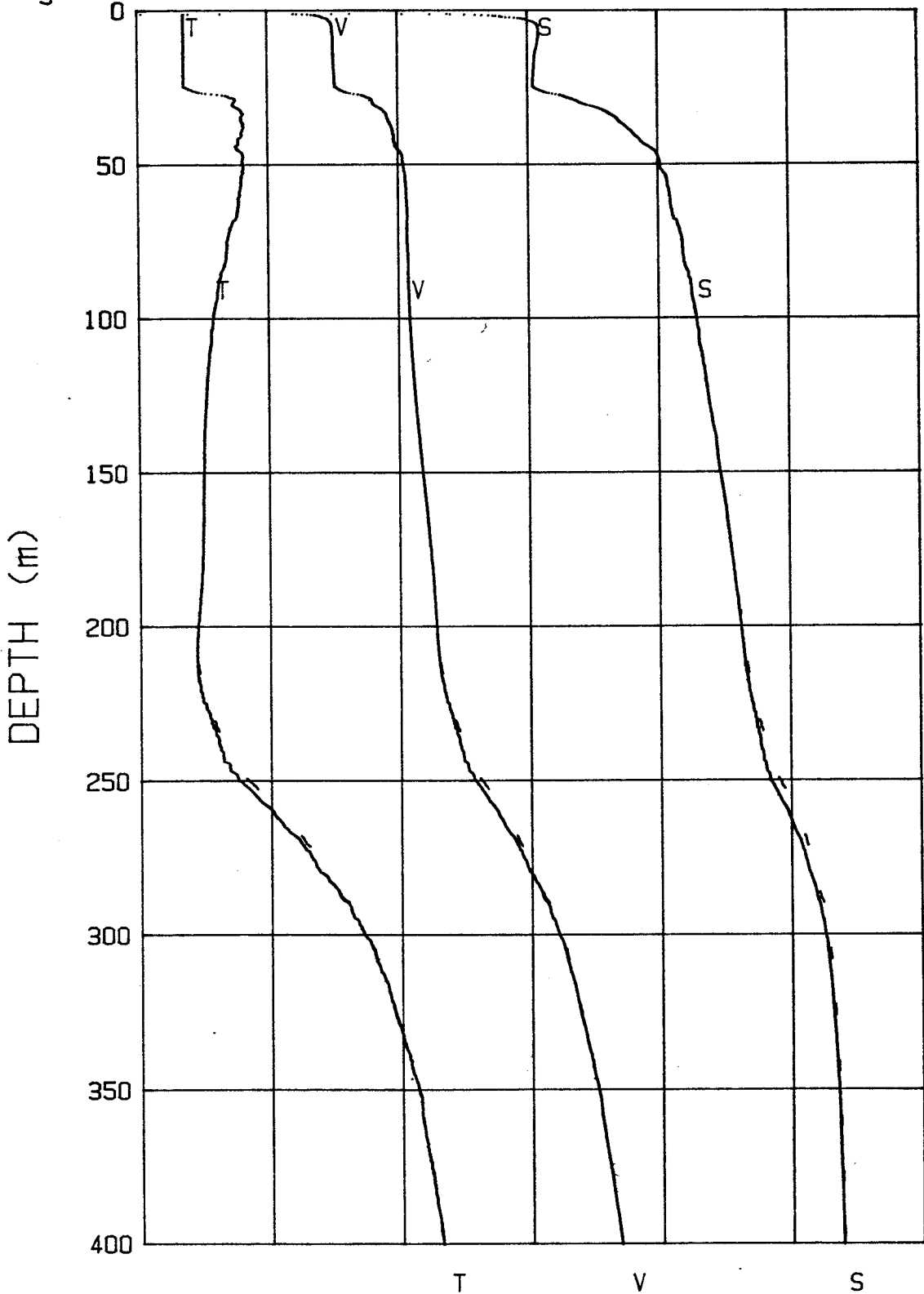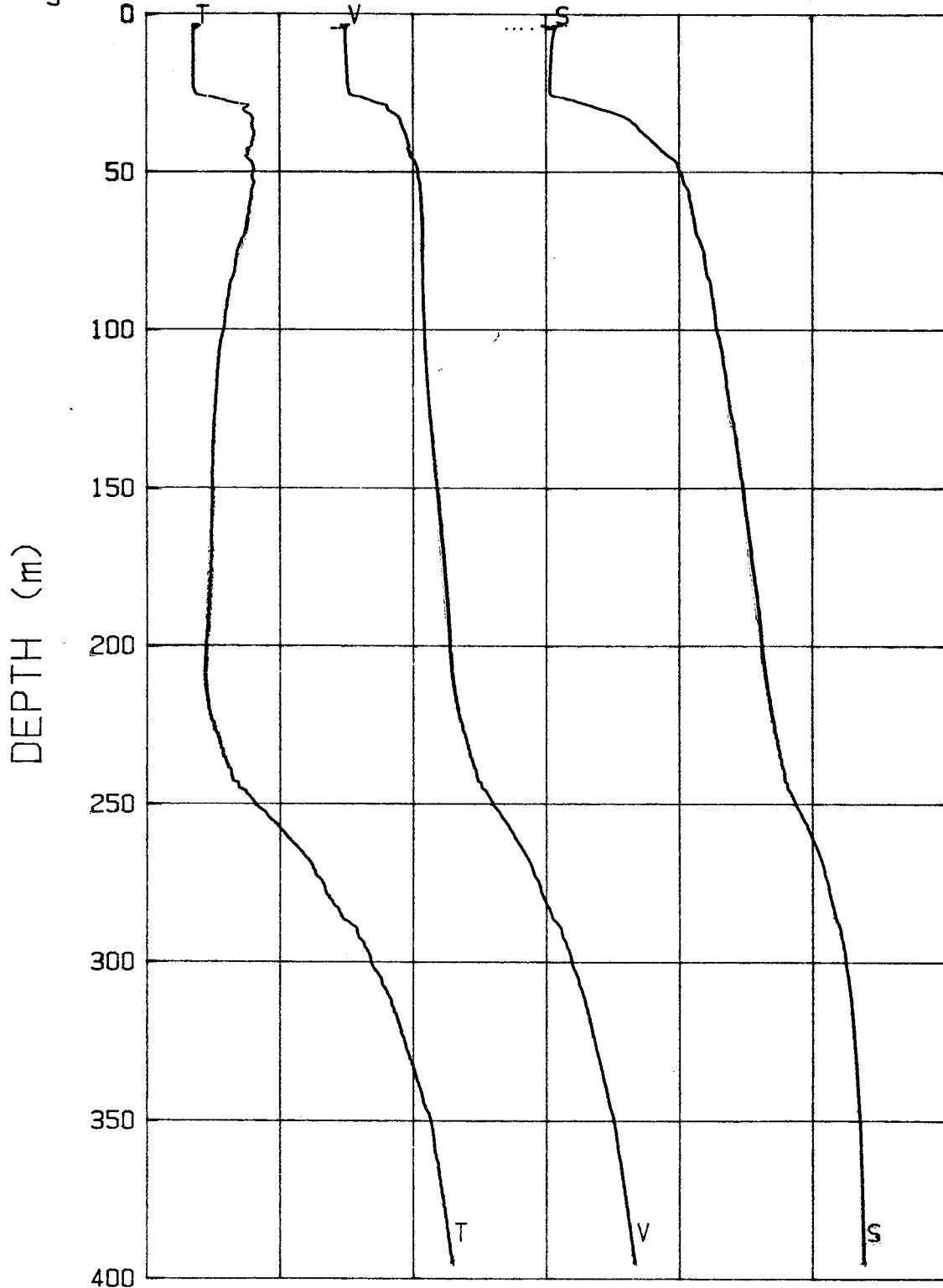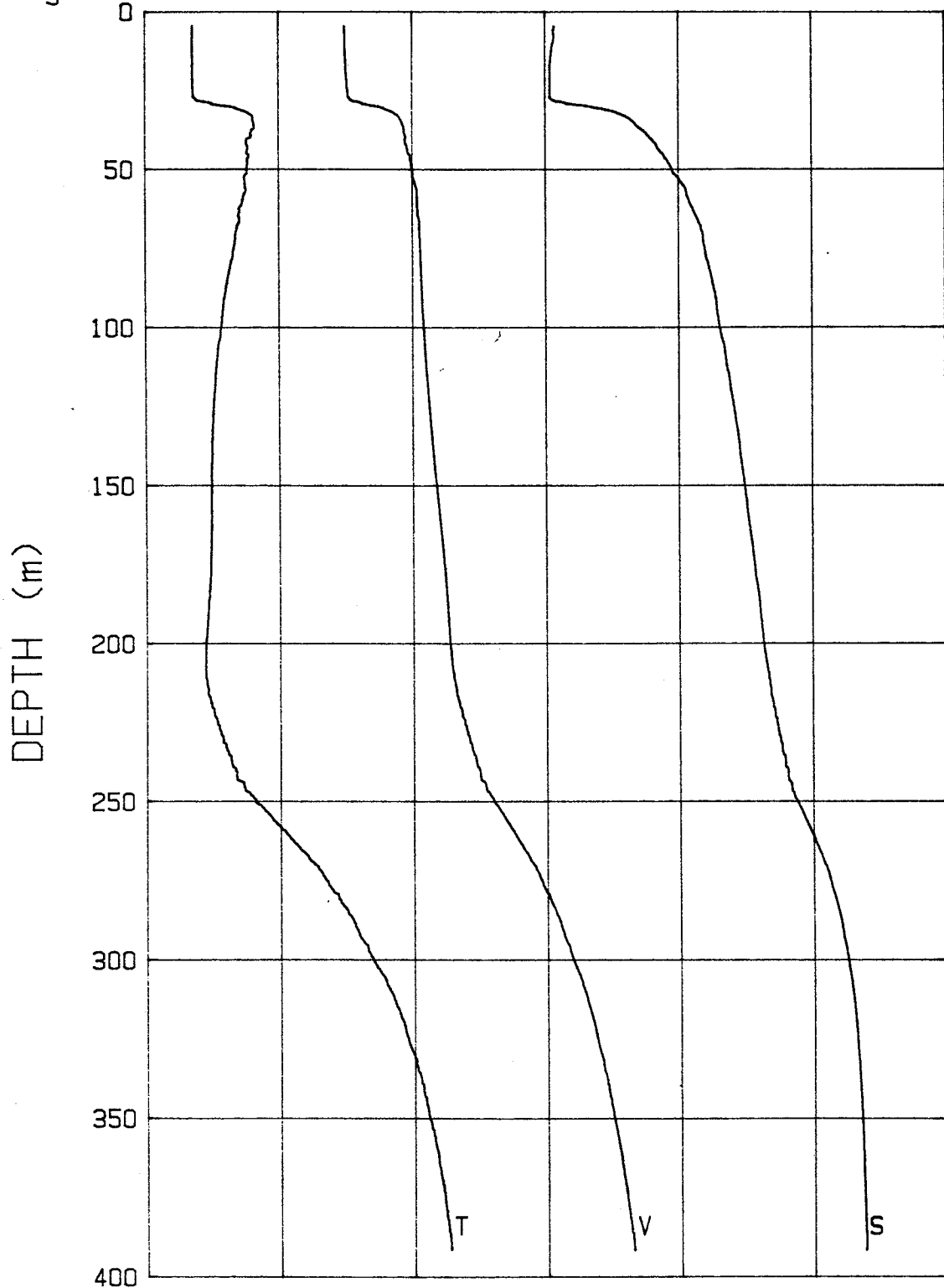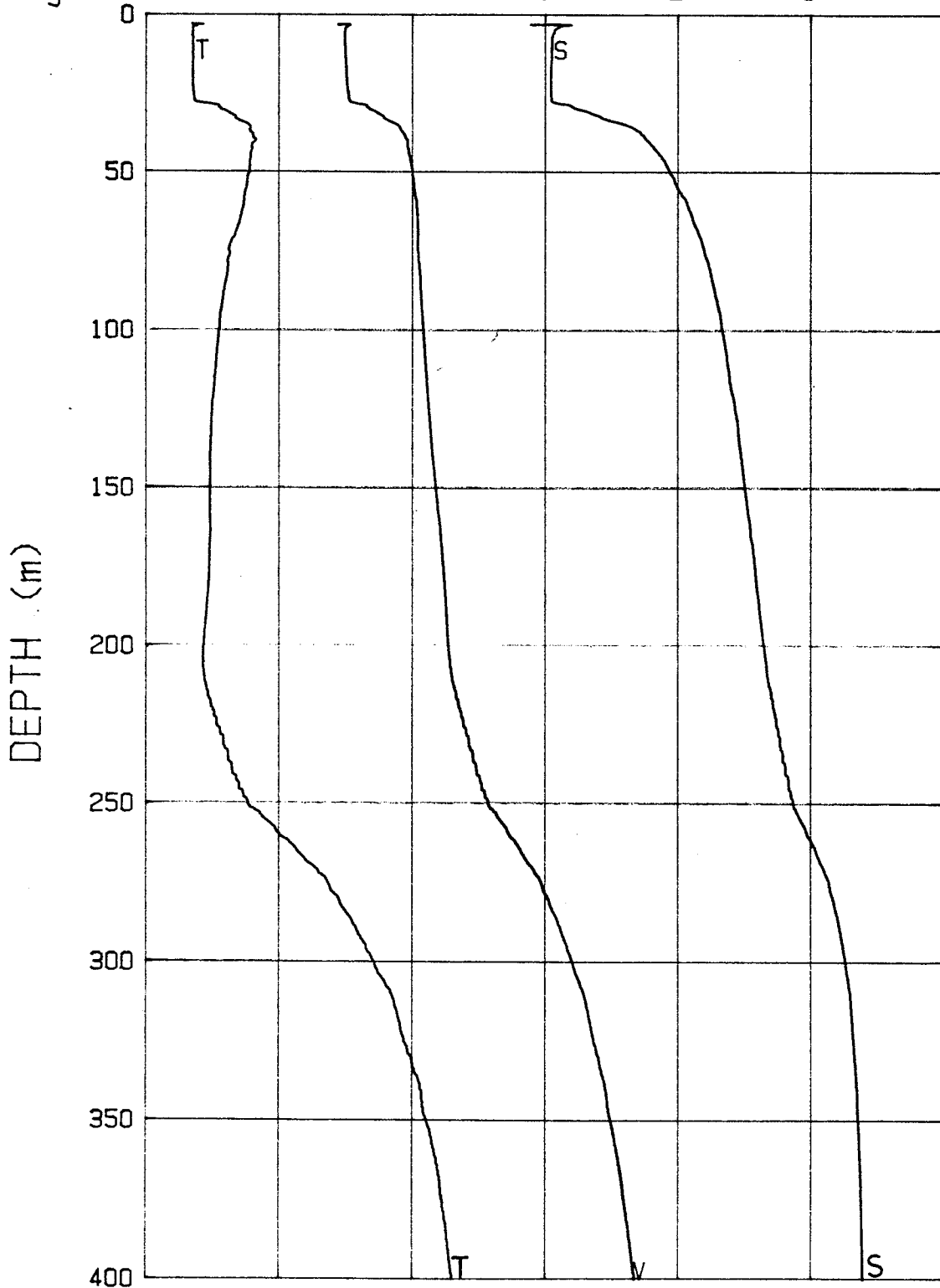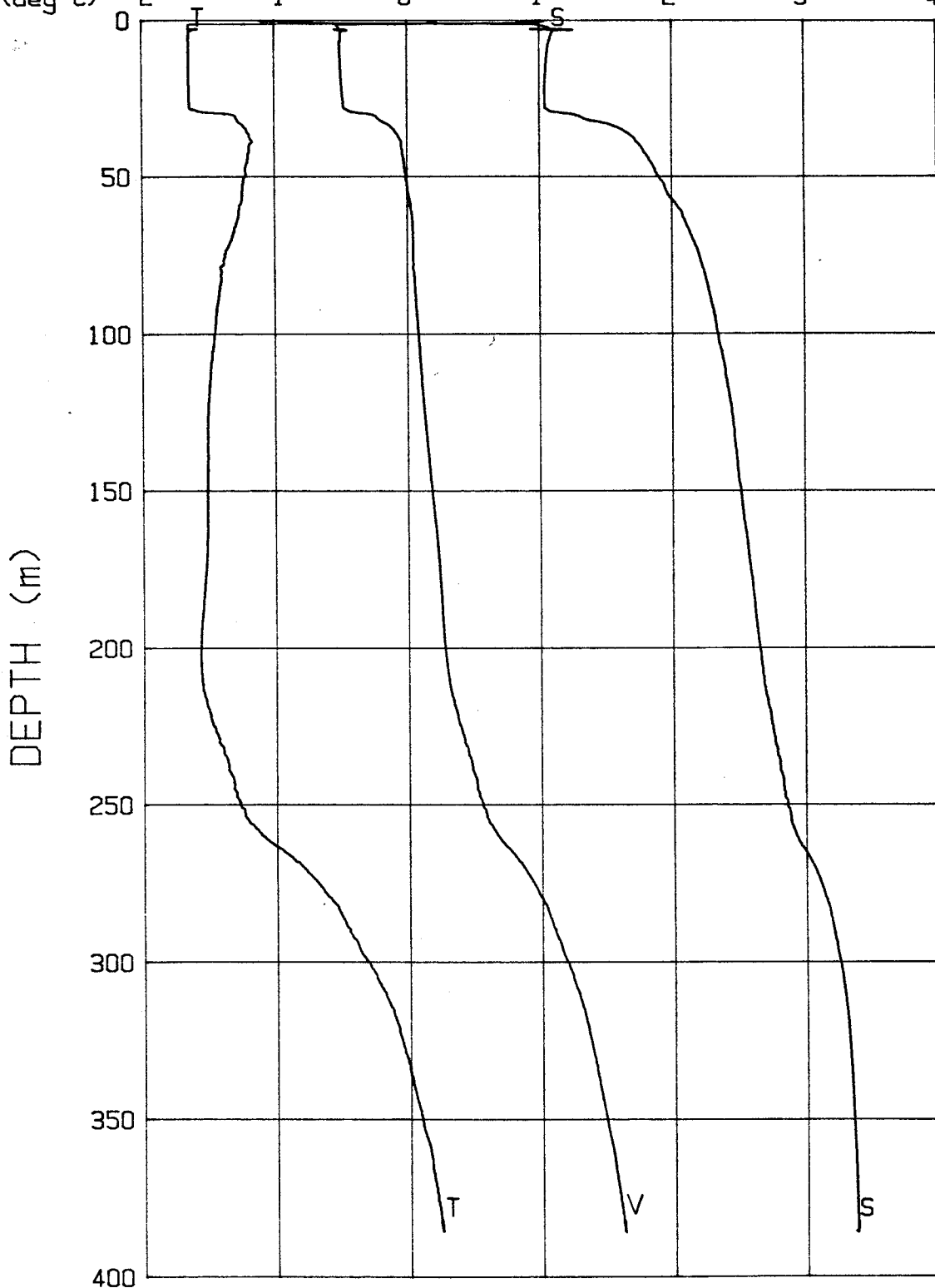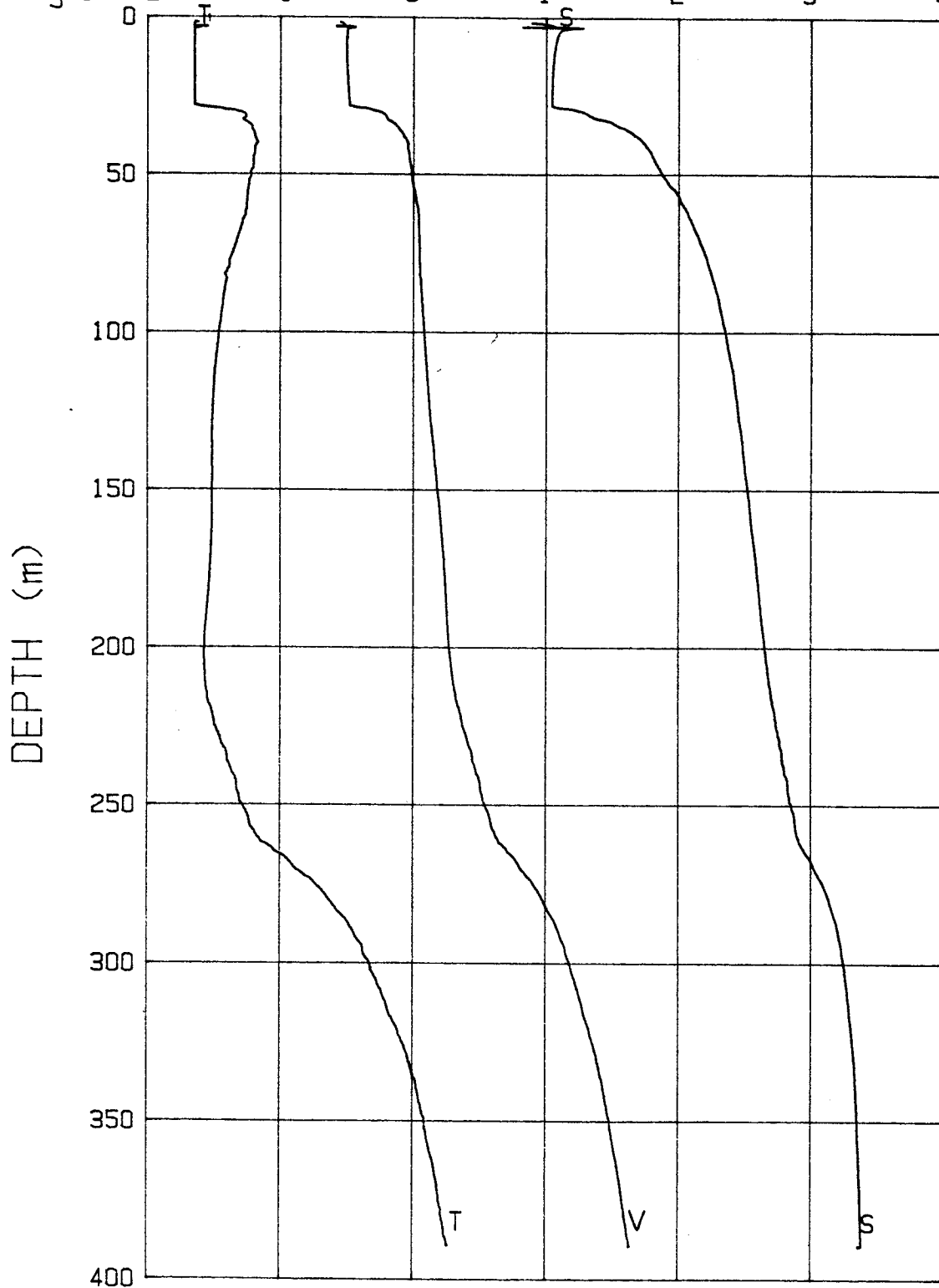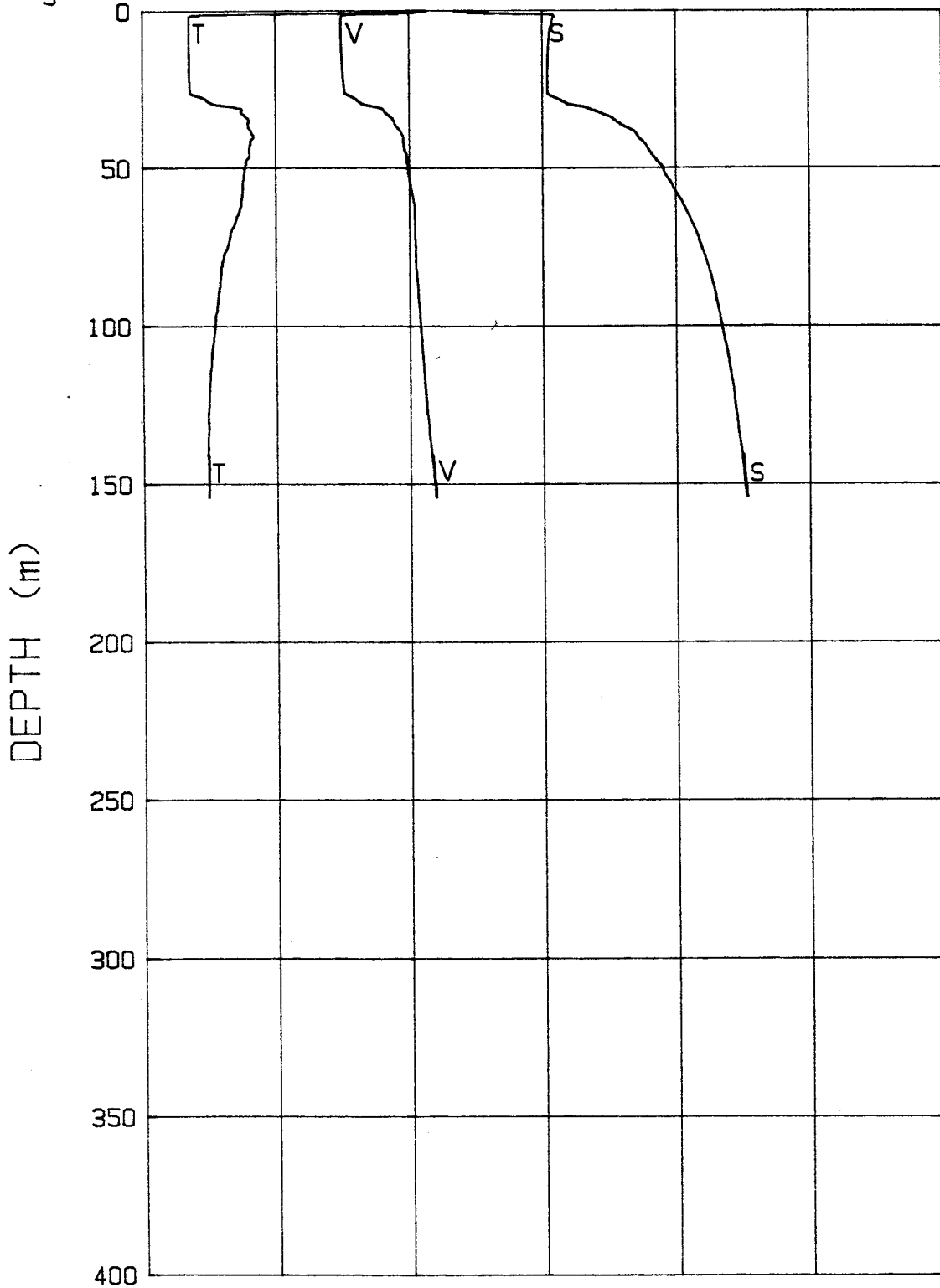T(deg C) -2   -1   0   1   2   3   4

DEPTH (m)

03-28-91 2254   CAST# 2   73-19.7N   145-41.4W

V (m/s)	1420	1430	1440	1450	1460	1470	1480
S (o/oo)	24	26	28	30	32	34	36
T (deg C)	-2	-1	0	1	2	3	4

-36-

03-29-91 0650 CAST# 3 73-19.7N 145-41.4W

V (m/s)	1420	1430	1440	1450	1460	1470	1480
S (o/oo)	24	26	28	30	32	34	36
T (deg C)	-2	-1	0	1	2	3	4

DEPTH (m)

03-29-91 2032 CAST# 4   73-19.7N   145-41.4W

V(m/s)	1420	1430	1440	1450	1460	1470	1480
S(o/oo)	24	26	28	30	32	34	36
T(deg C)	-2	-1	0	1	2	3	4

DEPTH (m)

03-30-91 0707   CAST# 5   73-19.7N 145-41.4W

Sigma-t 20   22   24   26   28   30   32
S(o/oo) 24   26   28   30   32   34   36
T(deg C) -2   -1   0   1   2   3   4

DEPTH (m)

T   Sig   S

03-30-91 2059 CAST# 6   73-19.7N 145-41.5W

V (m/s)	1420	1430	1440	1450	1460	1470	1480
S (o/oo)	24	26	28	30	32	34	36
T (deg C)	-2	-1	0	1	2	3	4

DEPTH (m)

03-31-91 0633 CAST# 8 73-19.8N 145-41.3W

V (m/s)	1420	1430	1440	1450	1460	1470	1480
S (o/oo)	24	26	28	30	32	34	36
T (deg C)	-2	-1	0	1	2	3	4

DEPTH (m)

V(m/s)	1420	1430	1440	1450	1460	1470	1480
S(o/oo)	24	26	28	30	32	34	36
T(deg C)	-2	-1	0	1	2	3	4

DEPTH (m)

T   V   S

04-01-91 0755   CAST# 10   73-19.7N   145-41.4W

V(m/s)	1420	1430	1440	1450	1460	1470	1480
S(o/oo)	24	26	28	30	32	34	36
T(deg C)	-2	-1	0	1	2	3	4

DEPTH .(m)

04-01-91 2132 CAST# 11   73-19.7N   145-41.4W

04-02-91 0721 CAST# 12   73-2 .3N 145-35.5W

V(m/s)	1420	1430	1440	1450	1460	1470	1480
S(o/oo)	24	26	28	30	32	34	36
T(deg C)	-2	-1	0	1	2	3	4

DEPTH (m)

04-02-91 1624   CAST# 13   73-19.7N   145-42.3W

V(m/s)	1420	1430	1440	1450	1460	1470	1480
S(o/oo)	24	26	28	30	32	34	36
T(deg C)	-2	-1	0	1	2	3	4

DEPTH (m)

04-02-91 2159 CAST# 14   73-19.7N 145-40.5W

Sigma-t 20   22   24   26   28   30   32
S(o/oo) 24   26   28   30   32   34   36
T(deg C) -2   -1   0   1   2   3   4
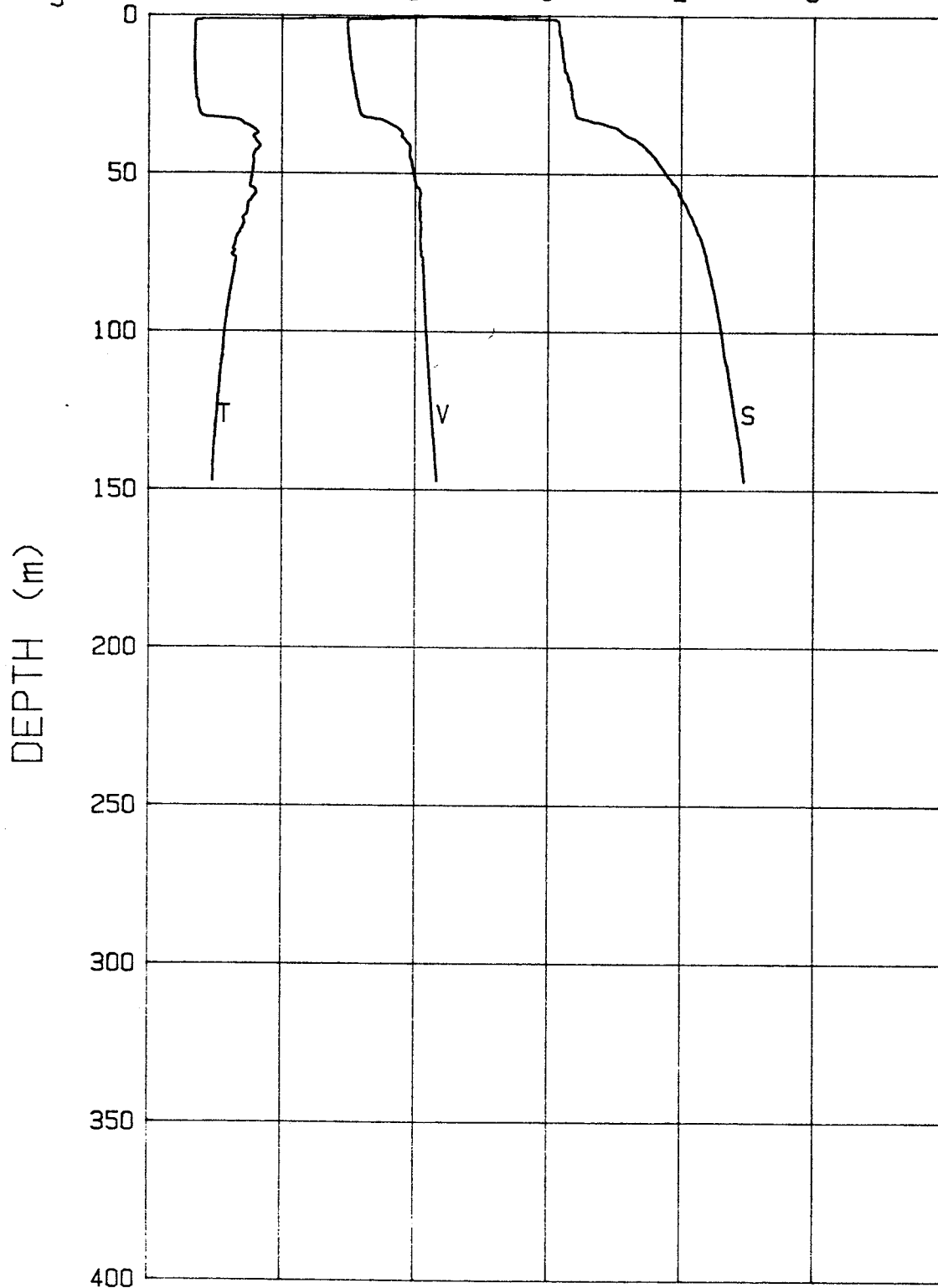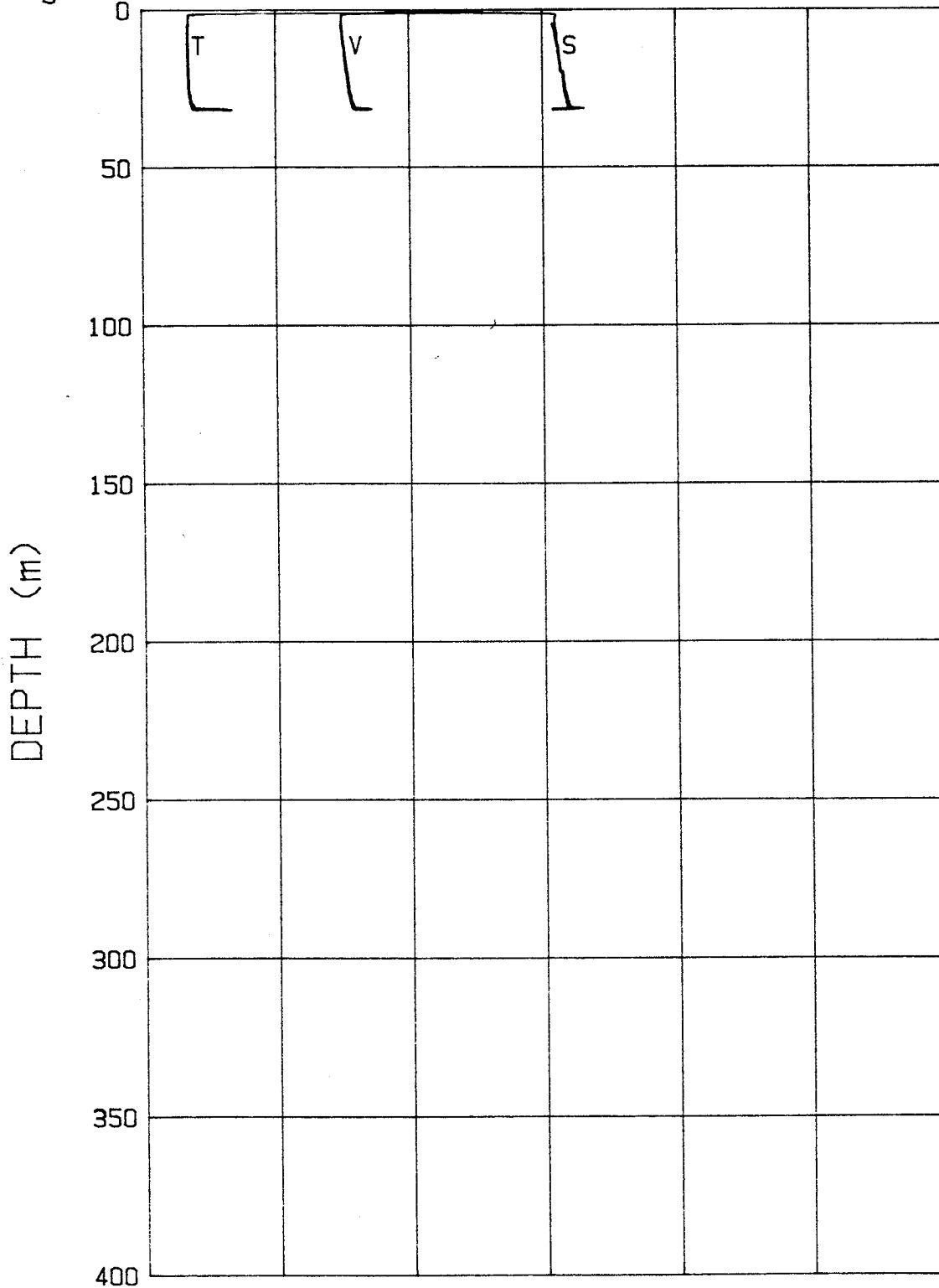
DEPTH (m)

04-03-91 0017 CAST# 15 73-19.7N 145-40.5W

04-03-91 0719 CAST# 16   73-19.7N 145-40.5W

04-03-91 1023   CAST# 17   73-19.7N   145-40.5W

04-03-91 1437   CAST# 19   73-19.7N   145-40.5W

04-03-91 2124   CAST# 20   73-19.7N   145-41.4W

V(m/s)	1420	1430	1440	1450	1460	1470	1480
S(o/oo)	24	26	28	30	32	34	36
T(deg C)	-2	-1	0	1	2	3	4

DEPTH (m)

04-04-91 0005   CAST# 21   73-19.7N   145-41.5W

V(m/s)	1420	1430	1440	1450	1460	1470	1480
S(o/oo)	24	26	28	30	32	34	36
T(deg C)	-2	-1	0	1	2	3	4

DEPTH (m)

T

V

S

-53-

04-04-91 0619   CAST# 22   73-19.8N   145-41.5W

-54-

04-04-91 1058 CAST# 23   73-19.8N 145-41.5W

04-04-91 1358 CAST# 24   73-19.8N 145-41.4W

V (m/s)	1420	1430	1440	1450	1460	1470	1480
S (o/oo)	24	26	28	30	32	34	36
T (deg C)	-2	-1	0	1	2	3	4

DEPTH (m)

04-04-91 1440 CAST# 25 73-19.8N 145-41.4W

V(m/s)	1420	1430	1440	1450	1460	1470	1480
S(o/oo)	24	26	28	30	32	34	36
T(deg C)	-2	-1	0	1	2	3	4

DEPTH (m)

04-04-91 1842   CAST# 26   73-19.8N   145-41.4W

V(m/s)	1420	1430	1440	1450	1460	1470	1480
S(o/oo)	24	26	28	30	32	34	36
T(deg C)	-2	-1	0	1	2	3	4
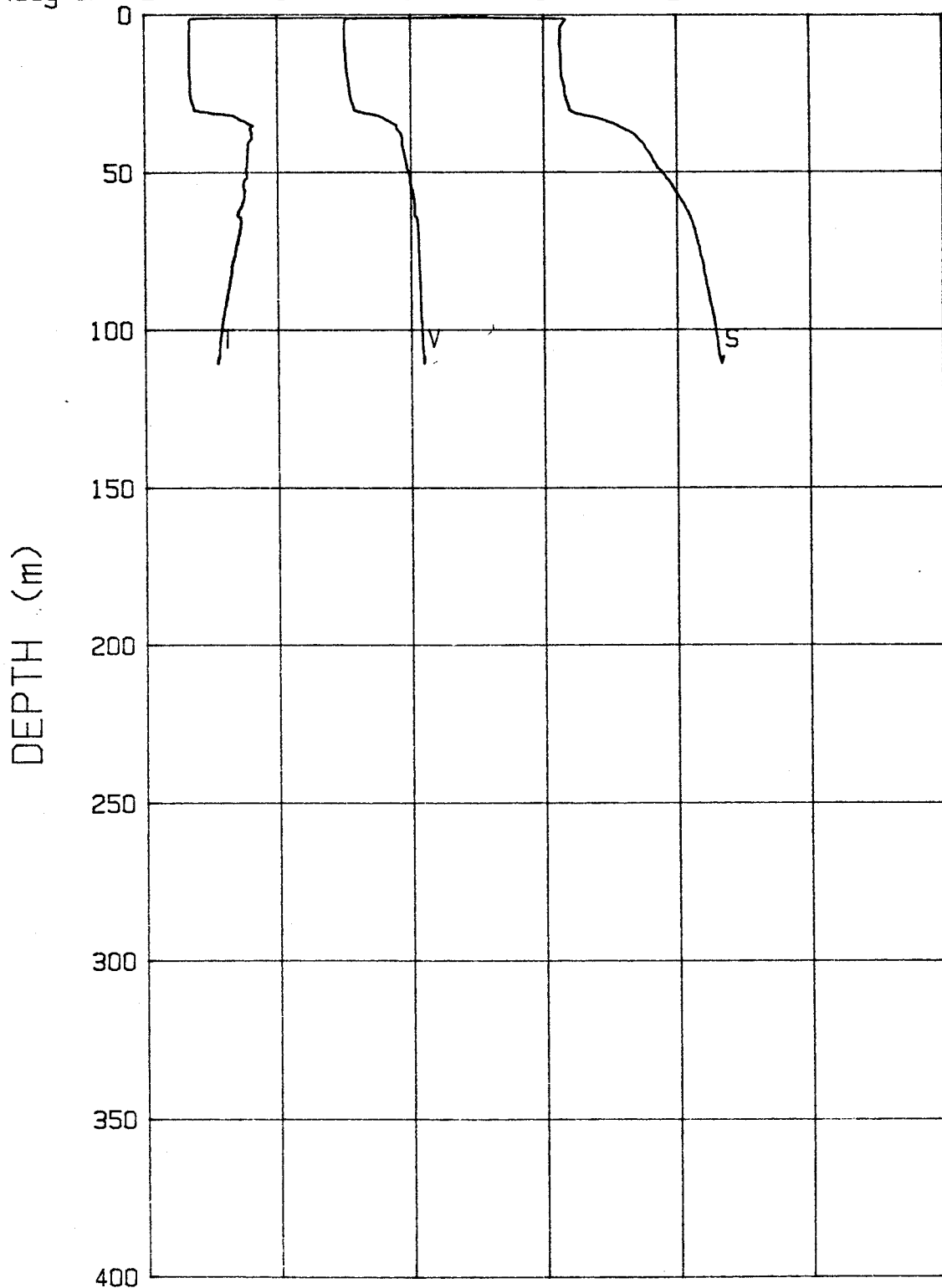
04-04-91 2159   CAST# 27   73-19.8   145-41.4W

V (m/s)	1420	1430	1440	1450	1460	1470	1480
S (o/oo)	24	26	28	30	32	34	36
T (deg C)	-2	-1	0	1	2	3	4

DEPTH (m)

04-05-91 0731 CAST# 28   73-19.7N 145-41.5W

V (m/s)	1420	1430	1440	1450	1460	1470	1480
S (o/oo)	24	26	28	30	32	34	36
T (deg C)	-2	-1	0	1	2	3	4

DEPTH (m)

T   V   S

04-05-91 1201   CAST# 29   73-19.7N 145-41.5W

V(m/s)	1420	1430	1440	1450	1460	1470	1480
S(o/oo)	24	26	28	30	32	34	36
T(deg C)	-2	-1	0	1	2	3	4

DEPTH (m)

04-05-91 2139 CAST# 30   73-19.7N 145-41.5W

V(m/s)	1420	1430	1440	1450	1460	1470	1480
S(o/oo)	24	26	28	30	32	34	36
T(deg C)	-2	-1	0	1	2	3	4

DEPTH (m)

04-06-91 0847 CAST# 31   73-19.7N 145-41.5W

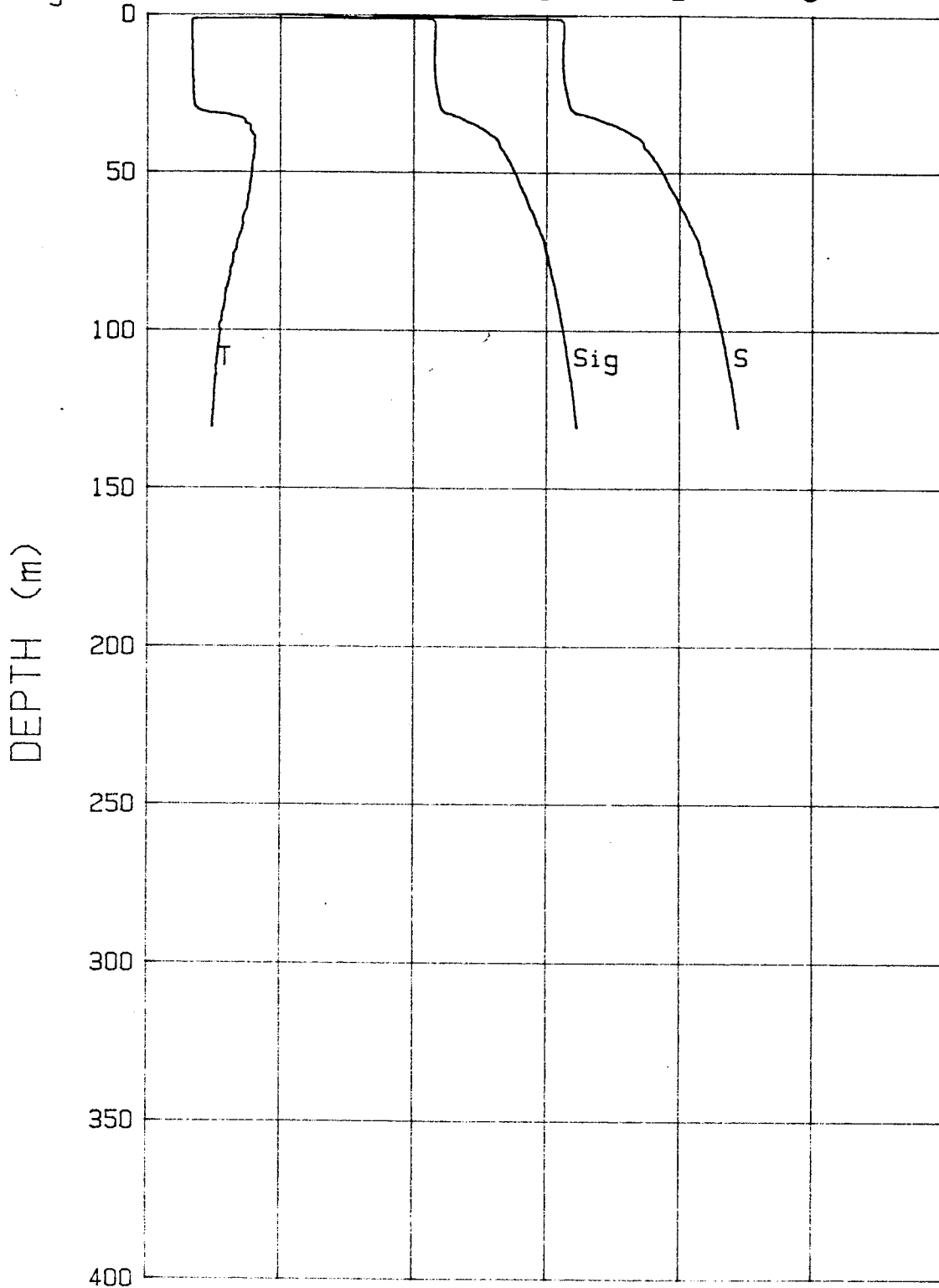| V(m/s)	1420	1430	1440	1450	1460	1470	1480
S(o/oo)	24	26	28	30	32	34	36
T(deg C)	-2	-1	0	1	2	3	4

DEPTH (m)

T   V   S

04-06-91 1245   CAST# 32   73-19.7N   145-41.5W

Sigma-t 20   22   24   26   28   30   32
S(o/oo) 24   26   28   30   32   34   36
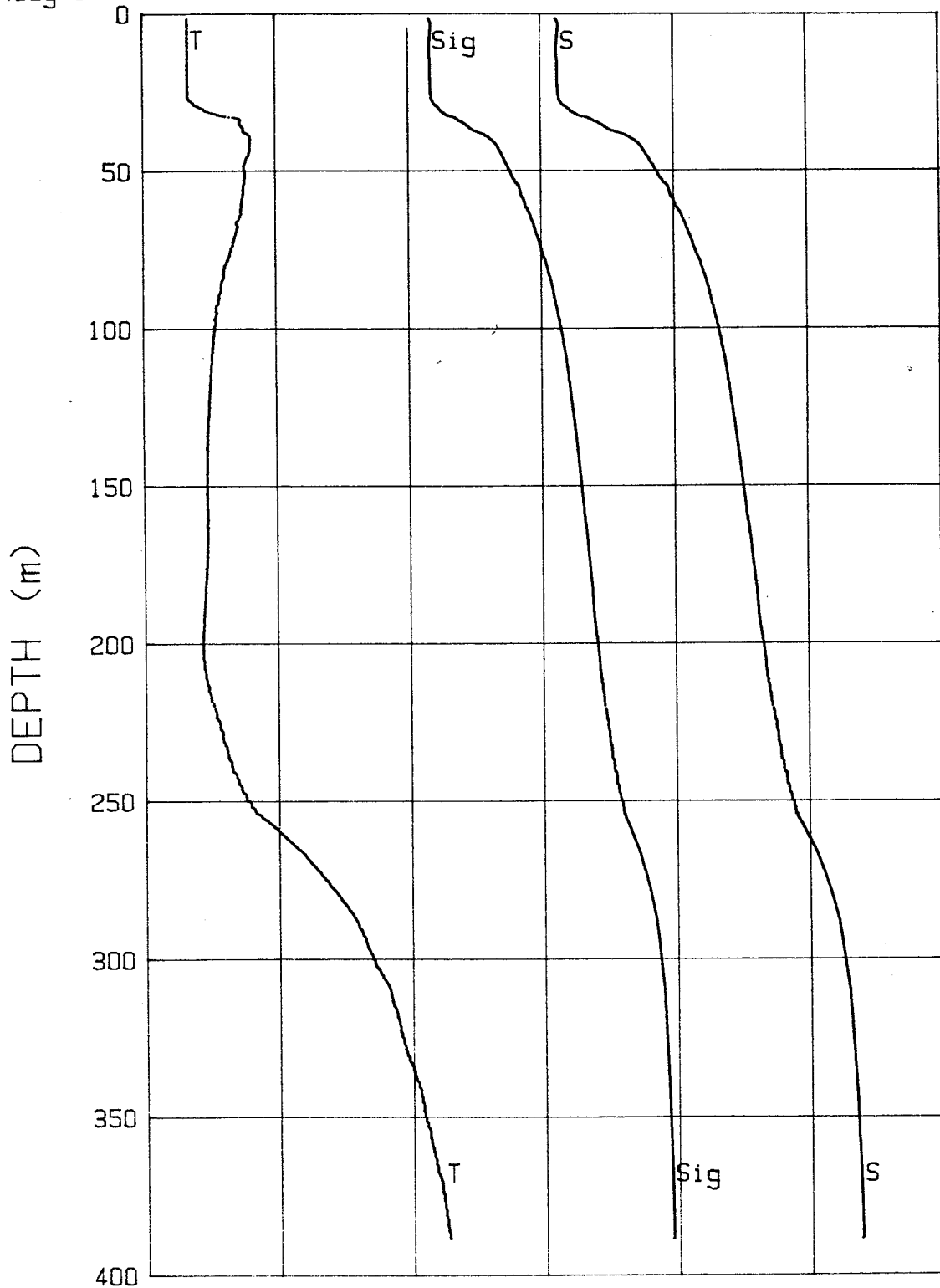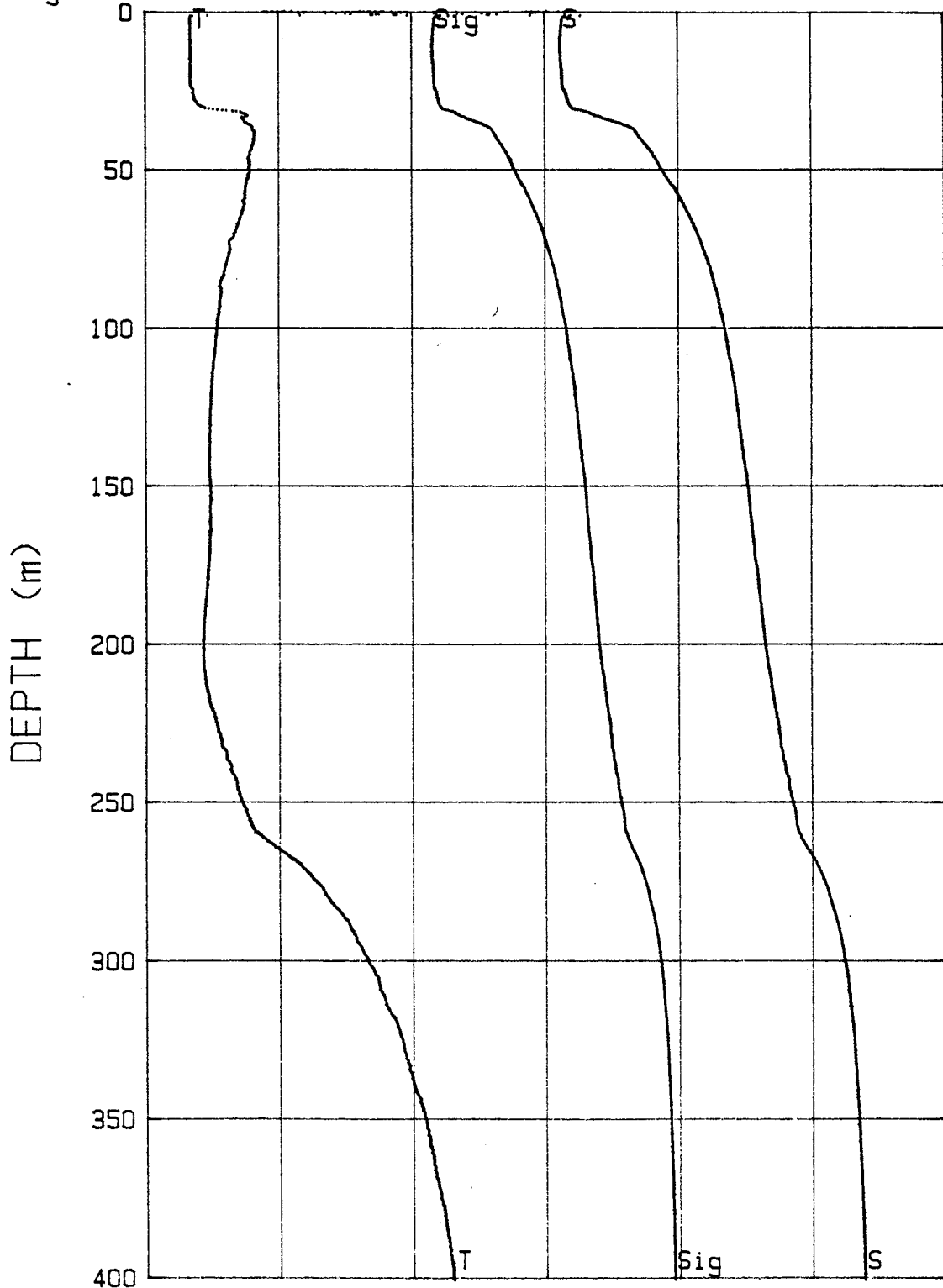T(deg C) -2   -1   0   1   2   3   4

DEPTH (m)

T   Sig   S

04-06-91 1934   CAST# 33   73-19.8N   145-41.5W

04-07-91 0933 CAST# 34   73-19.8N 145-41.6W

Sigma-t   20   22   24   26   28   30   32
S(o/oo)   24   26   28   30   32   34   36
T(deg C) -2   -1   0   1   2   3   4
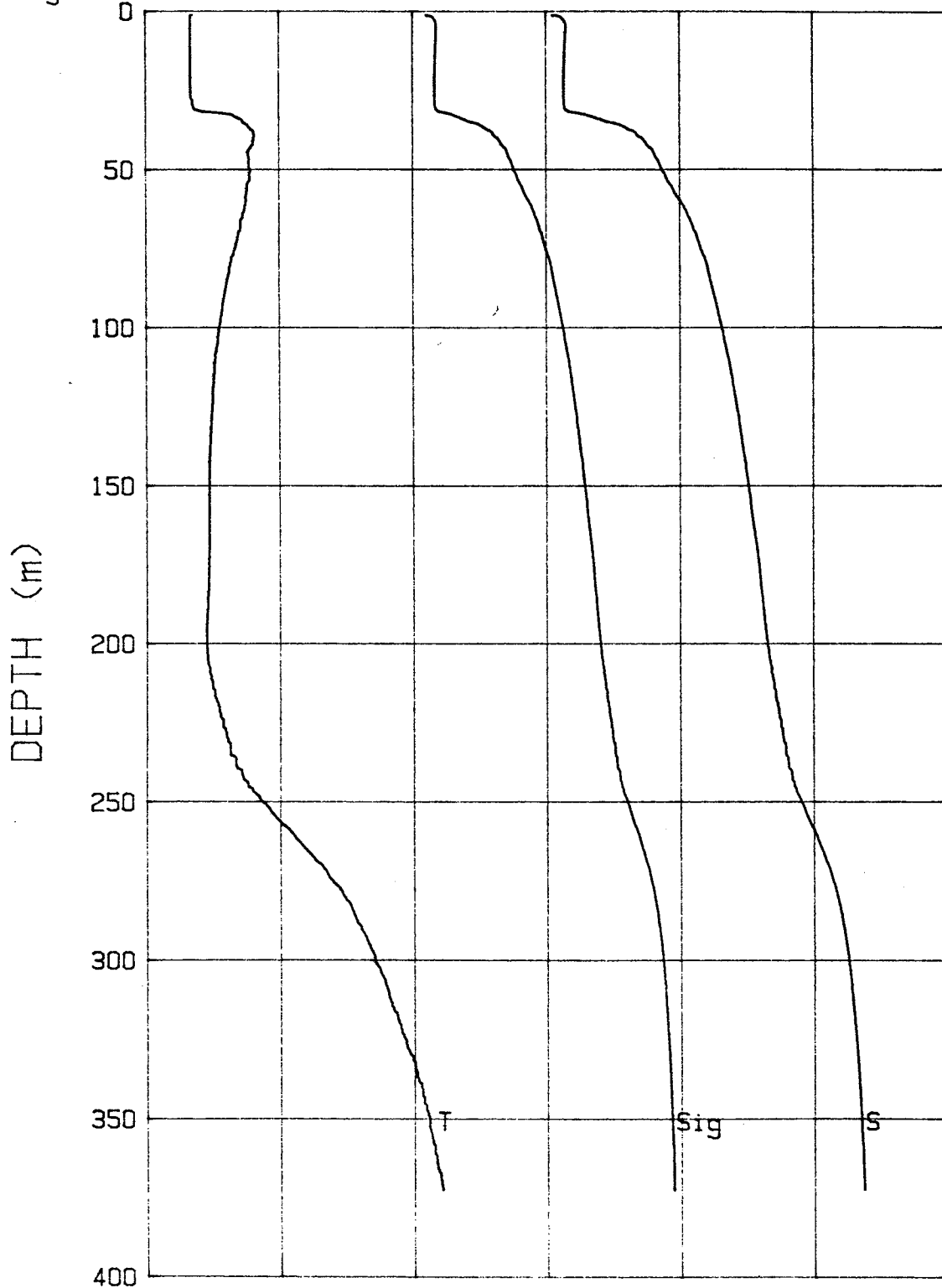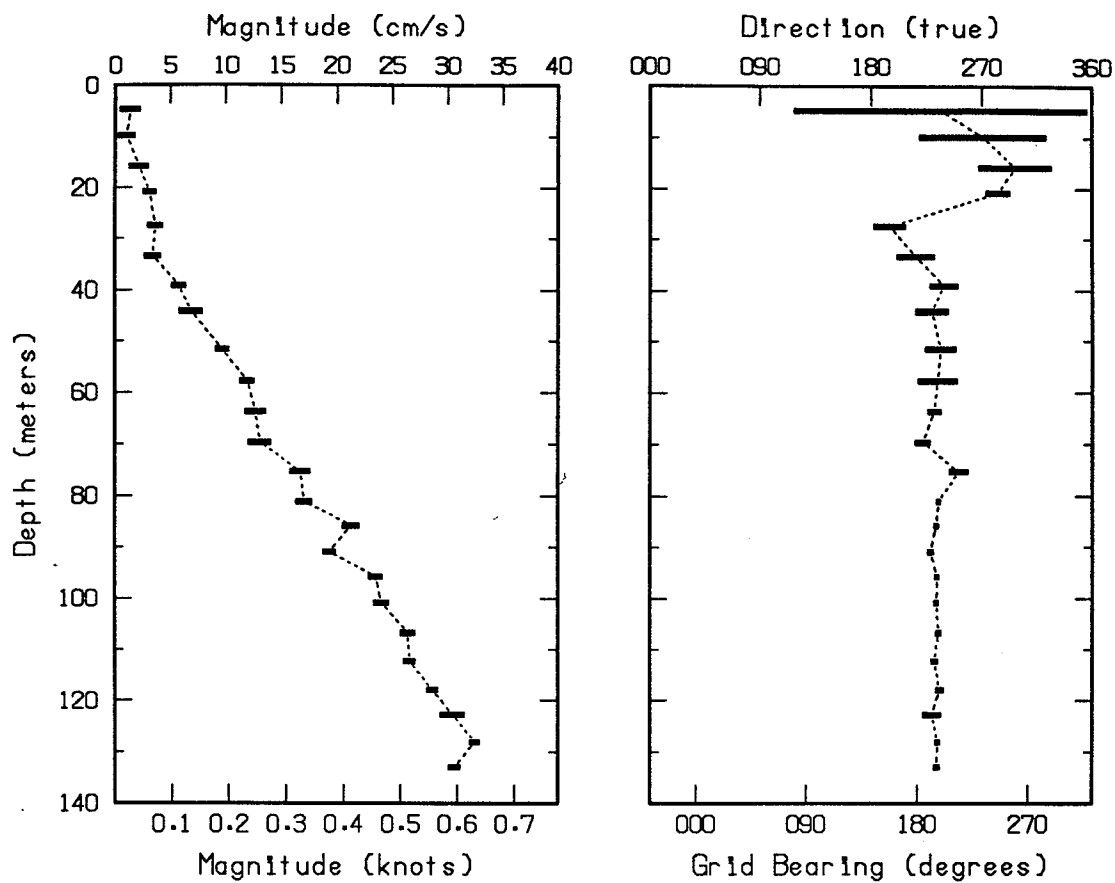
DEPTH (m)

04-07-91 2118   CAST# 35   73-19.8N   145-41.6W

Sigma-t	20	22	24	26	28	30	32
S(o/oo)	24	26	28	30	32	34	36
T(deg C)	-2	-1	0	1	2	3	4

DEPTH (m)

04-08-91 0920   CAST# 36   73-19.8N   145-41.5W

Sigma-t	20	22	24	26	28	30	32
S(o/oo)	24	26	28	30	32	34	36
T(deg C)	-2	-1	0	1	2	3	4

DEPTH (m)

T   Sig   S

APPENDIX B

Current Data

Table 3. Current meter casts at APLIS 91.

Date	Time-of-Day (L)	Cast #
04-01-91	1644	Cast #01
04-02-91	1407	Cast #02
04-02-91	2328	Cast #03
04-03-91	0743	Cast #04
04-03-91	1106	Cast #05
04-03-91	1458	Cast #06
04-03-91	2053	Cast #07
04-04-91	0638	Cast #08
04-04-91	1536	Cast #09
04-04-91	1952	Cast #10
04-05-91	0914	Cast #11
04-05-91	1100	Cast #12
04-05-91	2155	Cast #13
04-06-91	0638	Cast #14
04-06-91	1118	Cast #15
04-06-91	2250	Cast #16
04-07-91	0749	Cast #17
04-07-91	1412	Cast #18
04-08-91	0959	Cast #19

04-01-91 1644   CAST #01

Magnetic bearing + 34.3 degrees = True bearing
True bearing of +Y axis = 37.6 degrees

04-02-91 1407   CAST #02

Magnitude (cm/s)
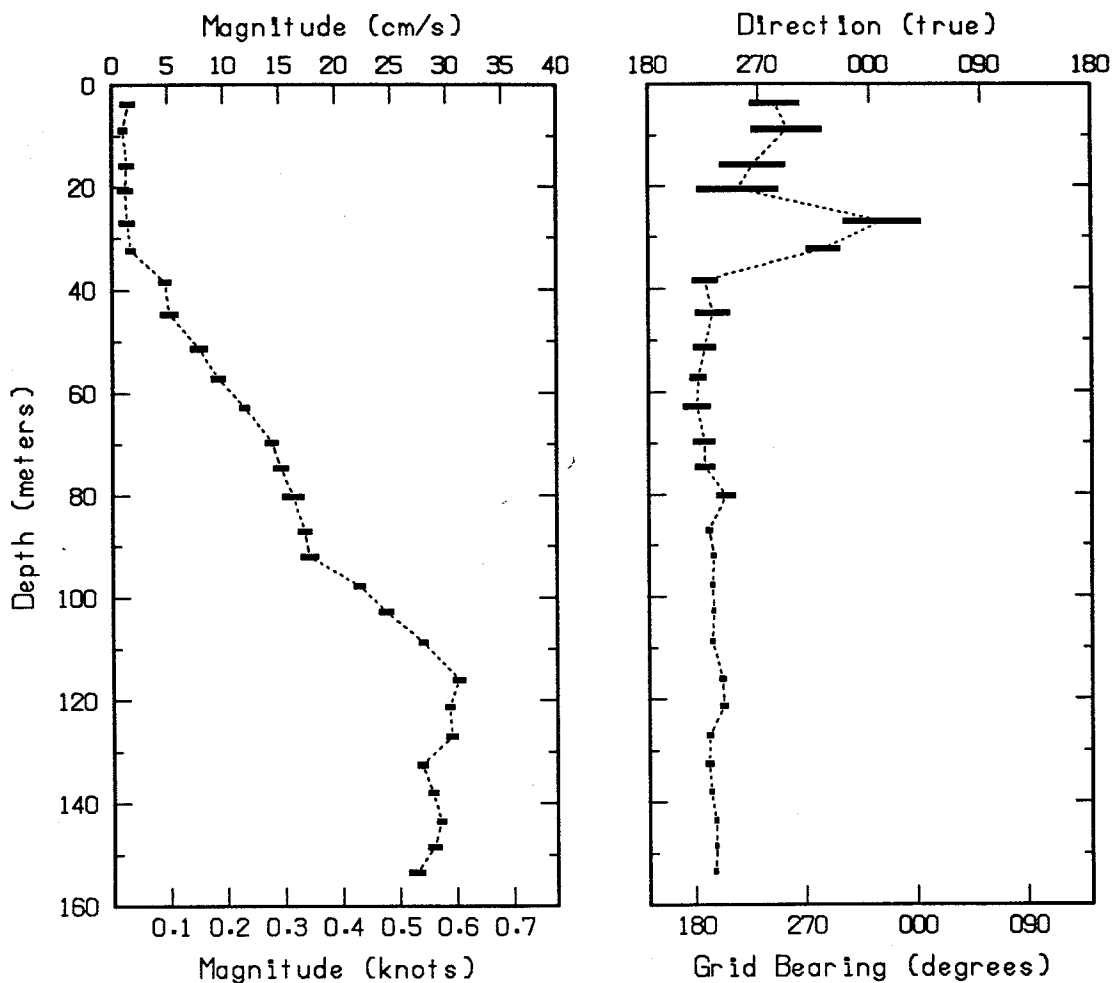
Direction (true)

Depth (meters)
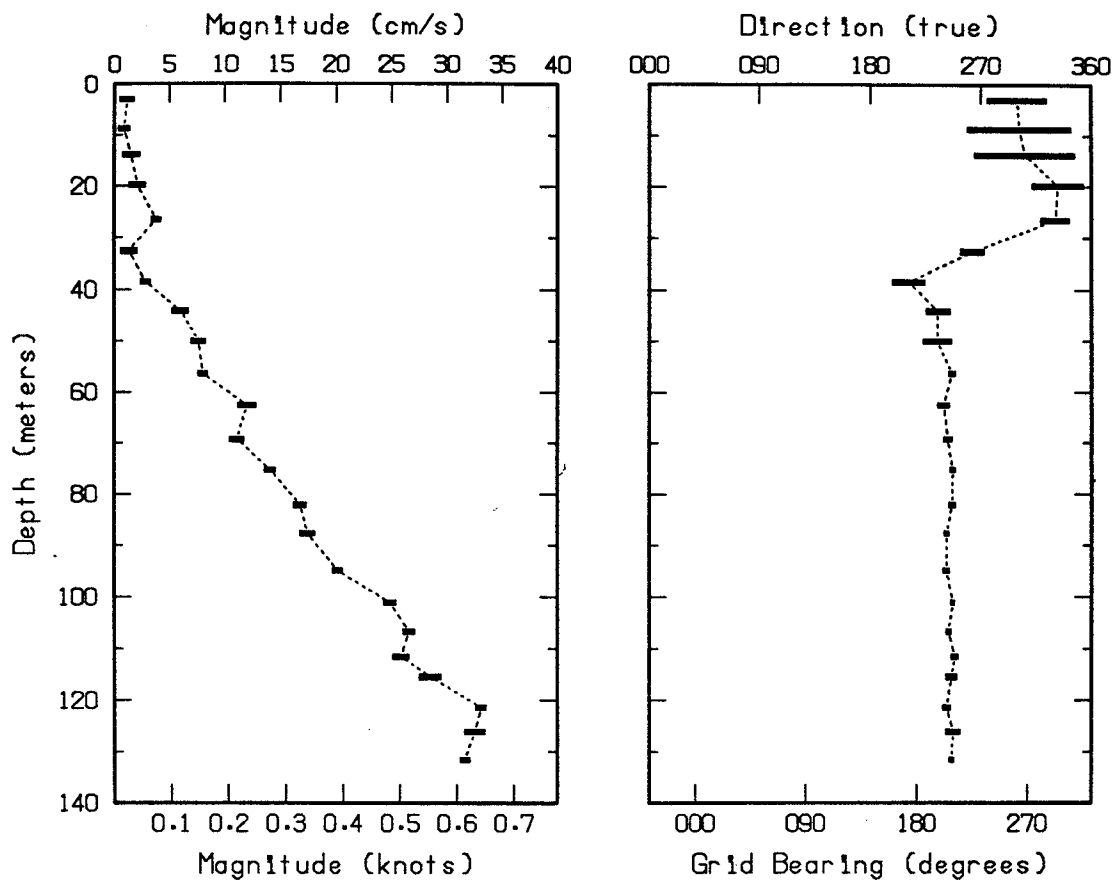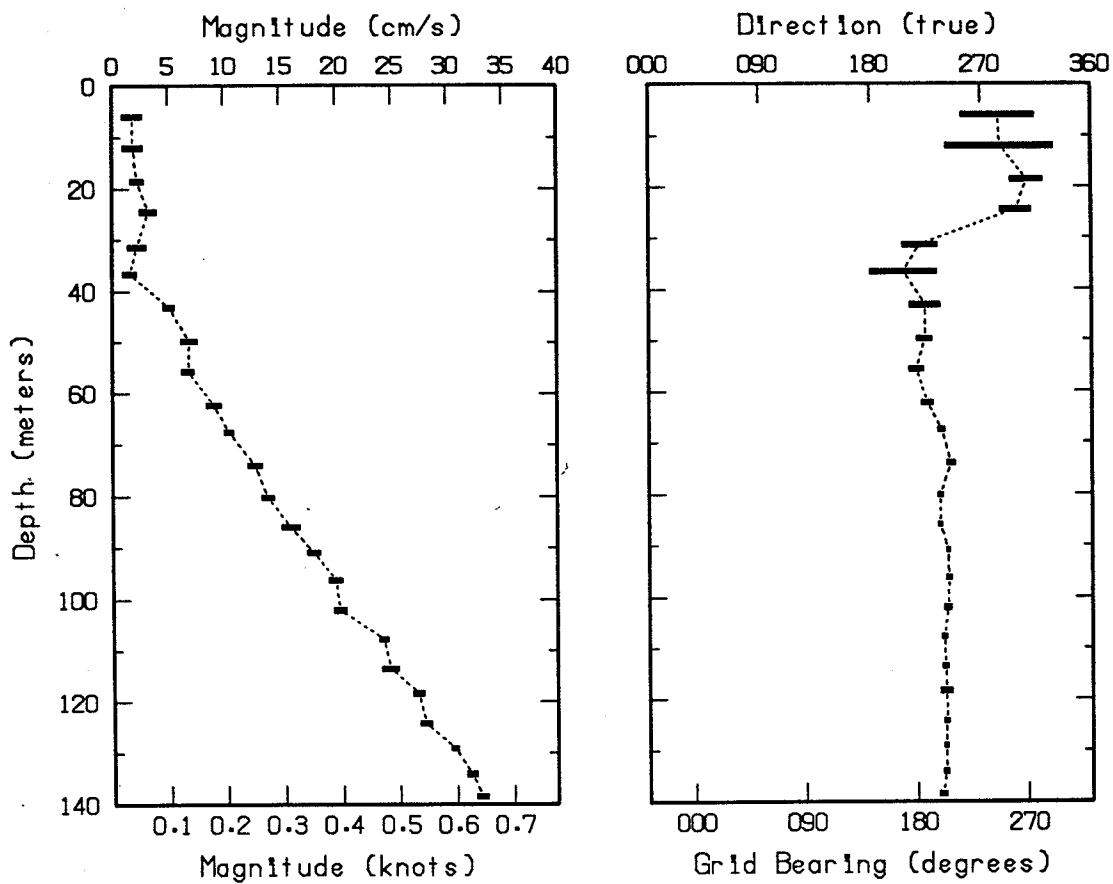
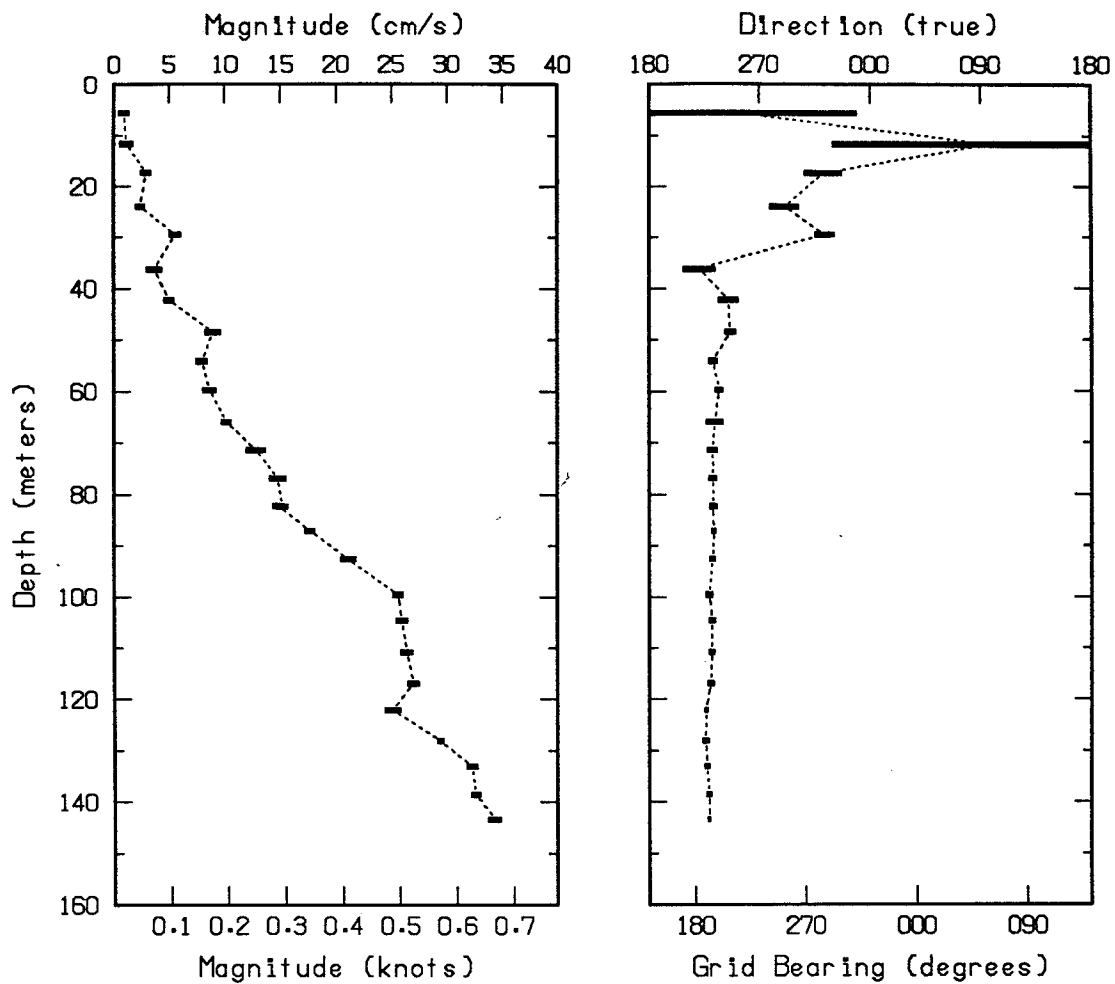Magnitude (knots)

Grid Bearing (degrees)

Magnetic bearing + 34.3 degrees = True bearing
True bearing of +Y axis = 37.6 degrees

Magnetic bearing + 34.3 degrees = True bearing
True bearing of +Y axis = 37.6 degrees

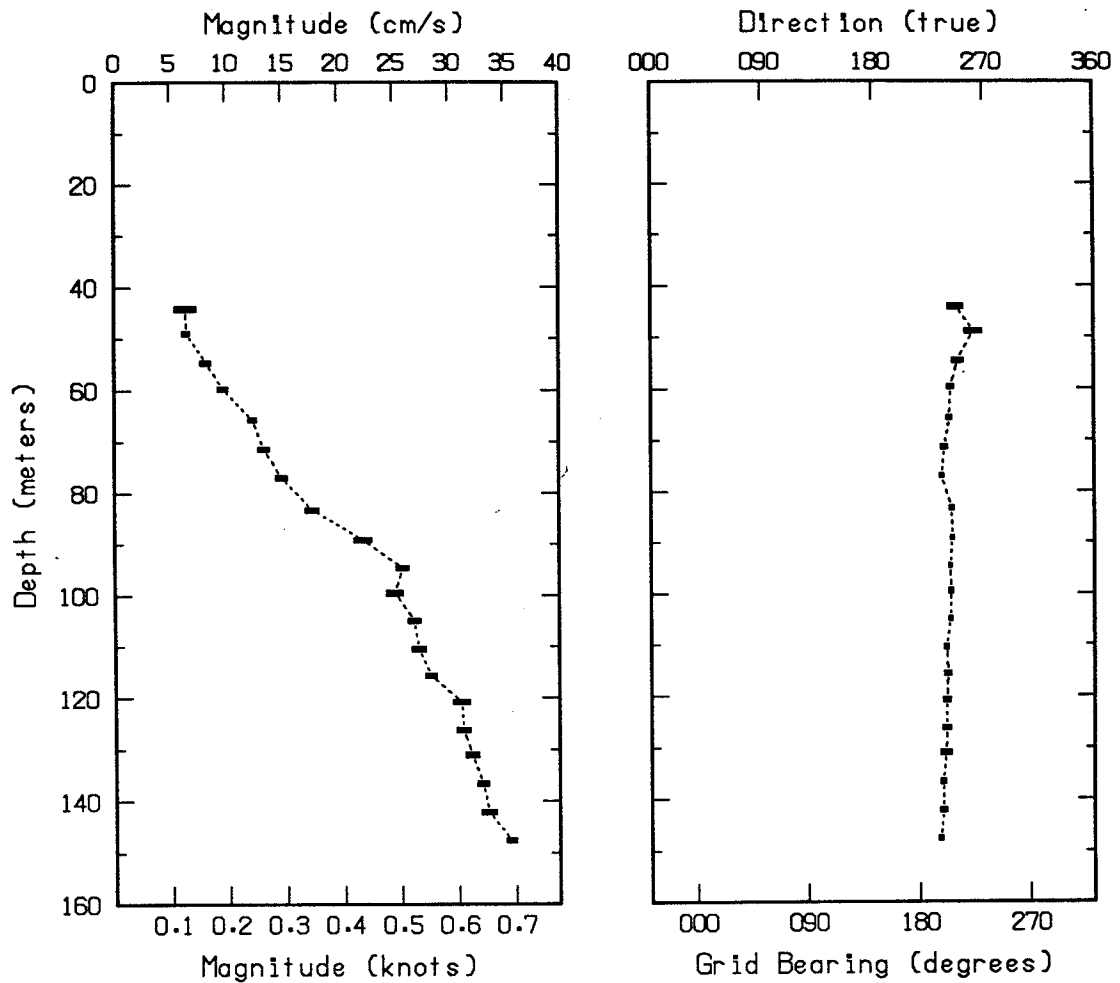Magnetic bearing + 34.3 degrees = True bearing
True bearing of +Y axis = 37.6 degrees

04-03-91 1106   CAST #05

Magnetic bearing + 34.3 degrees = True bearing
True bearing of +Y axis = 37.6 degrees

04-03-91 1458   CAST #06

Magnitude (cm/s)

Direction (true)

Magnitude (knots)

Grid Bearing (degrees)

Magnetic bearing + 34.3 degrees = True bearing
True bearing of +Y axis = 37.6 degrees

04-03-91 2053   CAST #07

Magnetic bearing + 34.3 degrees = True bearing
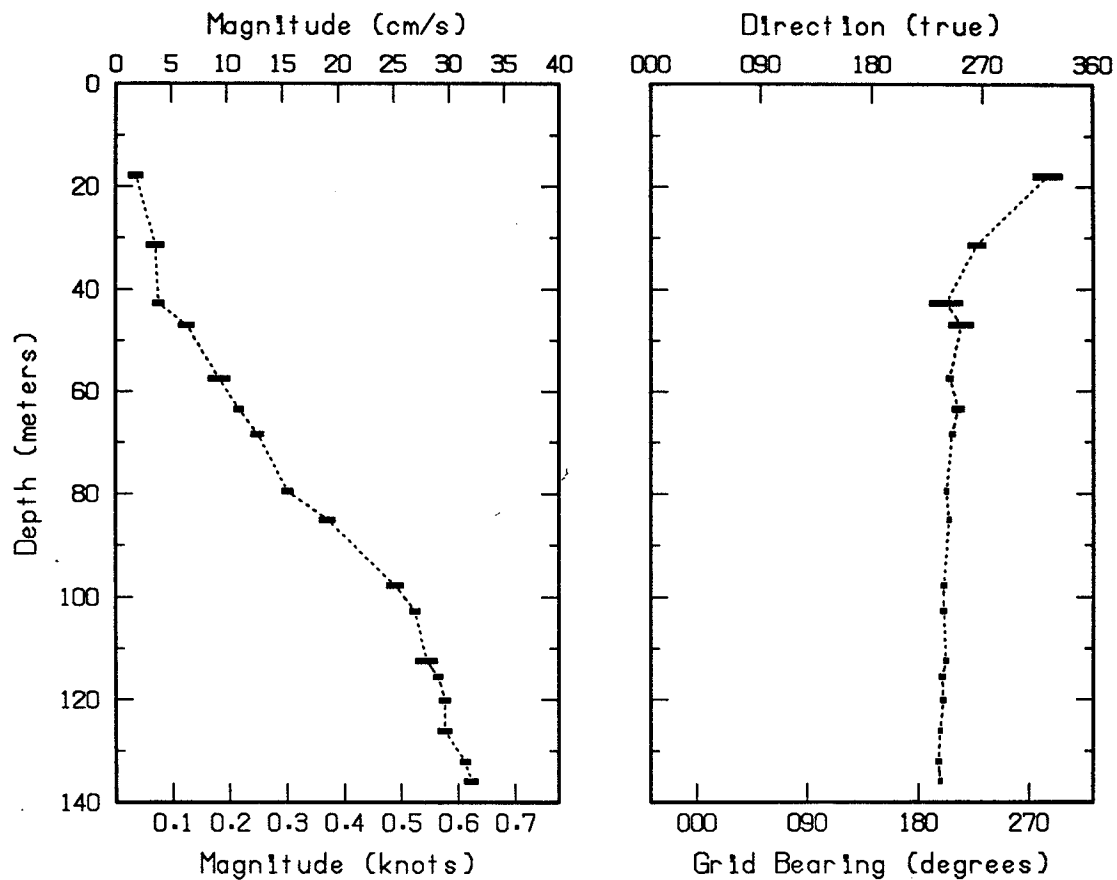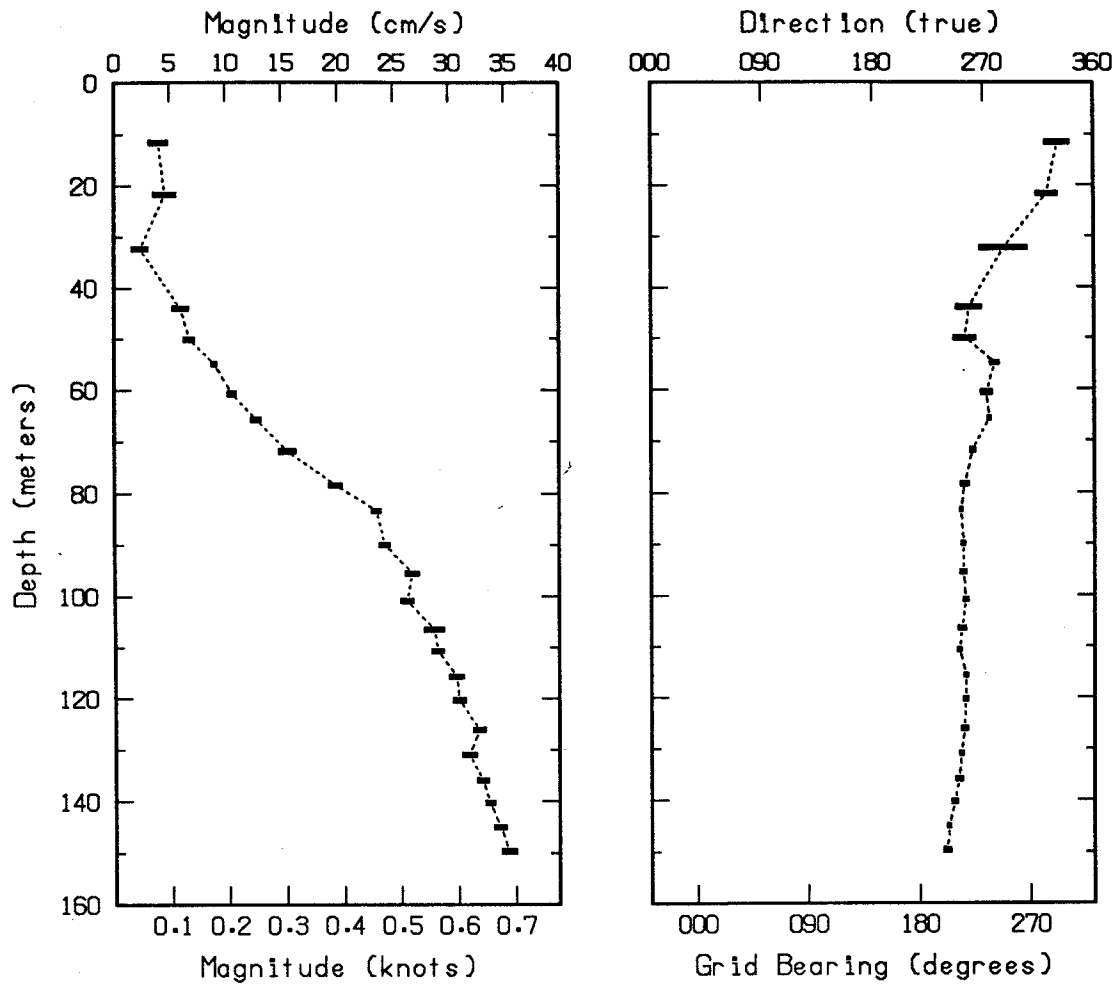True bearing of +Y axis = 37.6 degrees

04-04-91 0638   CAST #08

Magnetic bearing + 34.3 degrees = True bearing
True bearing of +Y axis = 37.6 degrees

04-04-91 1536   CAST #09

Magnitude (cm/s)

Direction (true)

Magnitude (knots)

Grid Bearing (degrees)

Depth (meters)

Magnetic bearing + 34.3 degrees = True bearing
True bearing of +Y axis = 37.6 degrees

04-04-91 1952   CAST #10
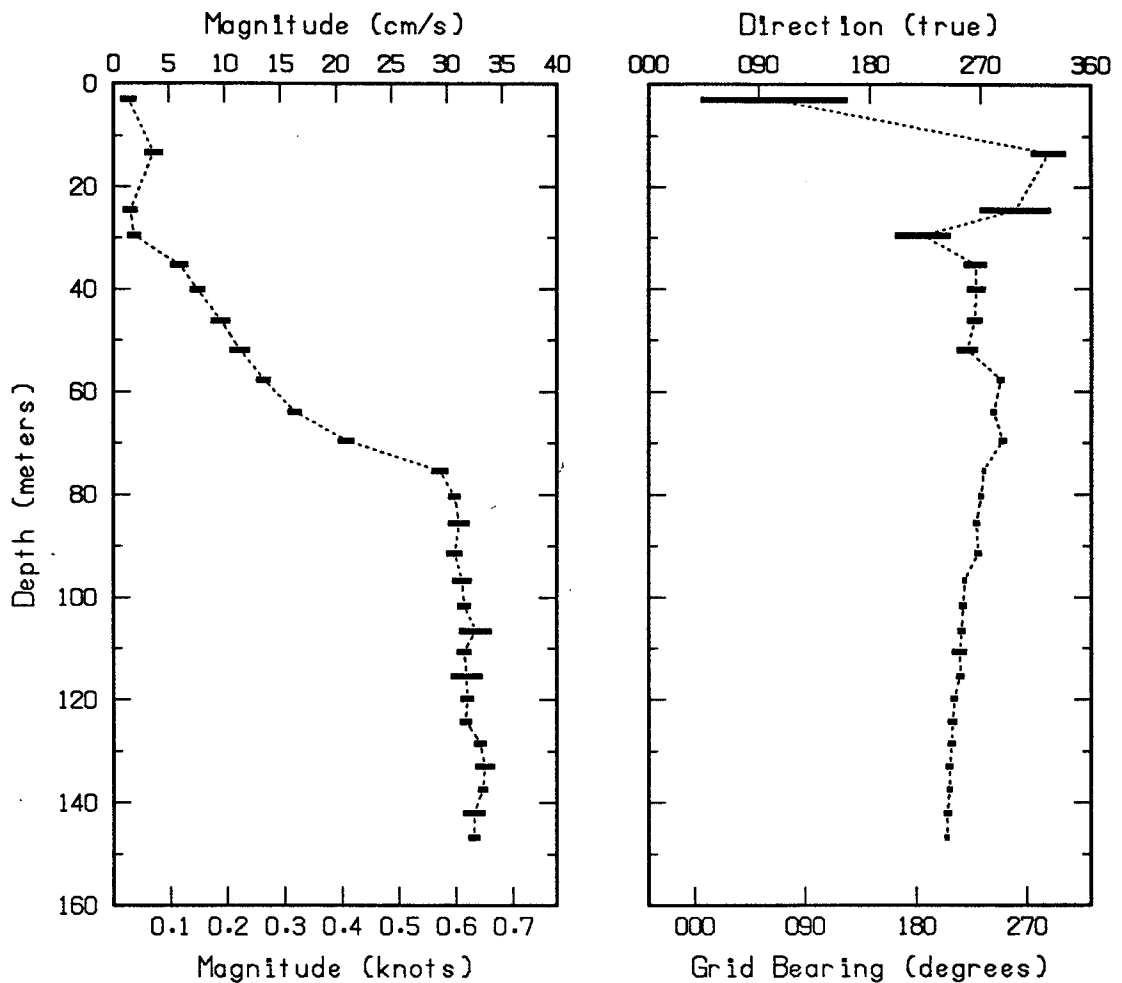
Magnetic bearing + 34.3 degrees = True bearing
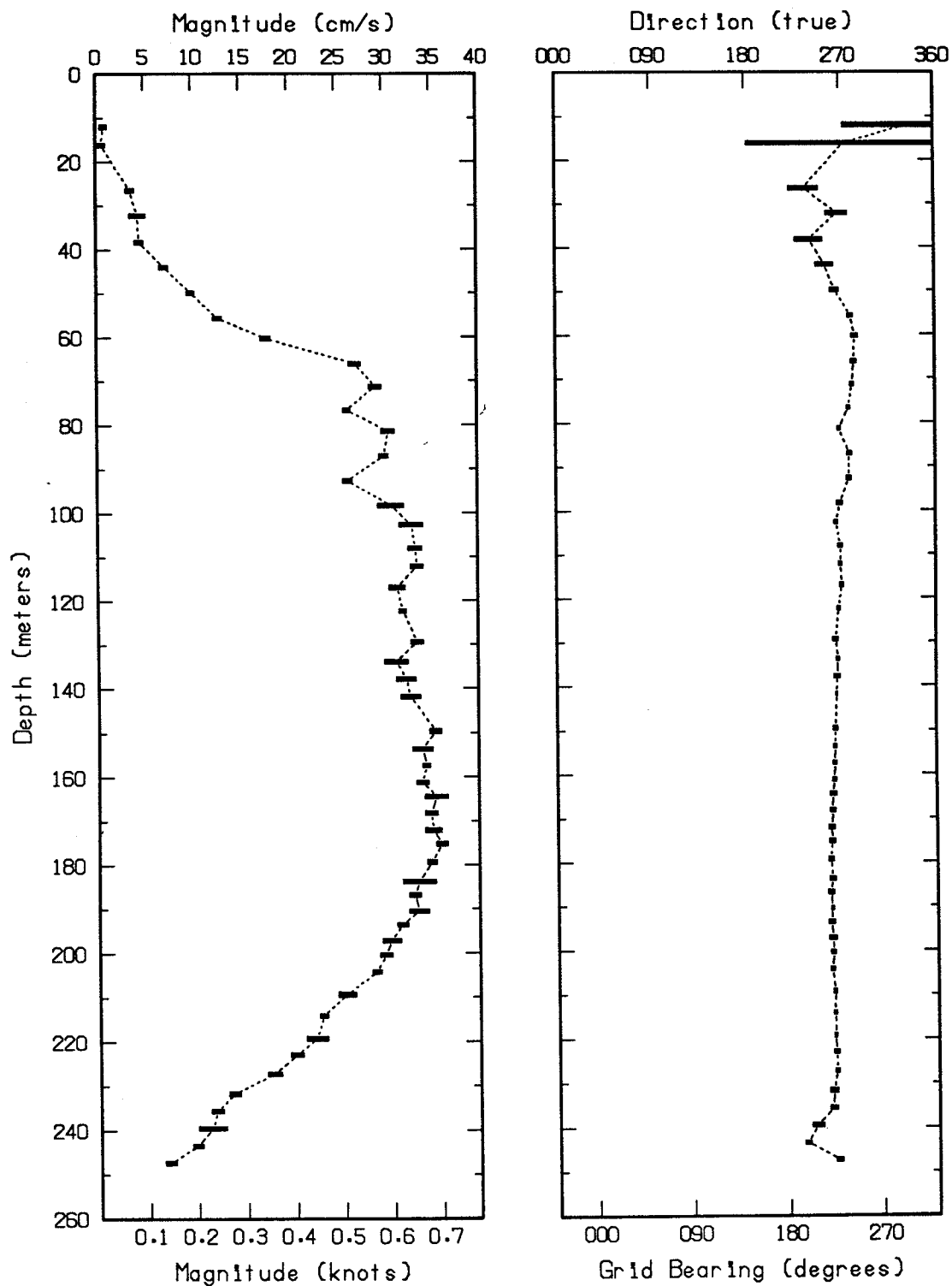True bearing of +Y axis = 37.6 degrees

04-05-91 0914   CAST #11

Magnetic bearing + 34.3 degrees = True bearing
True bearing of +Y axis = 37.6 degrees

04-05-91 1100   CAST #12

Magnitude (cm/s)

Direction (true)
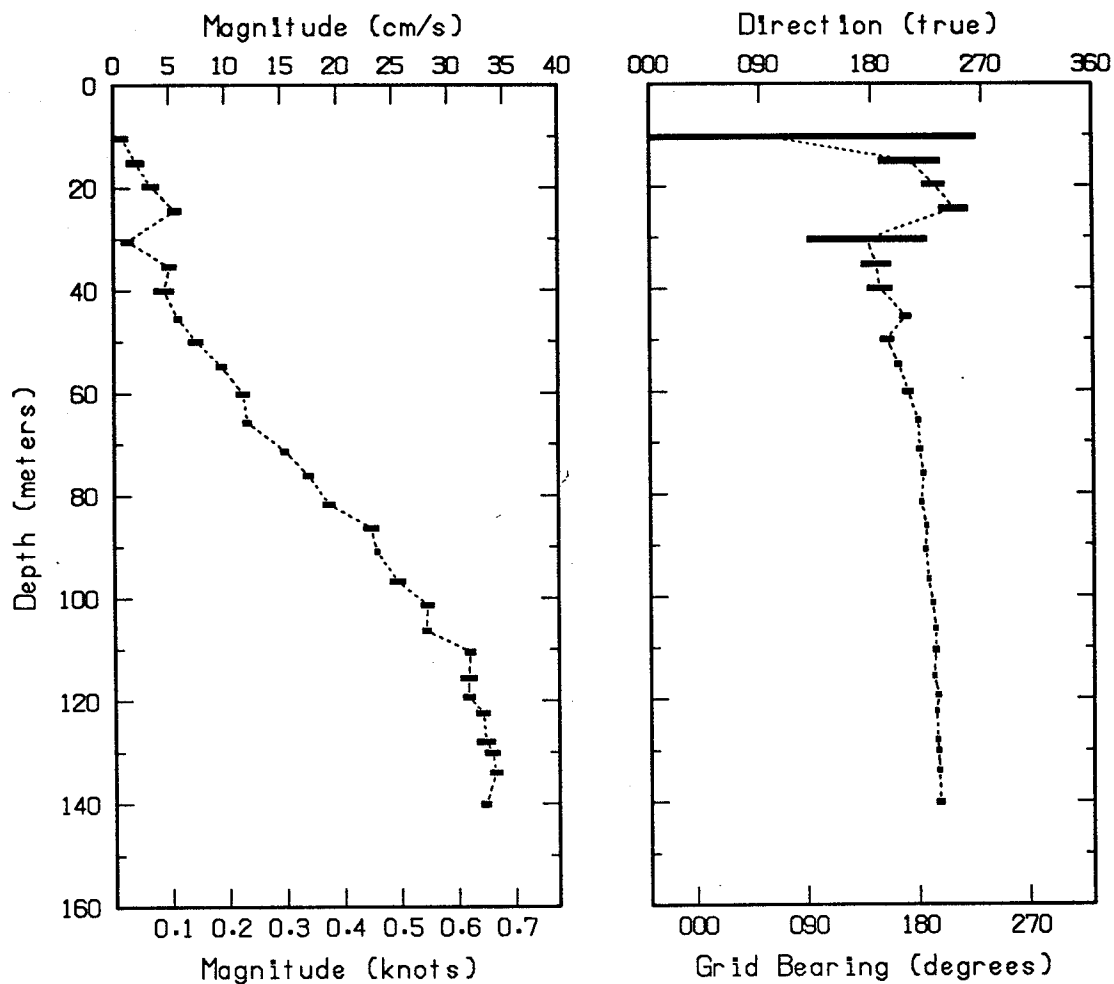
Magnetic bearing + 34.3 degrees = True bearing
True bearing of +Y axis = 37.6 degrees

04-05-91 2155   CAST #13

Magnetic bearing + 34.3 degrees = True bearing
True bearing of +Y axis = 37.6 degrees

04-06-91 0638   CAST #14

Magnetic bearing + 34.3 degrees = True bearing
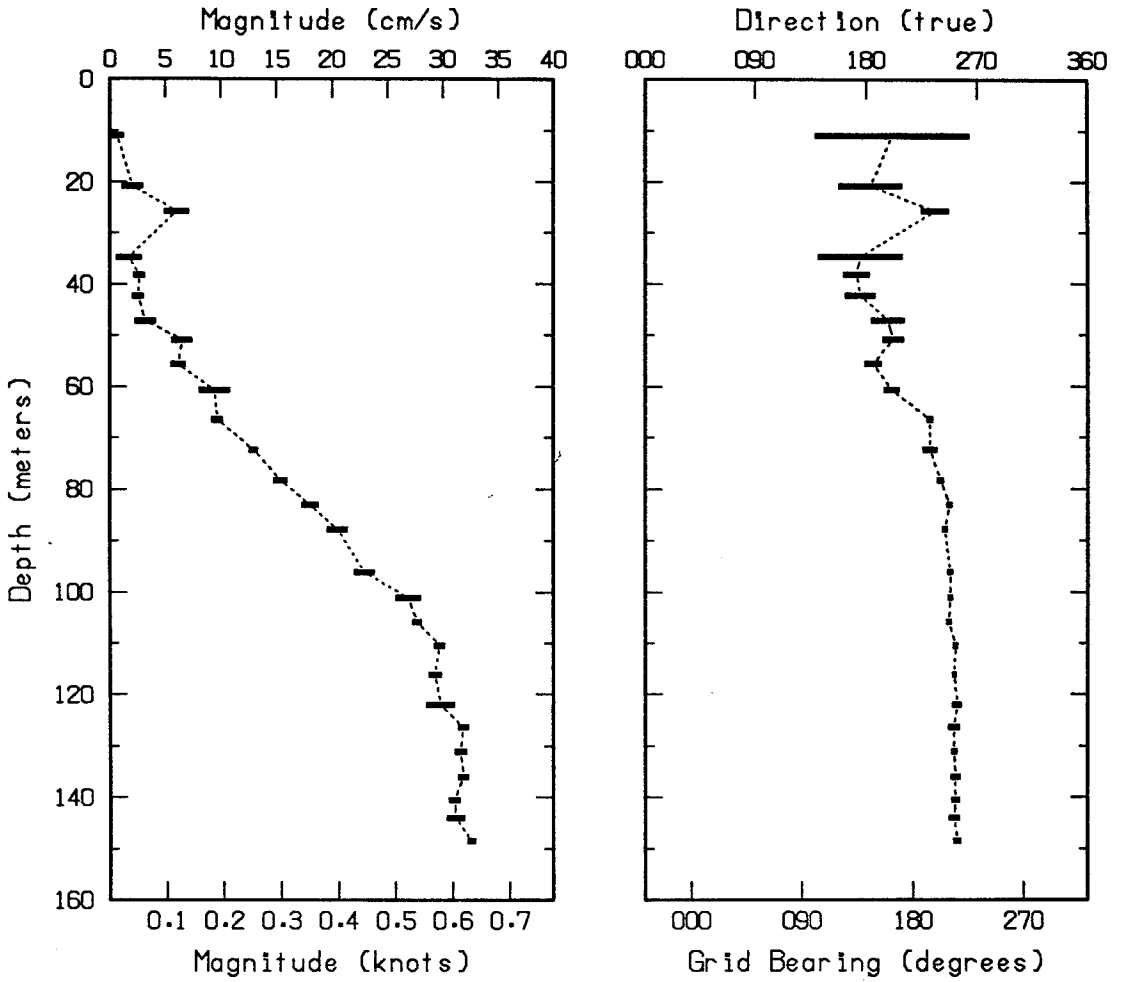True bearing of +Y axis = 37.6 degrees

04-06-91 1118   CAST #15

Magnetic bearing + 34.3 degrees = True bearing
True bearing of +Y axis = 37.6 degrees

04-06-91 2250   CAST #16
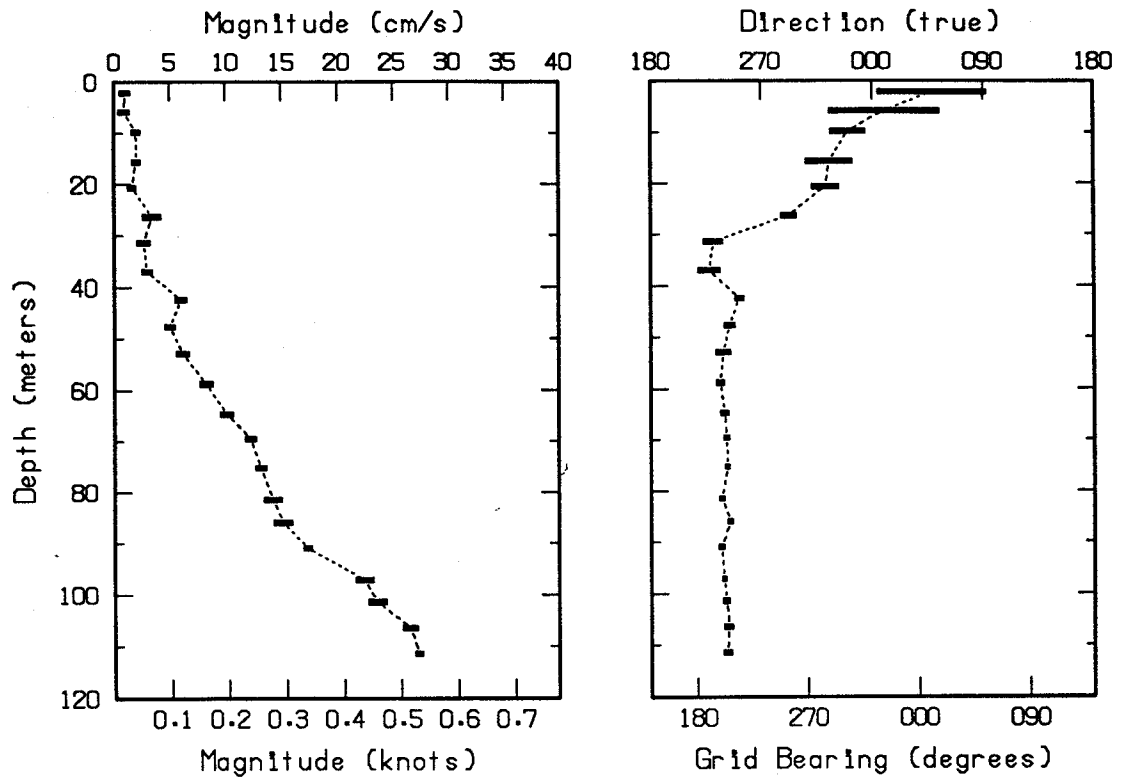
Magnetic bearing + 34.3 degrees = True bearing
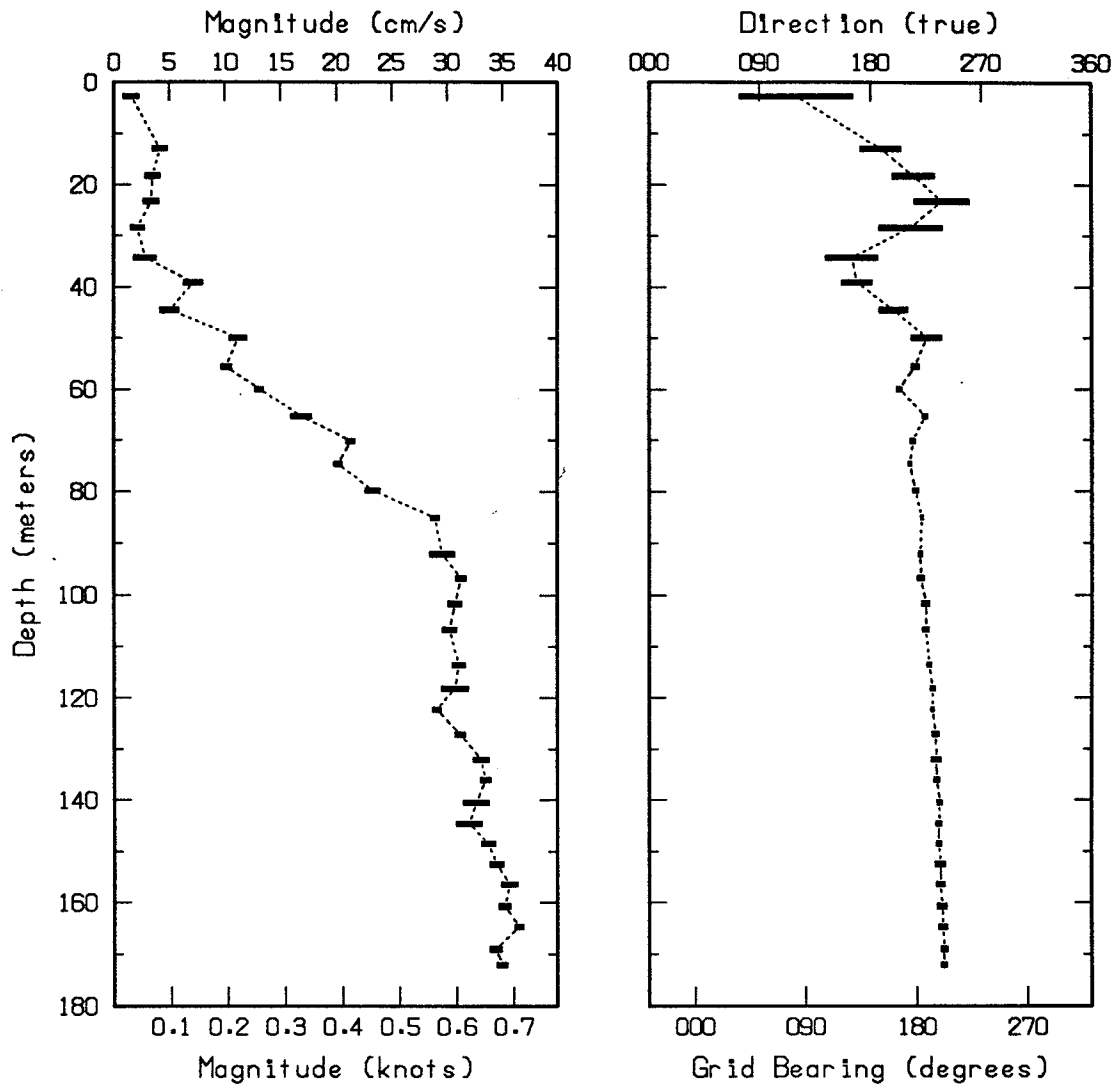True bearing of +Y axis = 37.6 degrees

04-07-91 0749   CAST #17
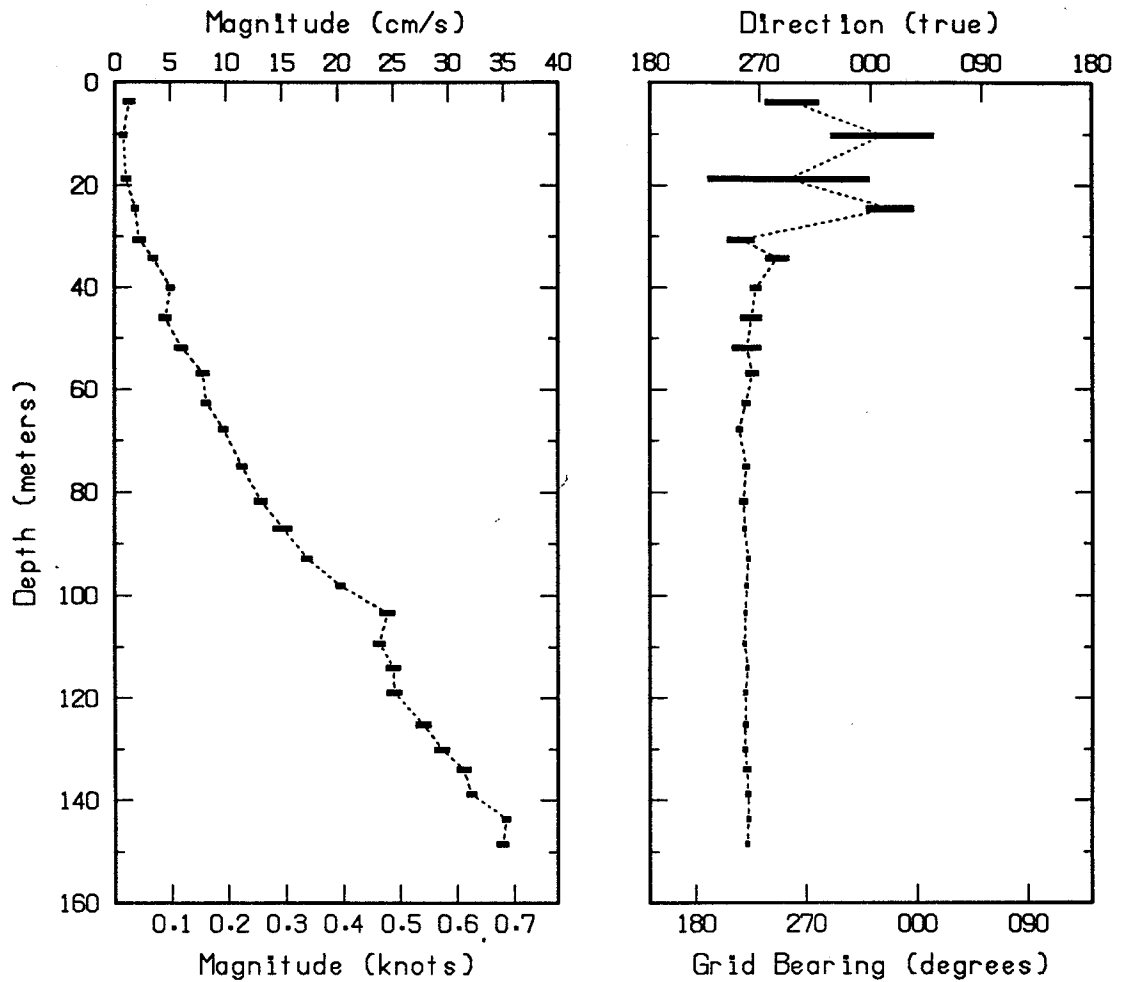
Magnetic bearing + 34.3 degrees = True bearing
True bearing of +Y axis = 37.6 degrees

04-07-91 1412   CAST #18
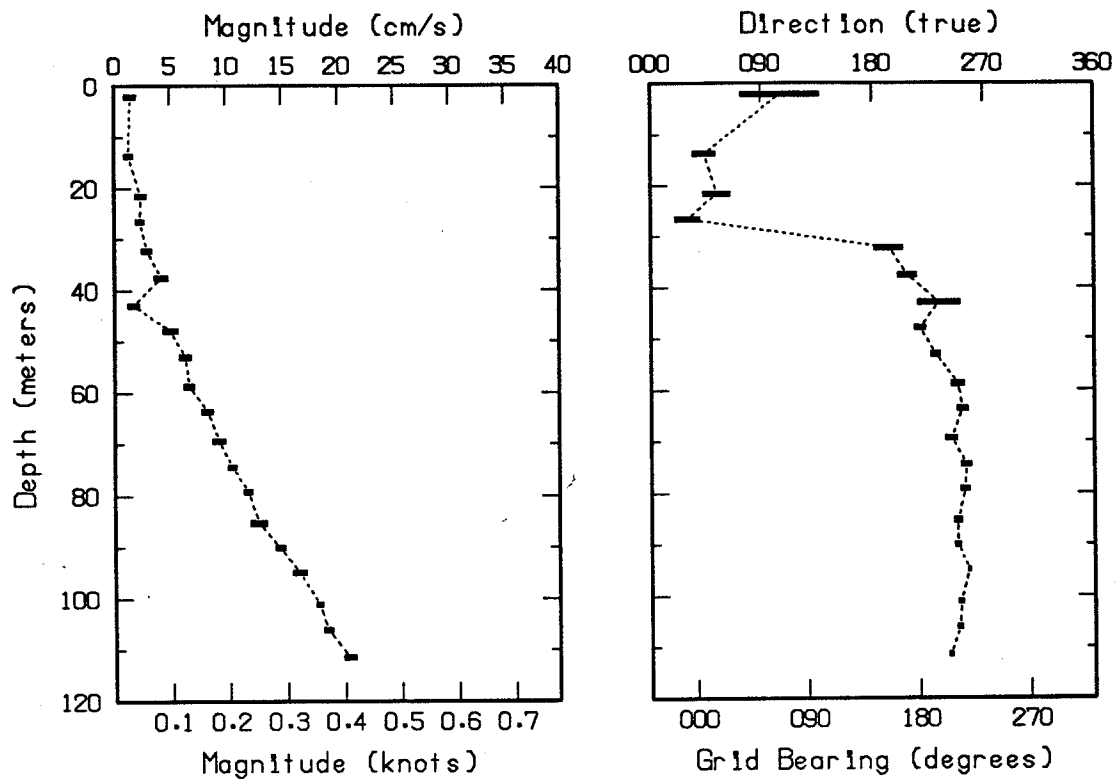
Magnetic bearing + 34.3 degrees = True bearing
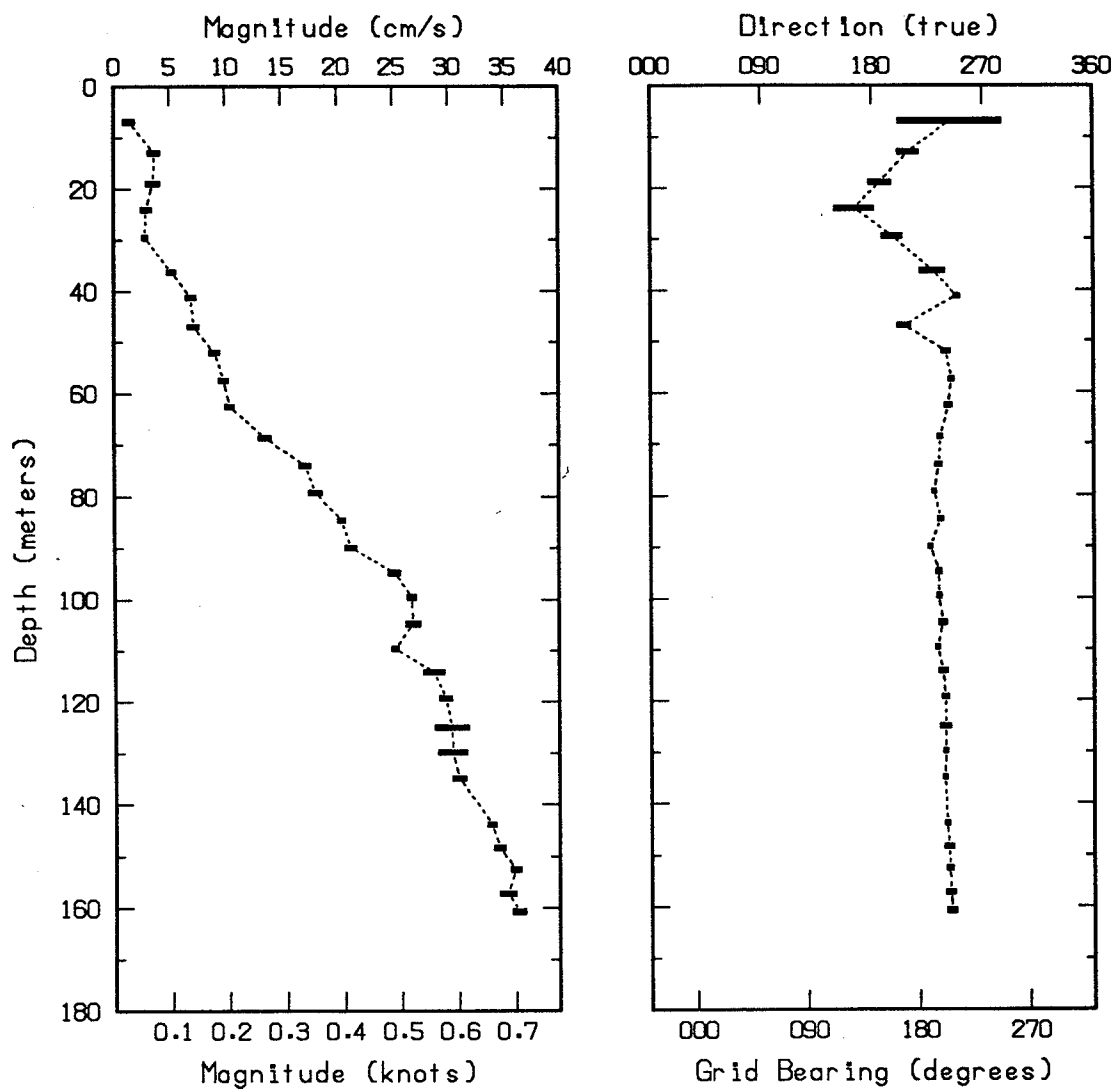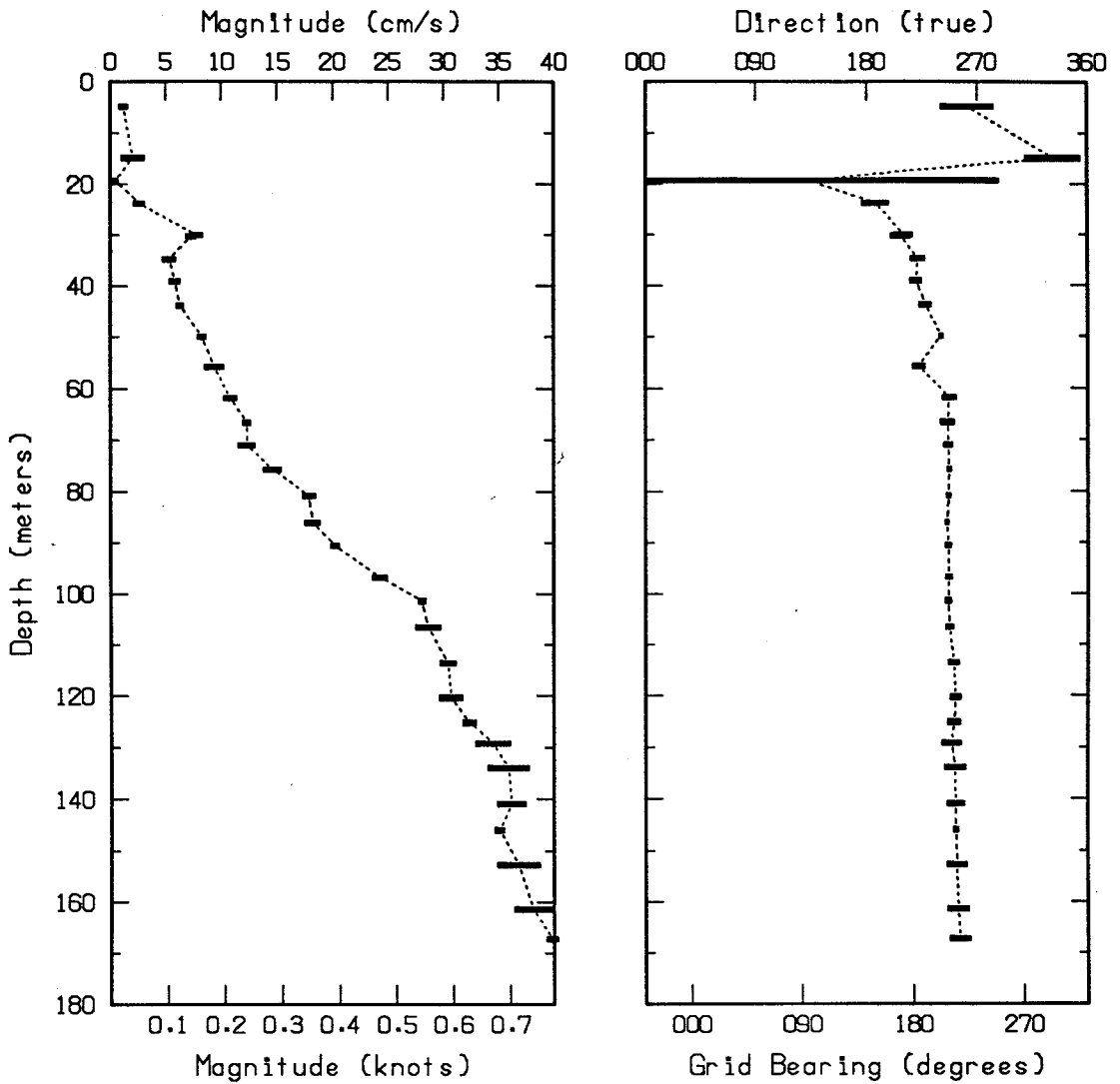True bearing of +Y axis = 37.6 degrees

04-08-91 0959   CAST #19
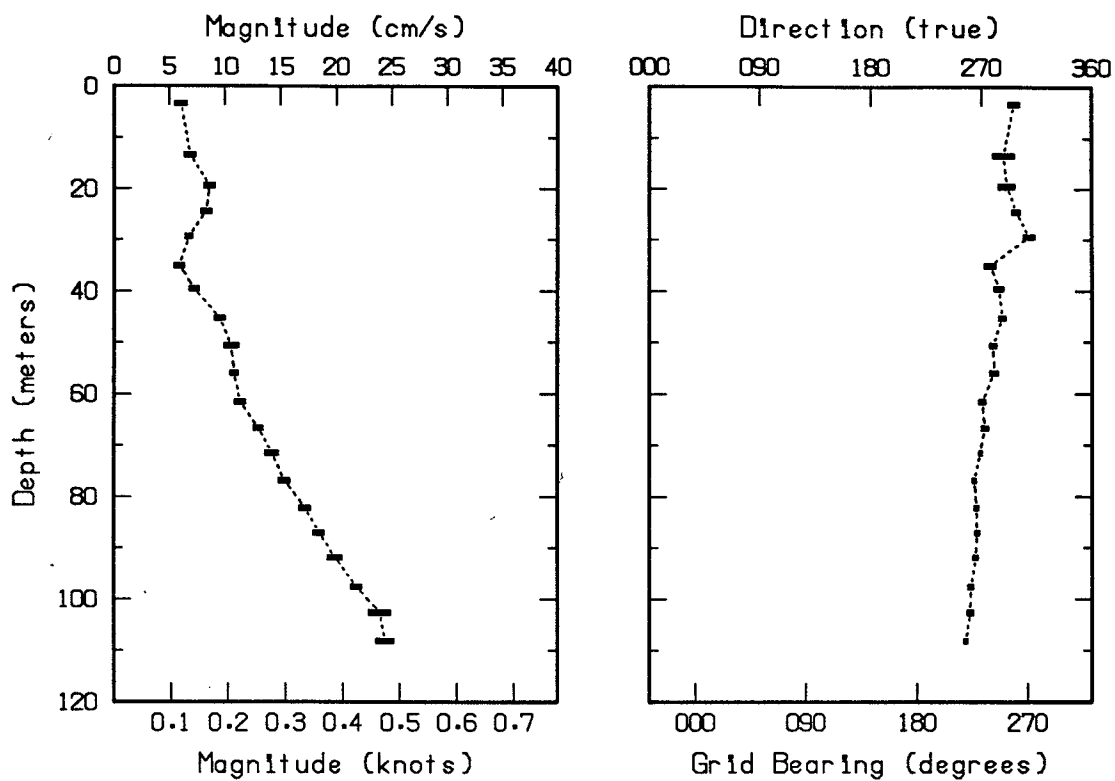
Magnet!c bear!ng + 34.3 degrees = True bear!ng
True bear!ng of +Y ax!s = 37.6 degrees

APPENDIX C

Time Series Plots of Parameters Measured by S4 Current Meters

Plot Identifier:

    letters
       f = fixed-depth array
       v = variable-depth array

    digits
       last two digits of respective S4 serial number and the run number

f191

Elapsed time (*10 s)

Time of day (mmddhhZ)

f192

-94-

f201

-95-

f202

Depth (m)

Temp (C)

S (o/oo)

Speed (cm/s)

Dir (deg)

Elapsed time (*10 s)

040700   040800

Time of day (mmddhhZ)

f251

-97-

f252

-98-

f261

-99-

f262

Elapsed time (*10 s)

040700   040800

Time of day (mmddhhZ)

-100-

v211

-101-

v212

-102-

v221

-103-

v222

Elapsed time (*10 s)

Time of day (mmddhhZ)

v231

-105-

v232

-106-

v241

-107-

v242

-108-
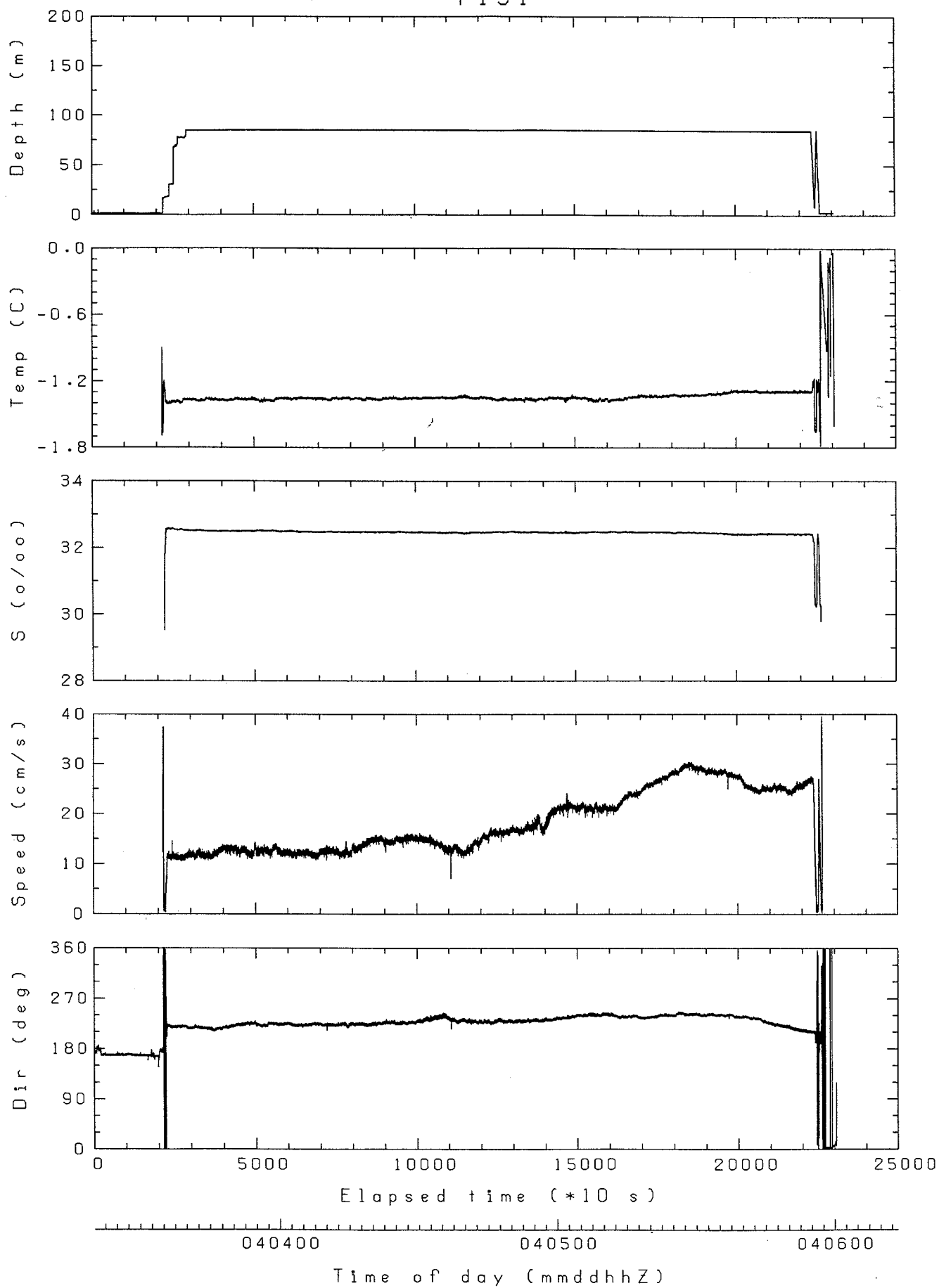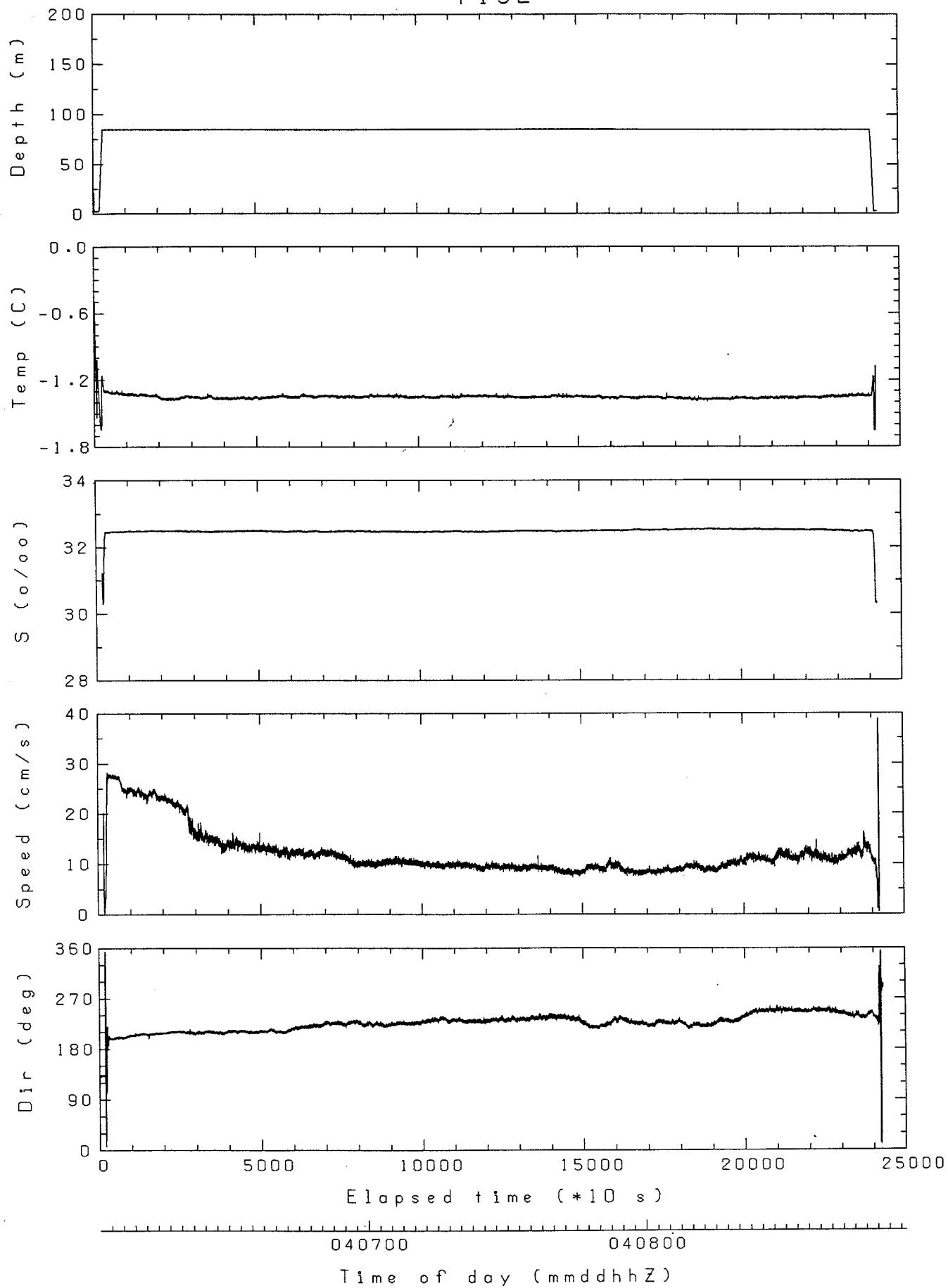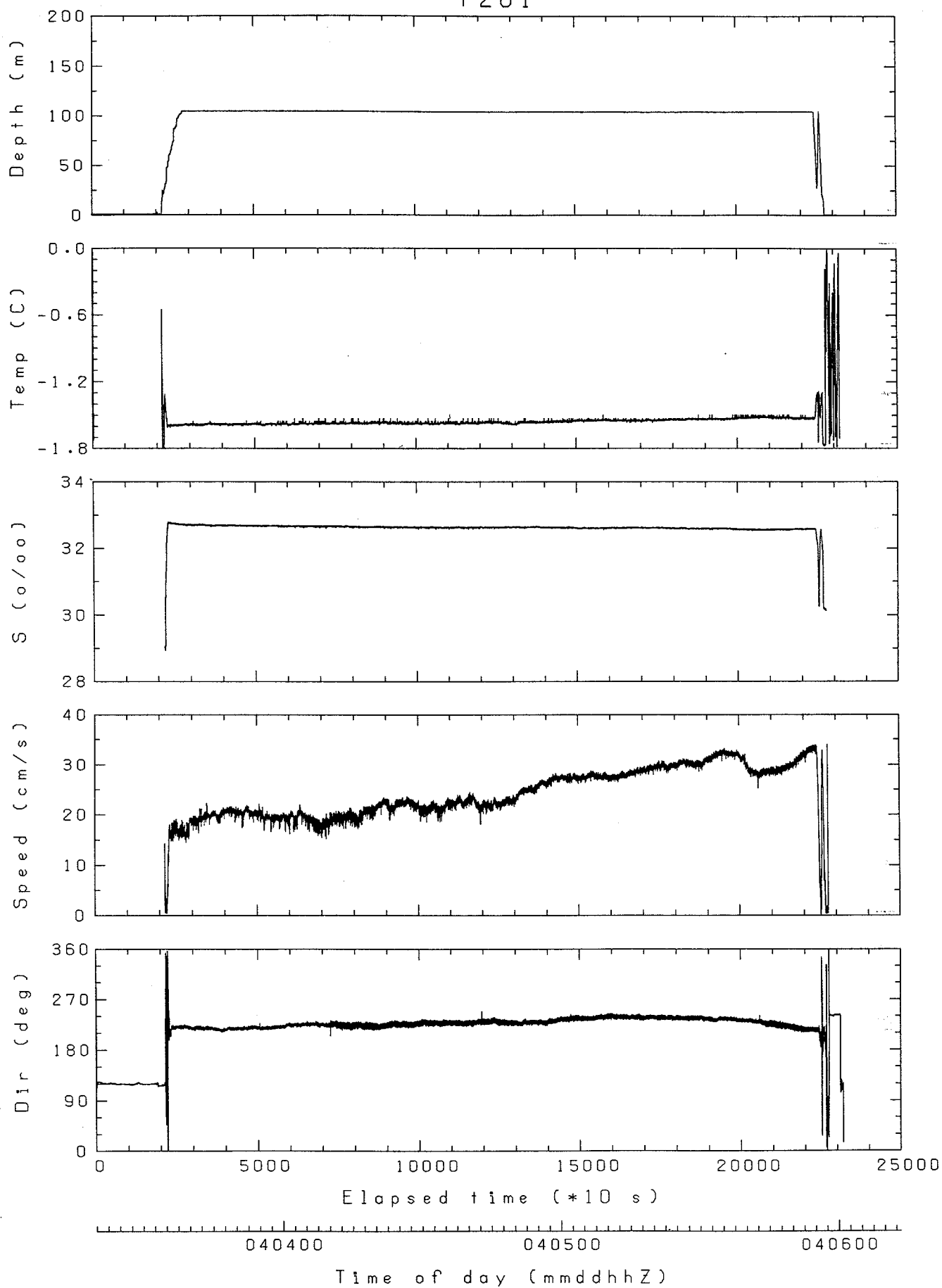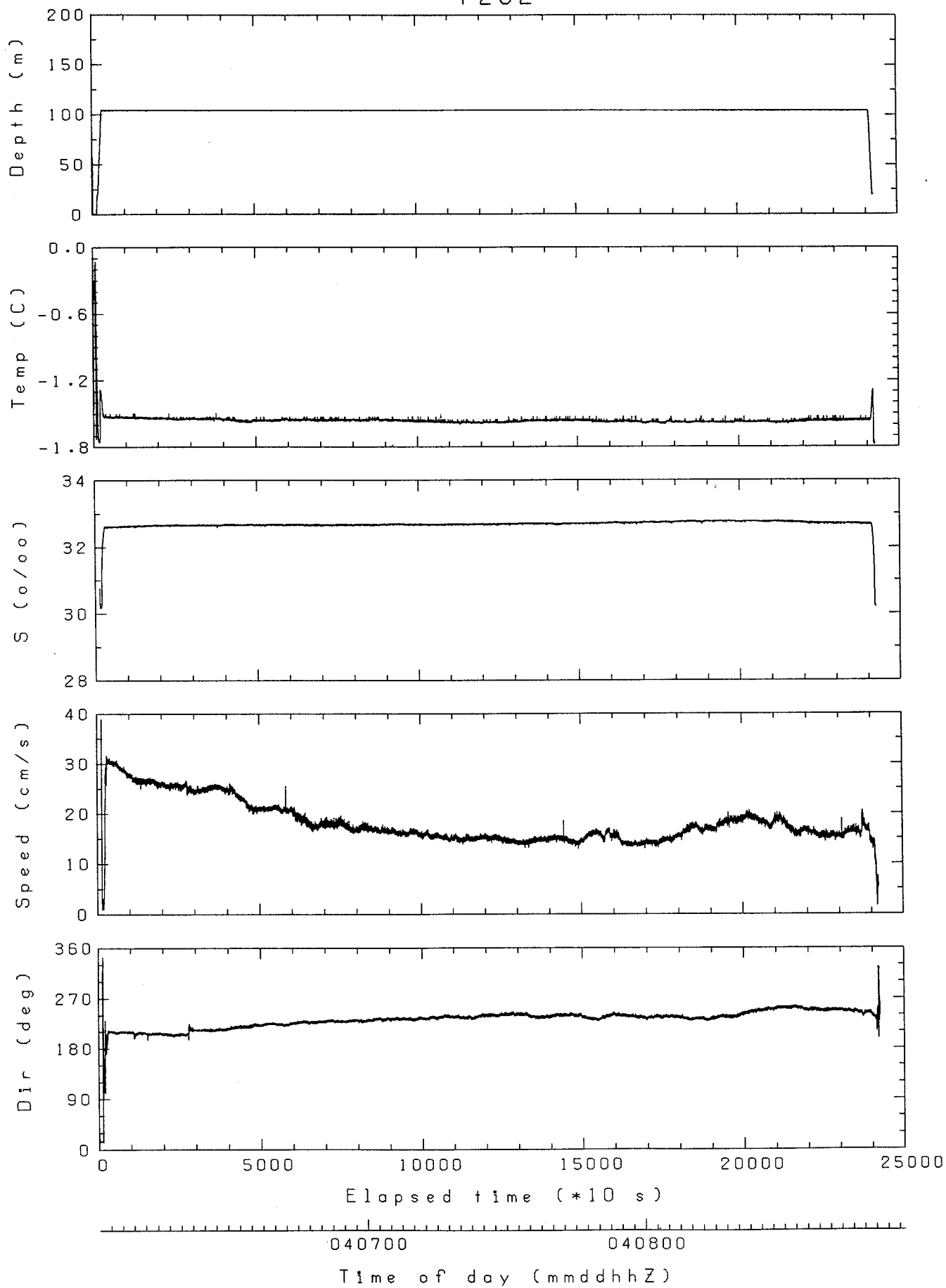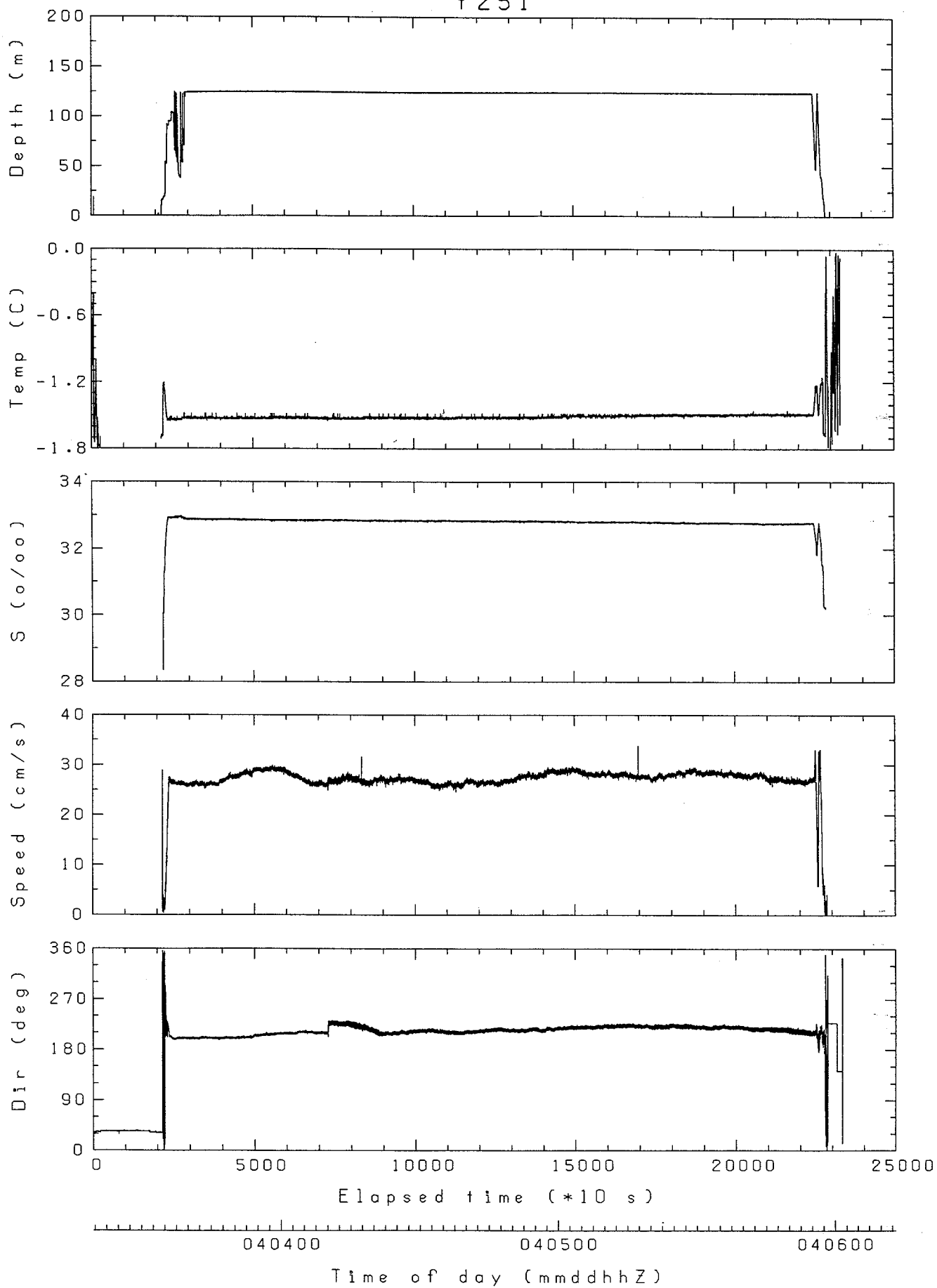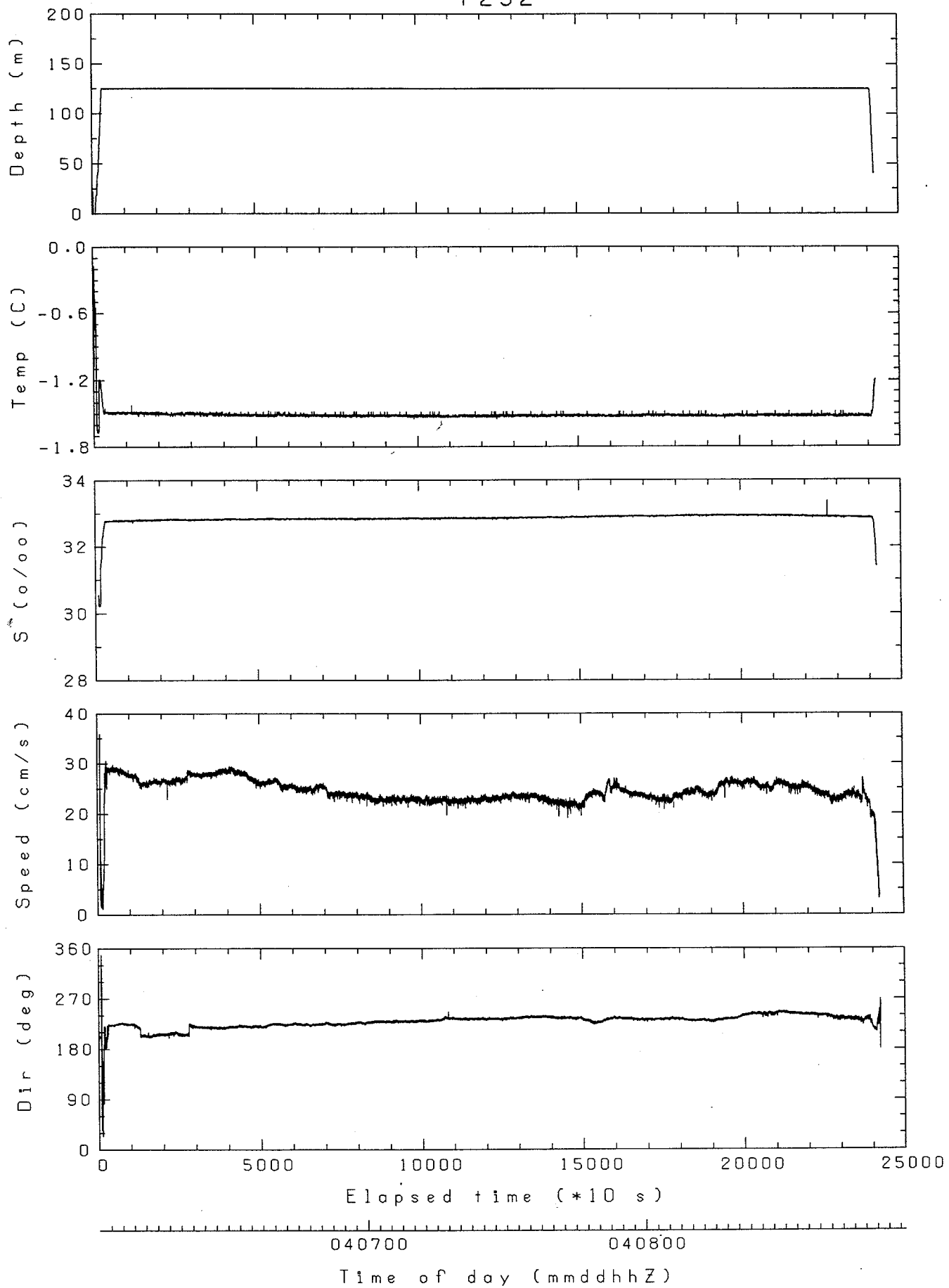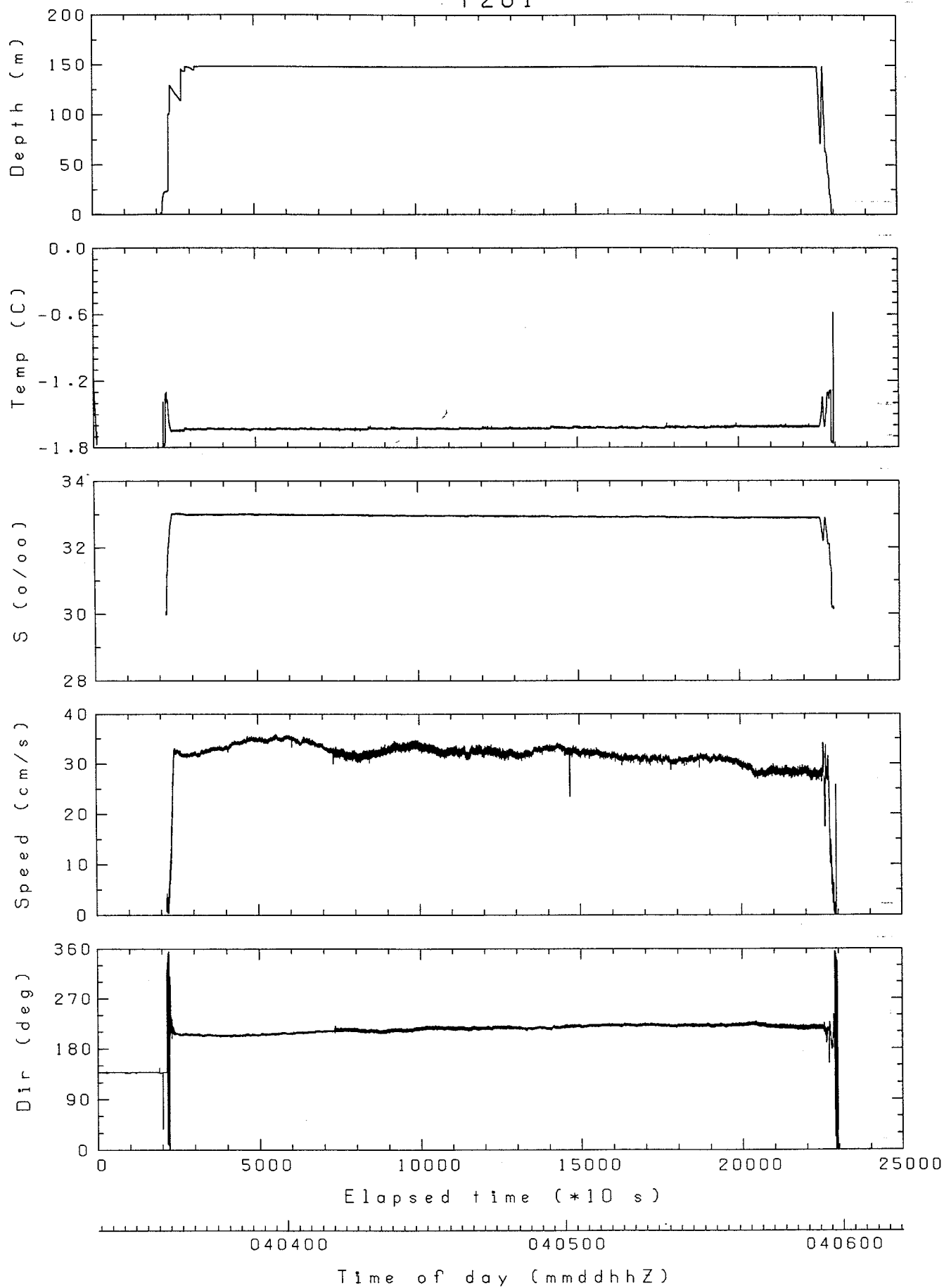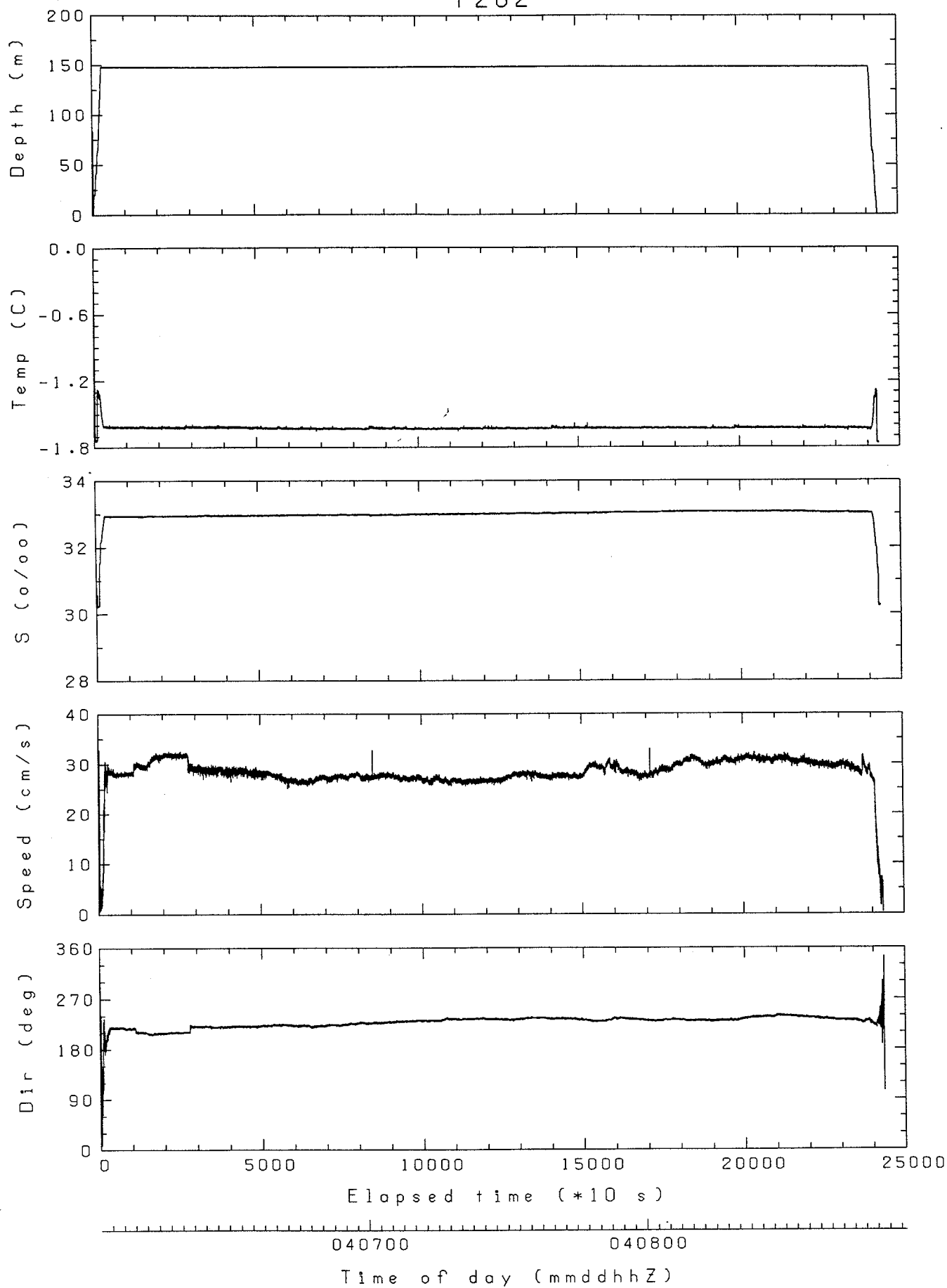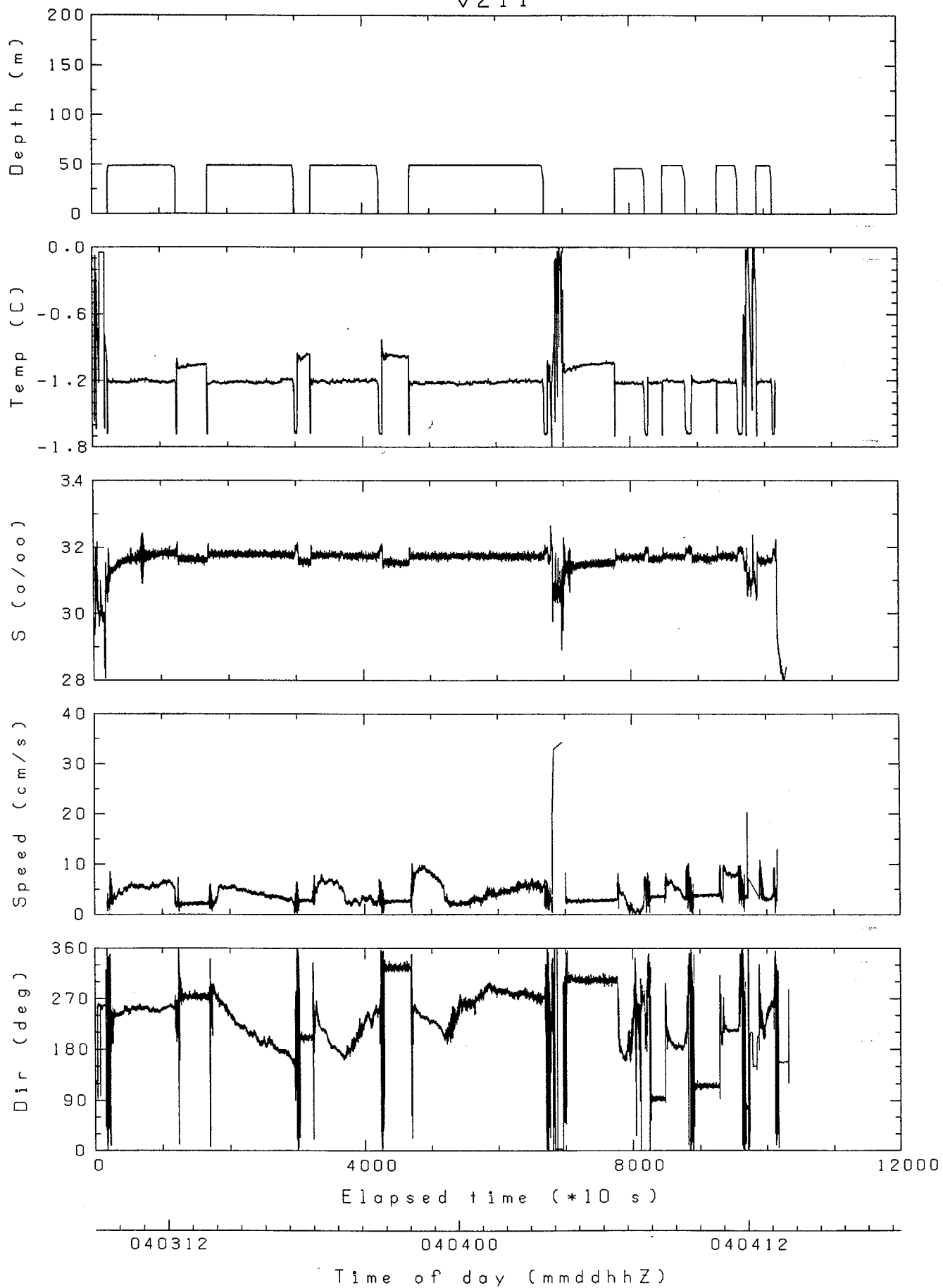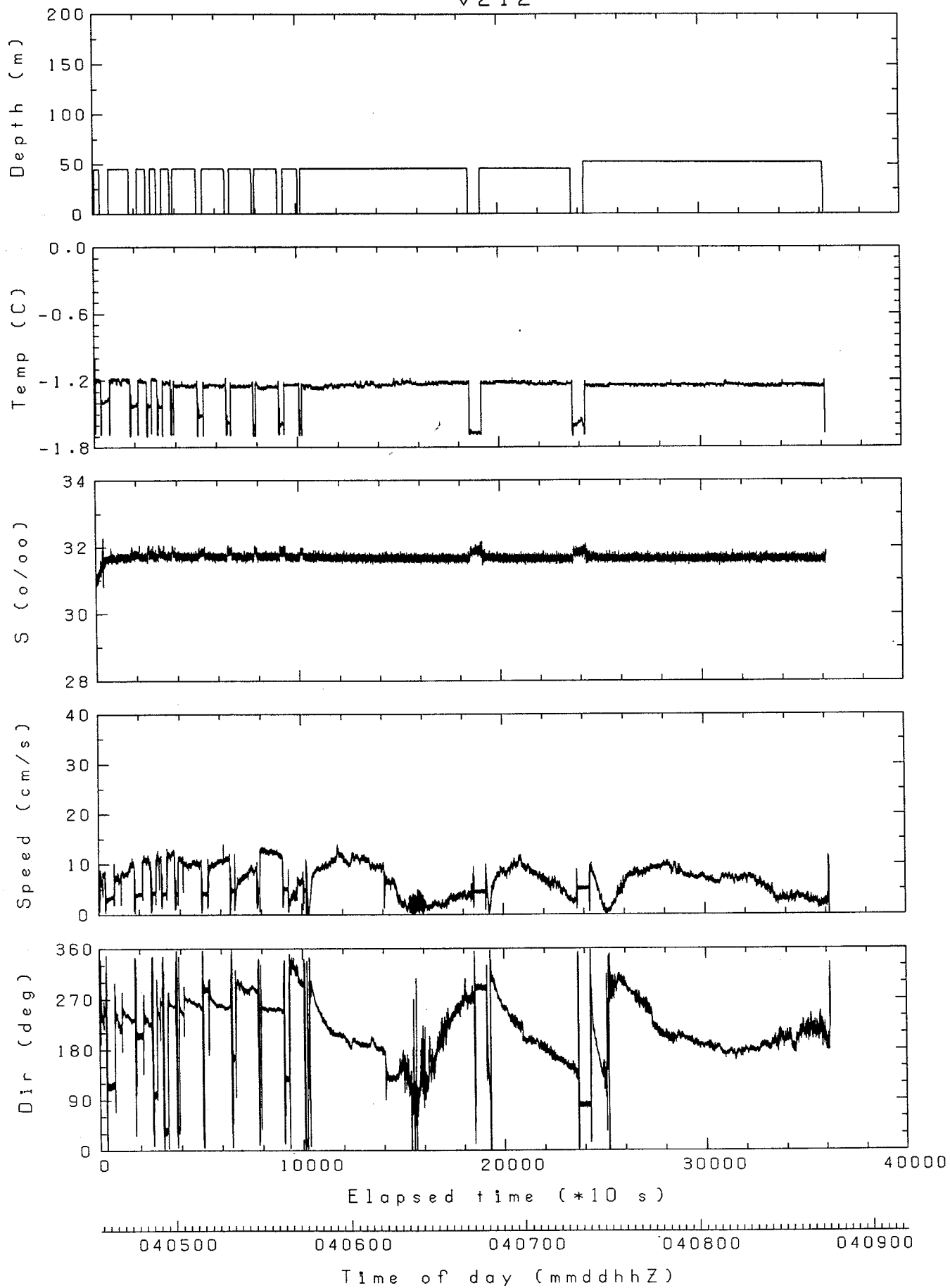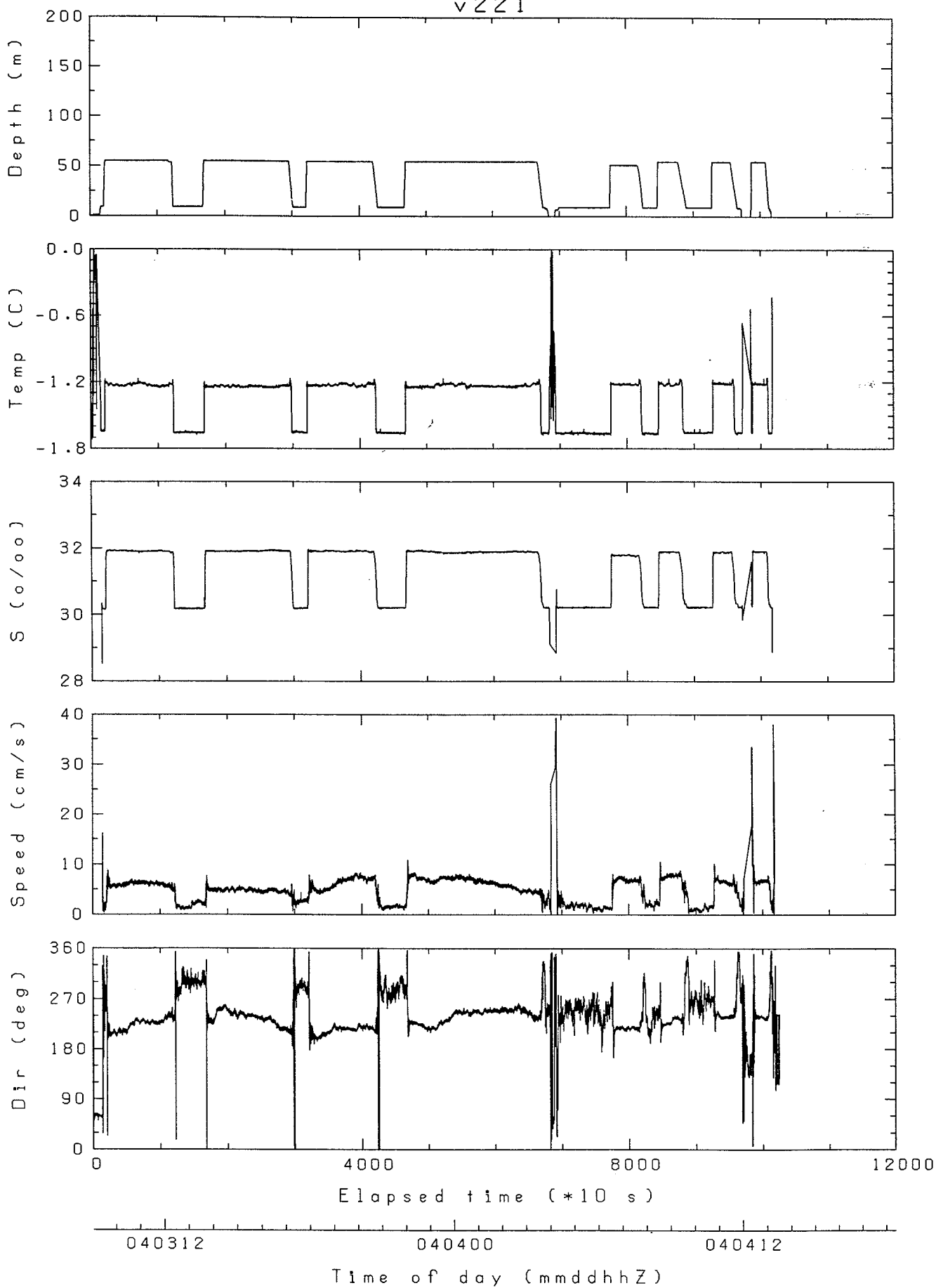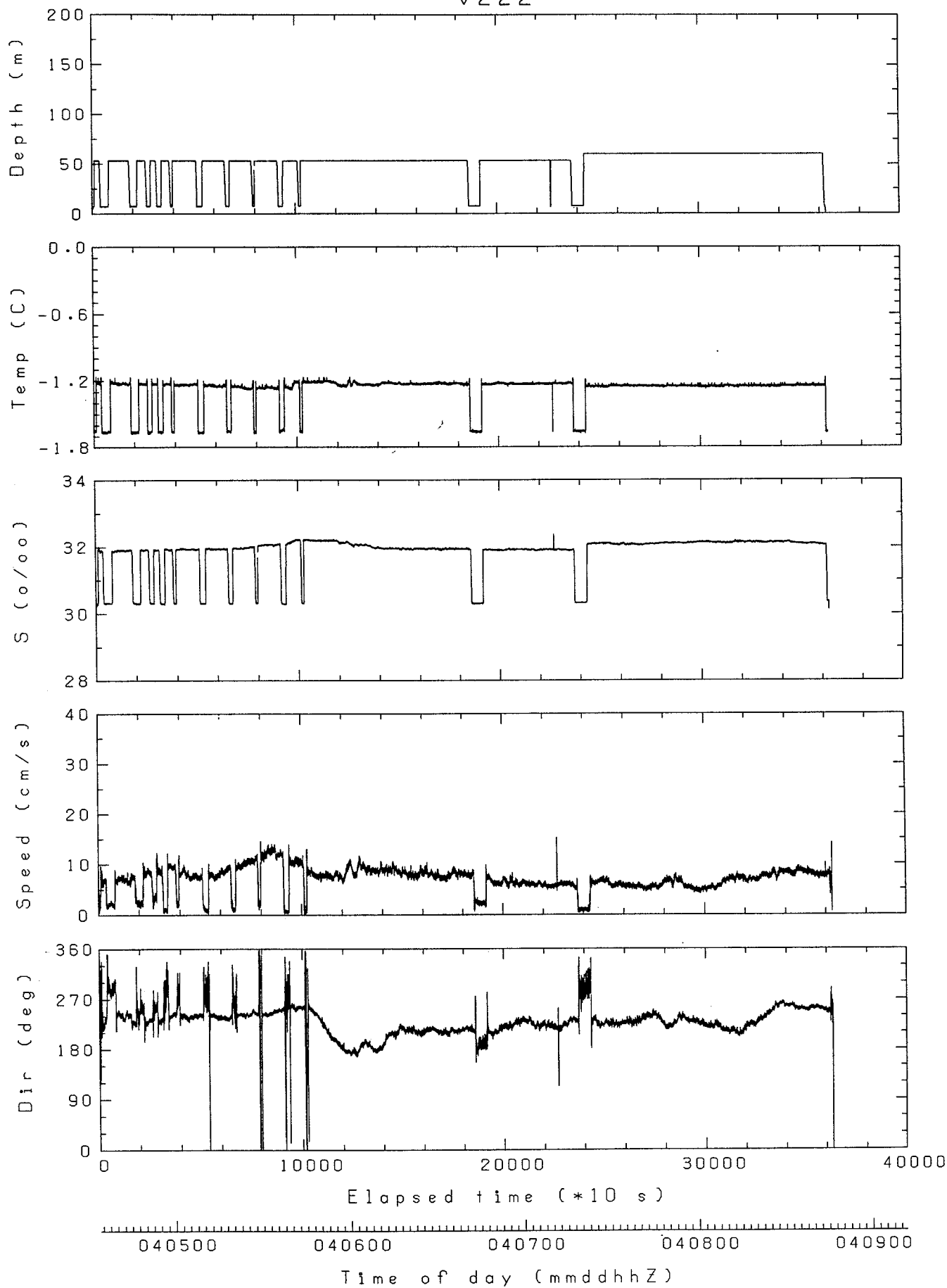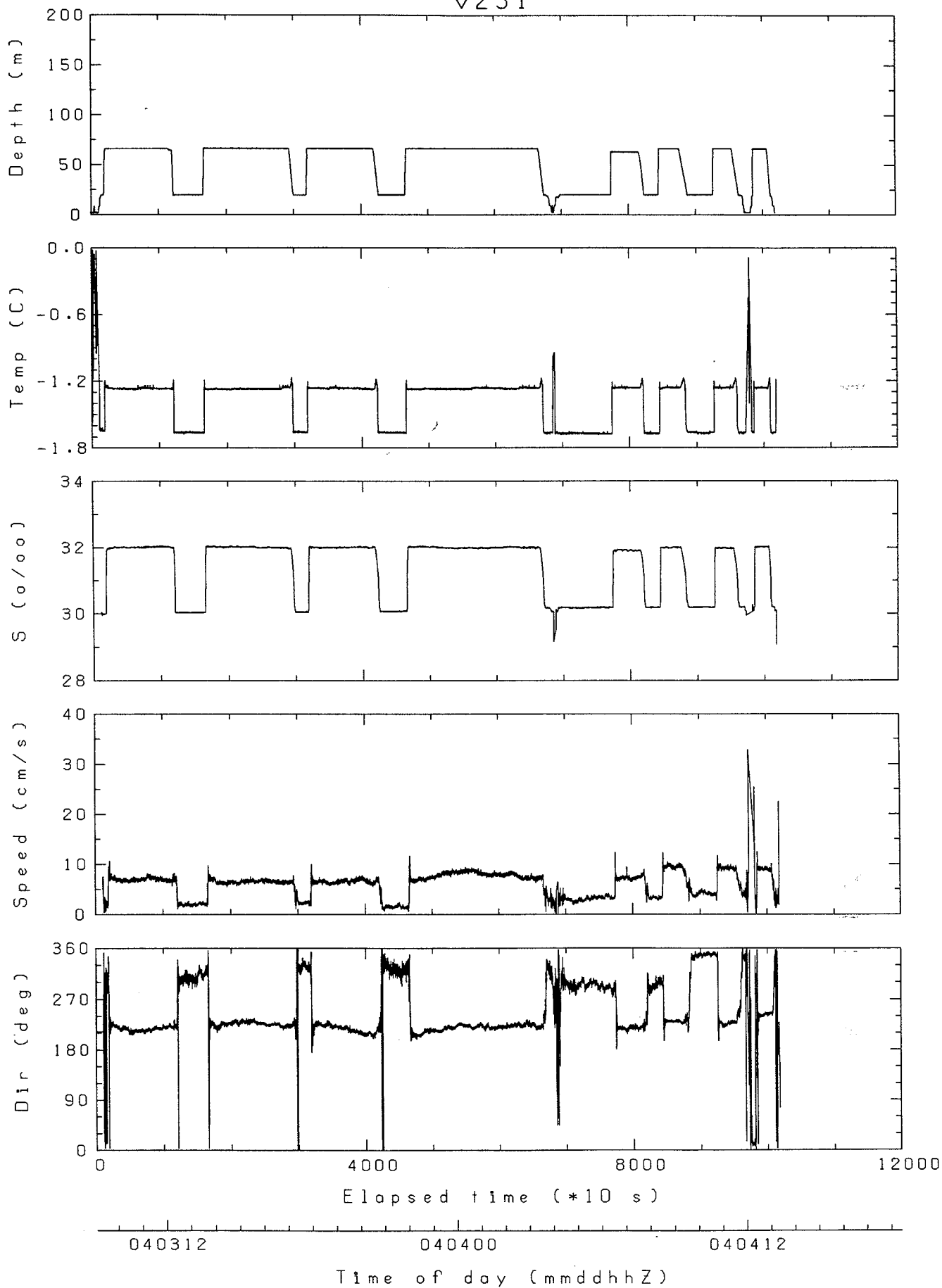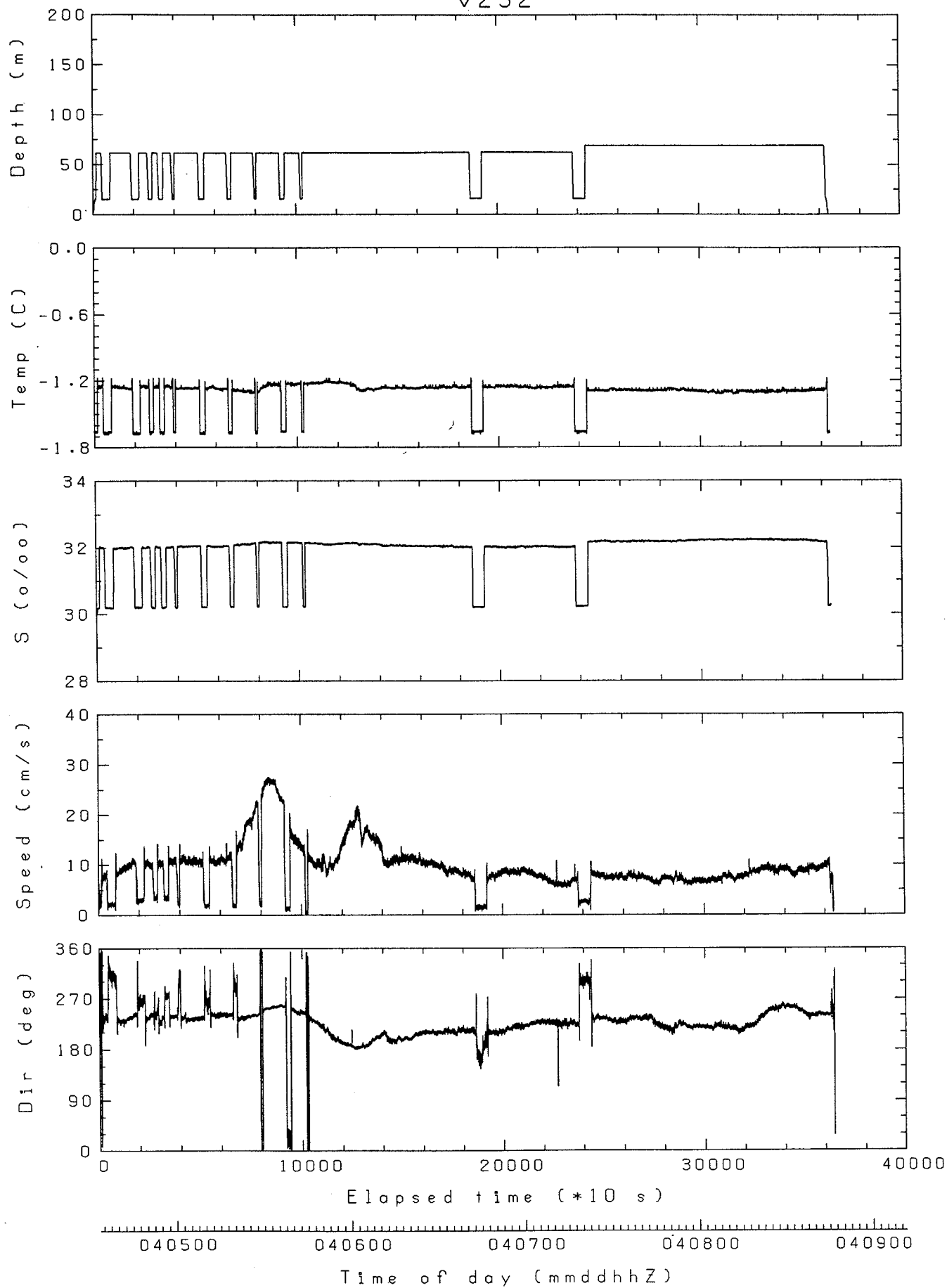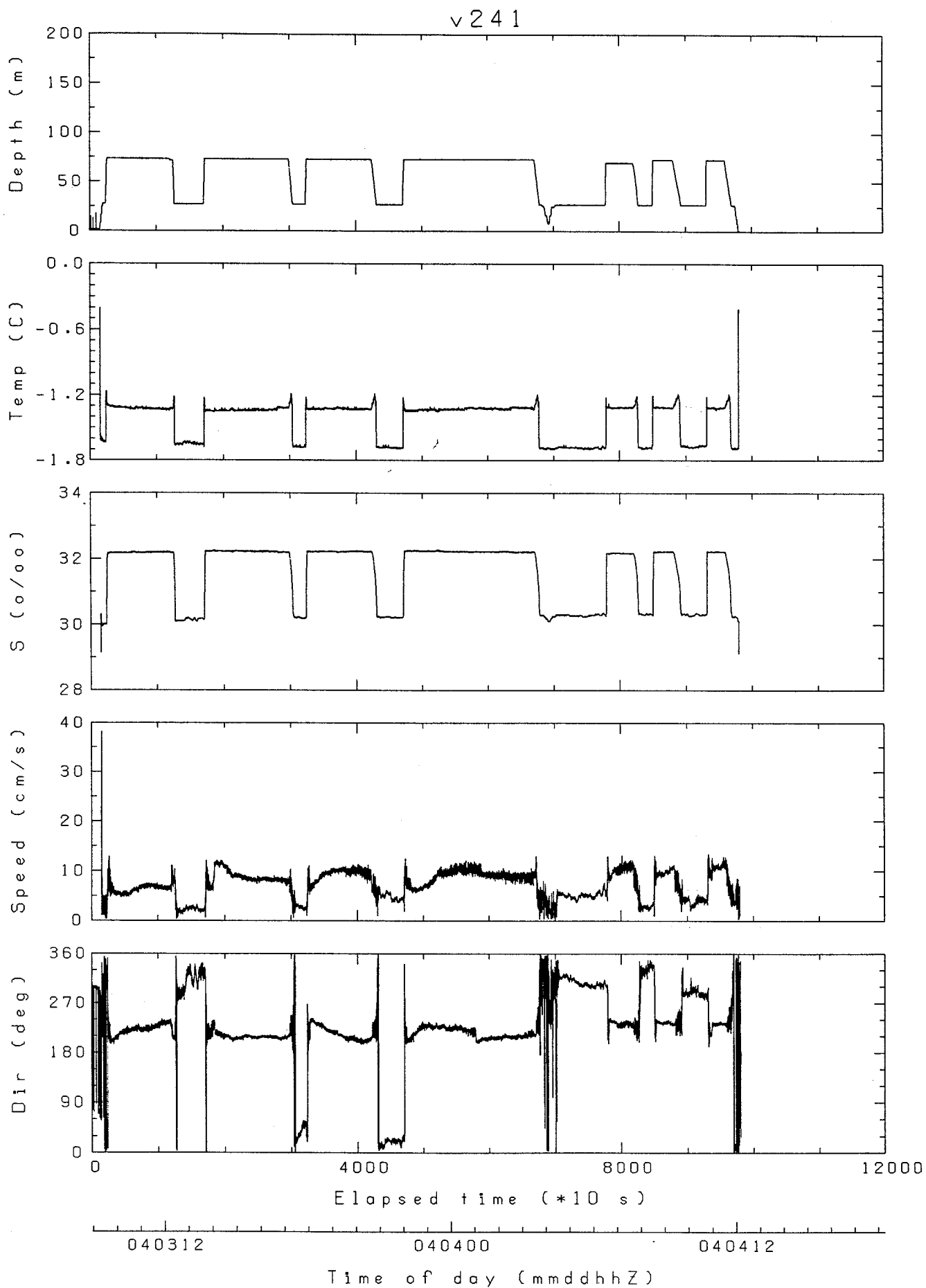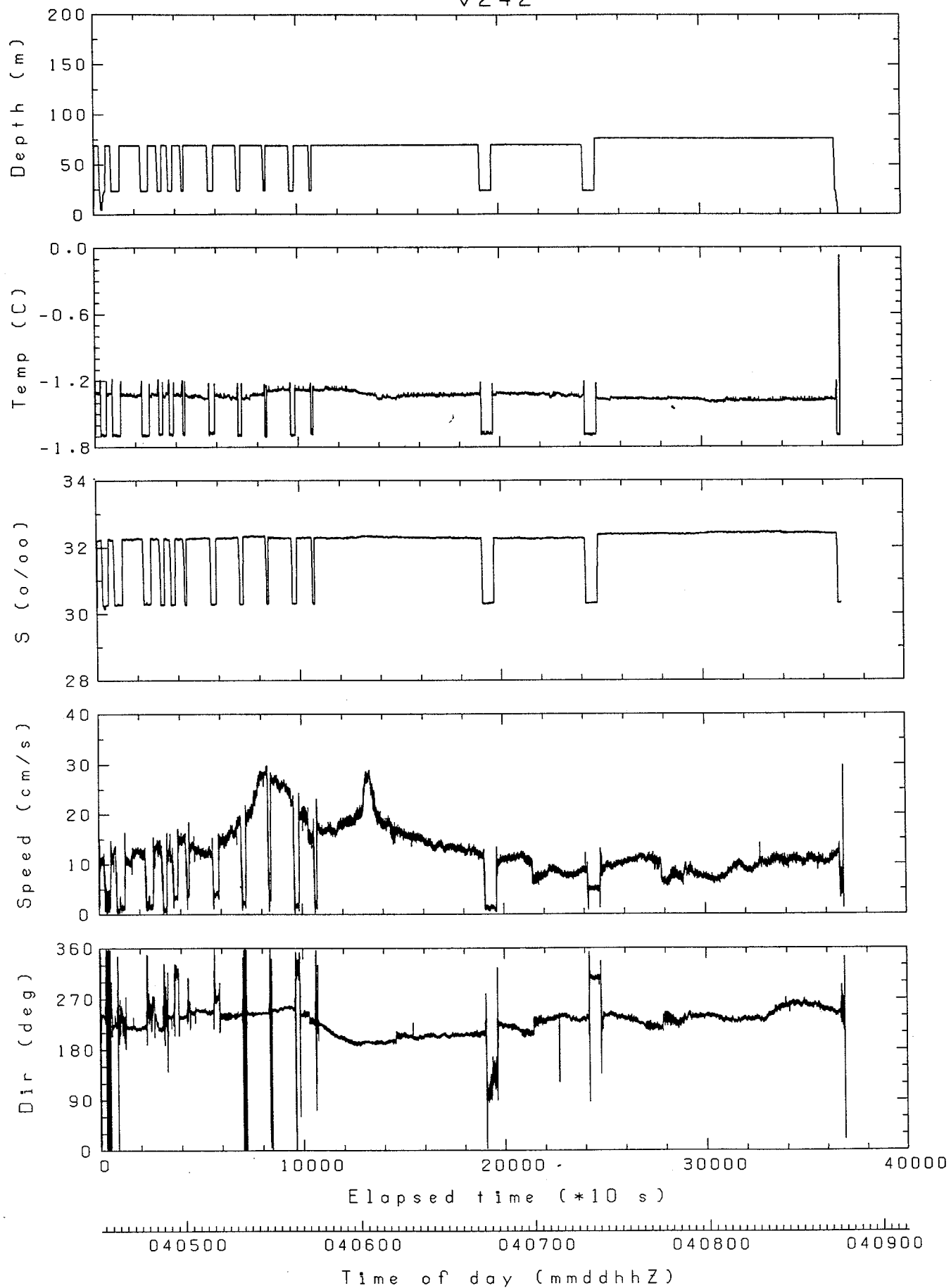
APPENDIX D

Measured & Computed Properties of the Ice Cores

Table D1. Properties of ice core NRL-1, APLIS 91. Computed properties to to the right of the line are based on a linear theoretical temperature profile.

4/6/91, thickness = 172 cm, snow cover = 7.6 cm

Sec #	Depth (cm)	Temp (C)	Salinity (o/oo)	Density (Mg/m^3)	Brine Vol. (o/oo)	Conductivity (mS/cm)	Temp (C)	Based on temperature Density (Mg/m^3)	theoretical profile Brine Vol. (o/oo)	Conductivity (mS/cm)
1	5.0	-21.4	10.54	0.930	34.0	0.239	-22.4	0.930	32.9	0.231
2	13.3	-21.2	3.44	0.923	11.1	0.078	-21.4	0.923	11.0	0.078
3	20.3	-20.5	4.23	0.924	14.0	0.098	-20.5	0.924	14.0	0.098
4	26.4	-19.4	4.10	0.924	14.1	0.099	-19.8	0.924	13.9	0.098
5	32.3	-18.5	5.18	0.924	18.4	0.130	-19.1	0.925	18.1	0.127
6	39.8	-17.7	4.63	0.924	17.0	0.119	-18.1	0.924	16.7	0.117
7	47.3	-17.0	4.05	0.923	15.3	0.107	-17.2	0.923	15.1	0.106
8	54.3	-16.3	4.00	0.923	15.5	0.109	-16.4	0.923	15.5	0.109
9	61.0	-15.3	4.74	0.924	19.3	0.135	-15.5	0.924	19.0	0.134
10	68.4	-14.8	4.41	0.923	18.3	0.129	-14.6	0.923	18.5	0.130
11	75.9	-14.1	4.89	0.924	21.0	0.148	-13.7	0.924	21.4	0.151
12	83.4	-13.5	4.83	0.924	21.4	0.150	-12.8	0.924	22.3	0.156
13	90.7	-13.3	4.59	0.924	20.6	0.145	-11.9	0.924	22.3	0.156
14	98.1	-12.3	4.54	0.924	21.5	0.151	-11.0	0.923	23.4	0.164
15	106.8	-11.7	4.03	0.923	19.8	0.139	-10.0	0.923	22.4	0.157
16	116.6	-10.0	4.50	0.923	25.0	0.175	-8.8	0.924	27.7	0.194
17	126.2	-8.8	4.71	0.924	28.9	0.203	-7.6	0.924	32.6	0.228
18	135.6	-7.6	4.59	0.924	31.7	0.222	-6.4	0.924	36.5	0.256
19	145.4	-6.6	4.54	0.924	35.3	0.248	-5.2	0.924	43.3	0.303
20	155.4	-5.4	4.85	0.925	45.1	0.316	-4.0	0.926	59.1	0.414
21	163.9	-4.9	4.89	0.925	49.6	0.348	-3.0	0.927	79.6	0.558

Table D2. Properties of ice core NRL-2, APLIS 91. Computed properties to
to the right of the line are based on a linear theoretical temperature profile.

4/6/91, thickness = 182 cm, snow cover = 7.6 cm

Sec #	Depth (cm)	Temp (C)	Salinity (o/oo)	Density (Mg/m^3)	Brine Vol. (o/oo)	Conductivity (mS/cm)	Temp (C)	Based on temperature Density (Mg/m^3)	theoretical profile Brine Vol. (o/oo)	Conductivity (mS/cm)
	1.0	-	-	-	-	-	-21.1	-	-	-
1	5.8	-19.5	7.96	0.927	27.4	0.192	-20.6	0.927	26.4	0.185
	14.6	-19.8	-	-	-	-	-19.7	-	-	-
2	23.4	-18.8	3.91	0.923	13.7	0.097	-18.7	0.923	13.8	0.097
	32.0	-18.0	-	-	-	-	-17.8	-	-	-
3	40.5	-17.0	4.95	0.924	18.7	0.131	-16.9	0.924	18.7	0.132
	44.9	-	-	-	-	-	-16.5	-	-	-
	48.9	-	-	-	-	-	-16.0	-	-	-
4	56.1	-16.0	5.23	0.924	20.6	0.145	-15.3	0.924	21.3	0.149
	63.7	-15.6	-	-	-	-	-14.5	-	-	-
5	71.3	-15.0	6.02	0.925	24.8	0.174	-13.7	0.925	26.5	0.186
	76.3	-	-	-	-	-	-13.1	-	-	-
6	81.1	-15.2	4.72	0.924	19.3	0.135	-12.6	0.924	21.9	0.154
	89.5	-13.4	-	-	-	-	-11.8	-	-	-
7	98.3	-12.6	4.02	0.923	18.7	0.132	-10.8	0.923	21.0	0.147
	105.9	-11.3	-	-	-	-	-10.0	-	-	-
8	112.3	-11.0	3.86	0.923	19.9	0.140	-9.4	0.923	22.5	0.158
	117.3	-12.2	-	-	-	-	-8.8	-	-	-
9	123.3	-9.6	4.18	0.923	23.9	0.168	-8.2	0.923	27.2	0.191
	130.9	-8.6	-	-	-	-	-7.4	-	-	-
10	138.4	-7.3	4.64	0.924	33.2	0.233	-6.6	0.924	36.1	0.253
	145.9	-6.8	-	-	-	-	-5.8	-	-	-
11	153.4	-6.6	4.54	0.924	35.3	0.248	-5.0	0.925	45.0	0.316
12	160.9	-3.7	4.12	0.925	54.3	0.381	-4.2	0.924	47.8	0.335
13	167.1	-3.1	4.30	0.926	67.4	0.473	-3.6	0.925	58.7	0.411
14	172.1	-2.0	3.47	0.927	85.3	0.598	-3.0	0.924	55.3	0.388
15	178.4	-2.5	5.00	0.929	97.7	0.684	-2.4	0.929	102.8	0.720

APPENDIX E

Ambient Noise Level Plots

ave .932002

ave .932202

ave .952229
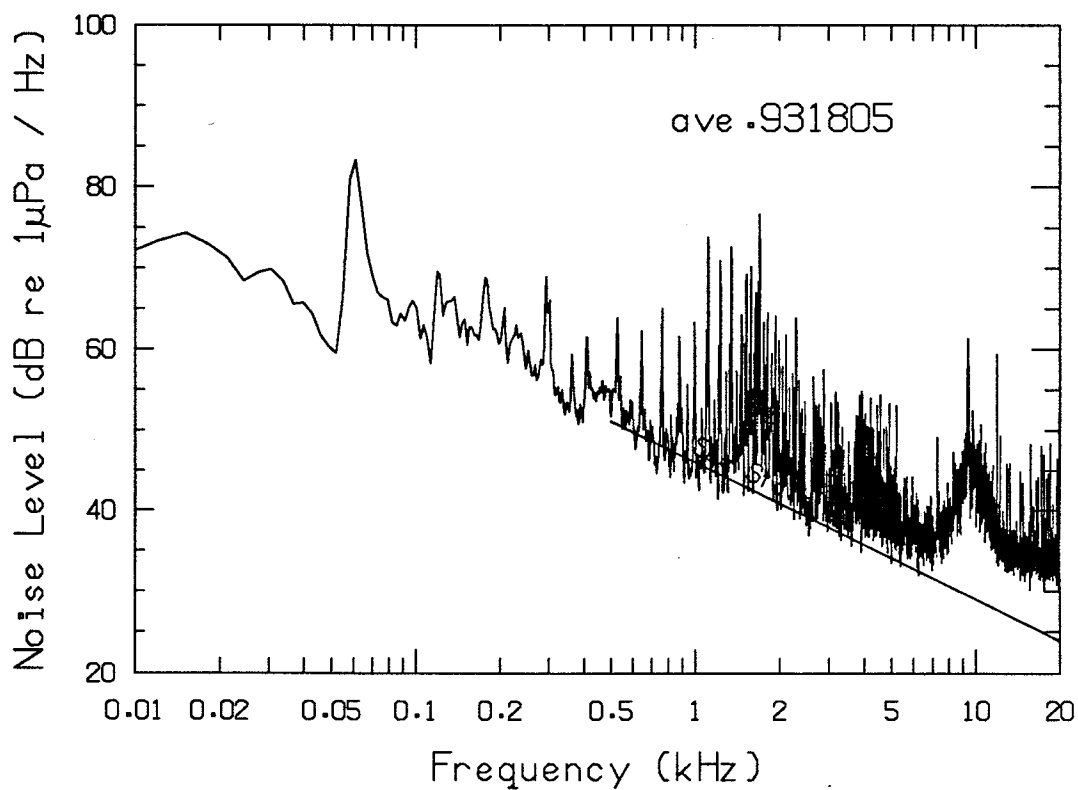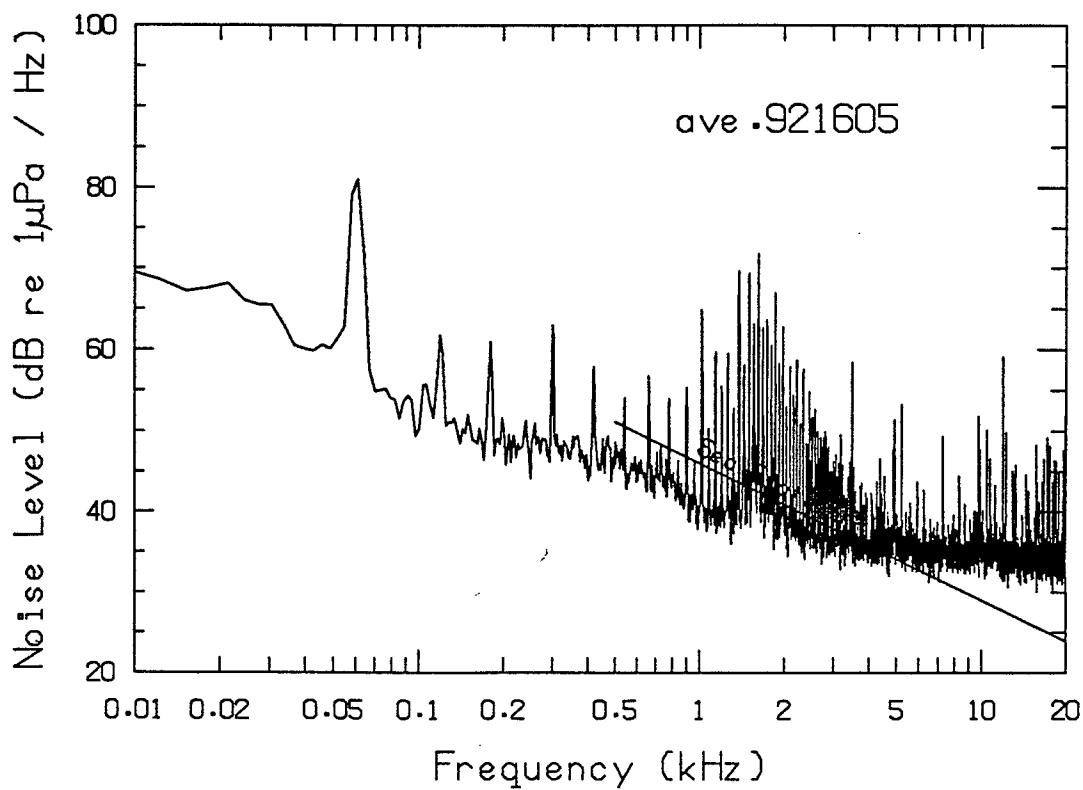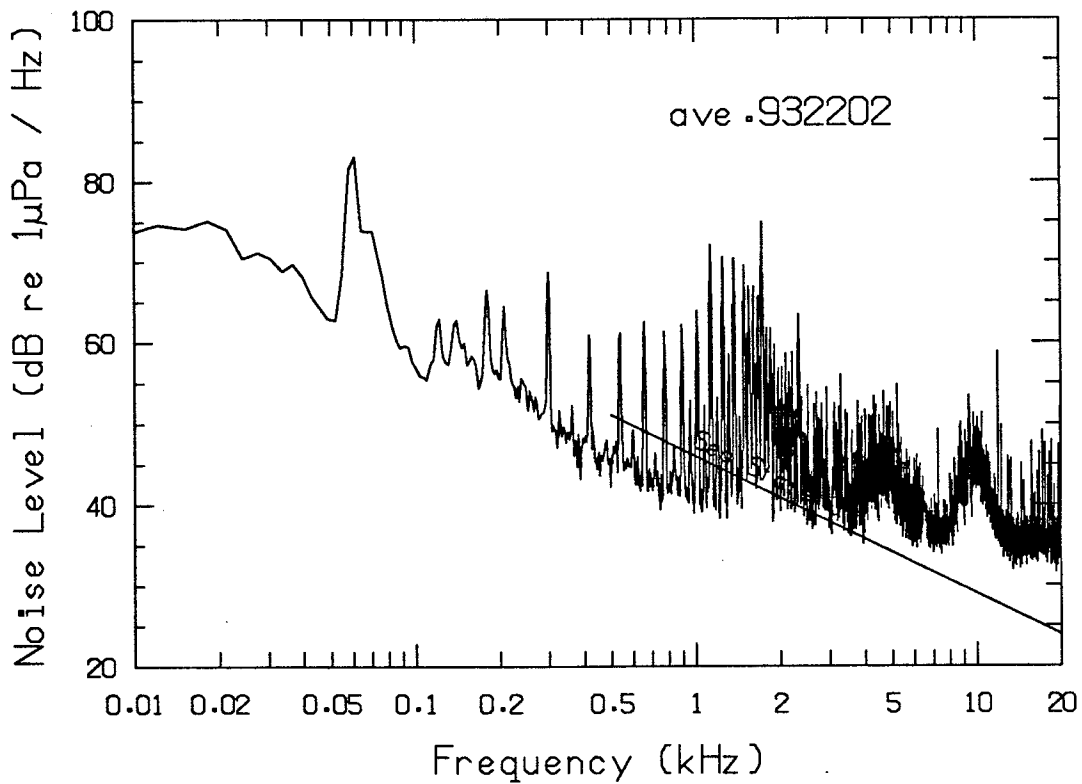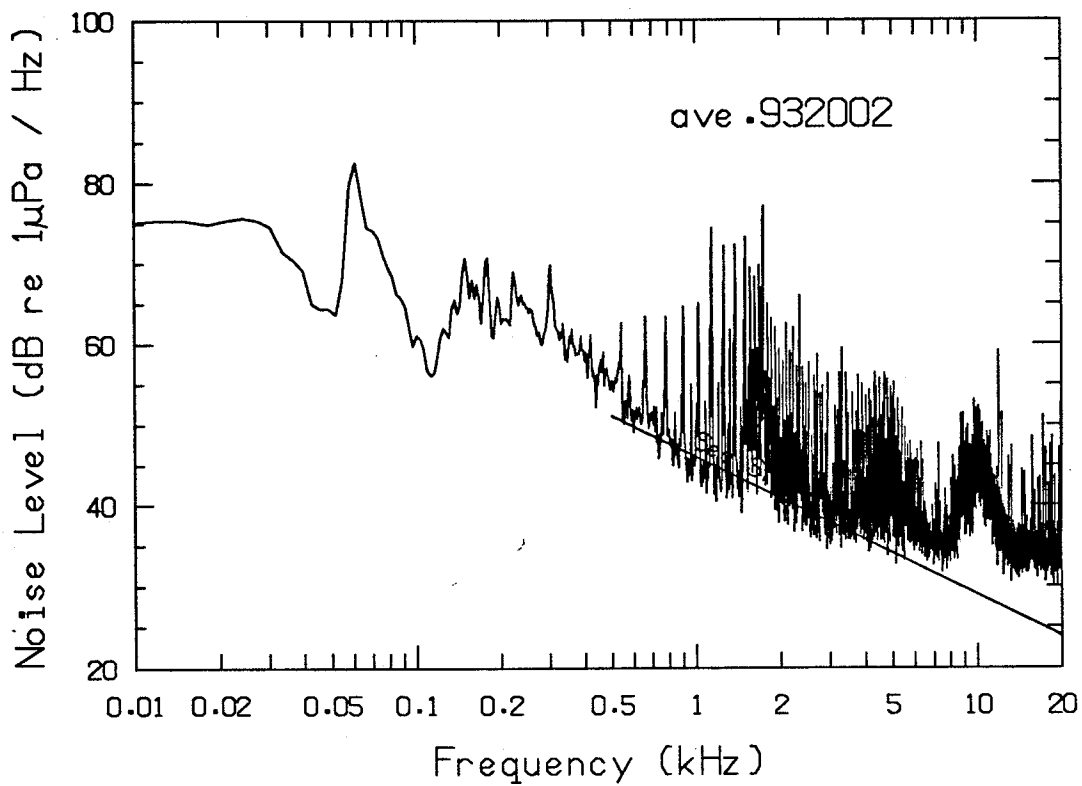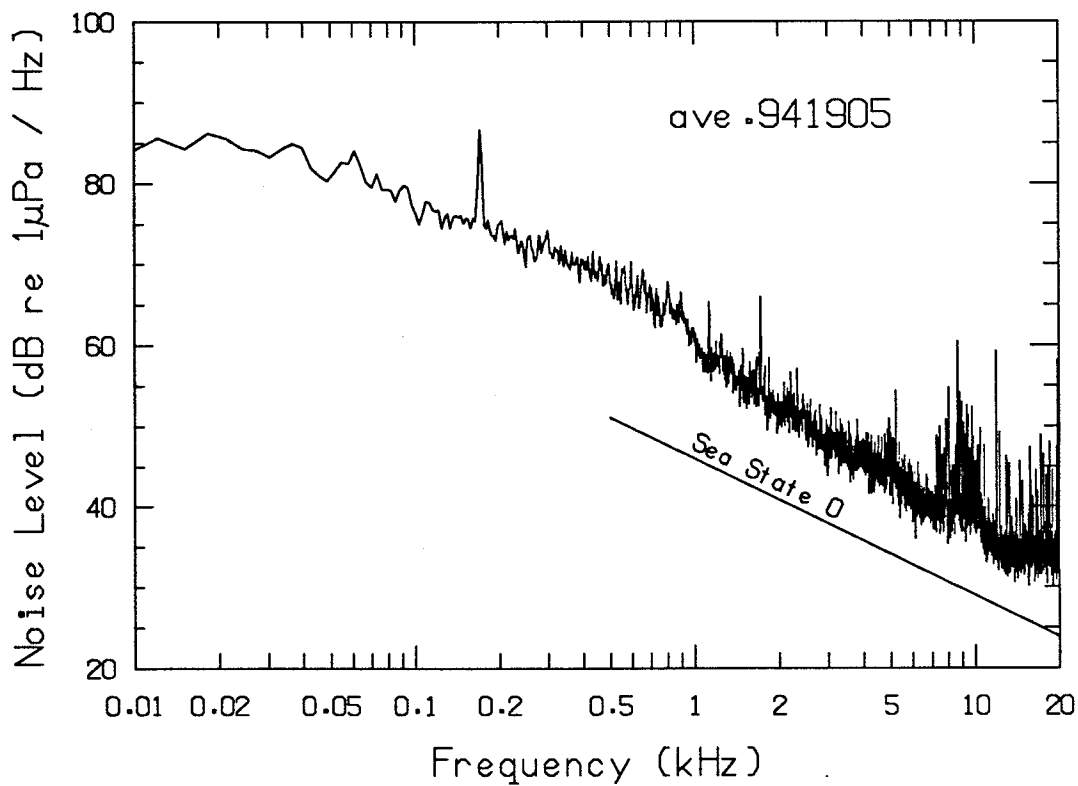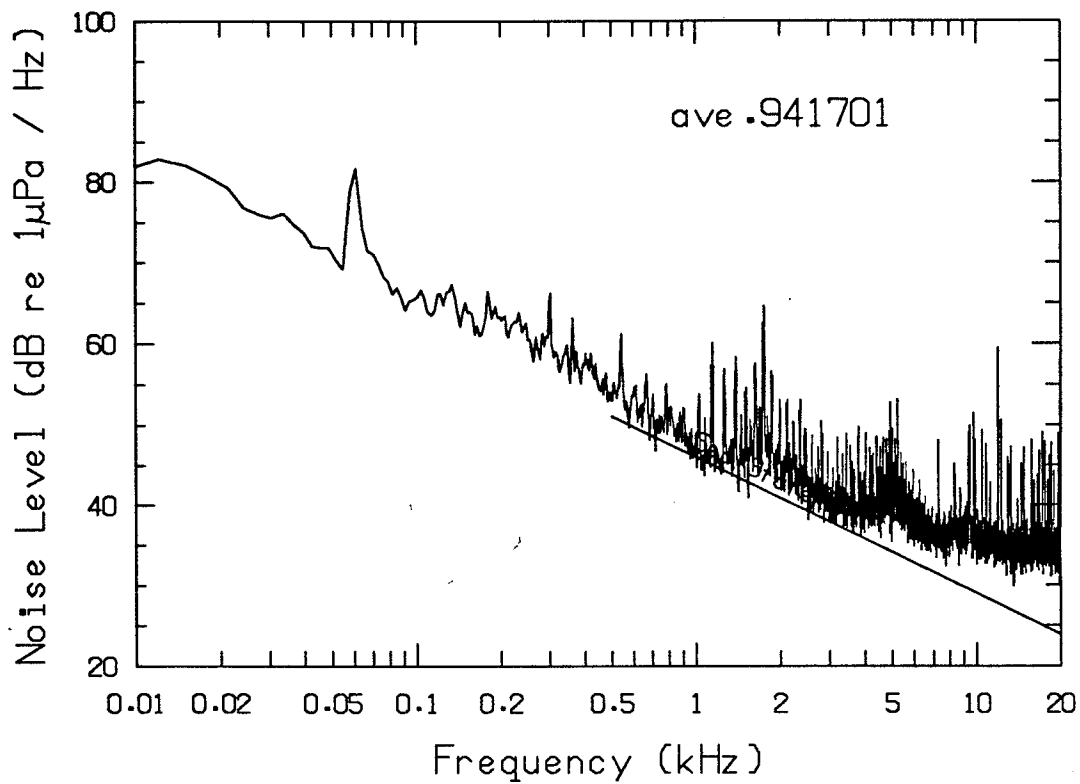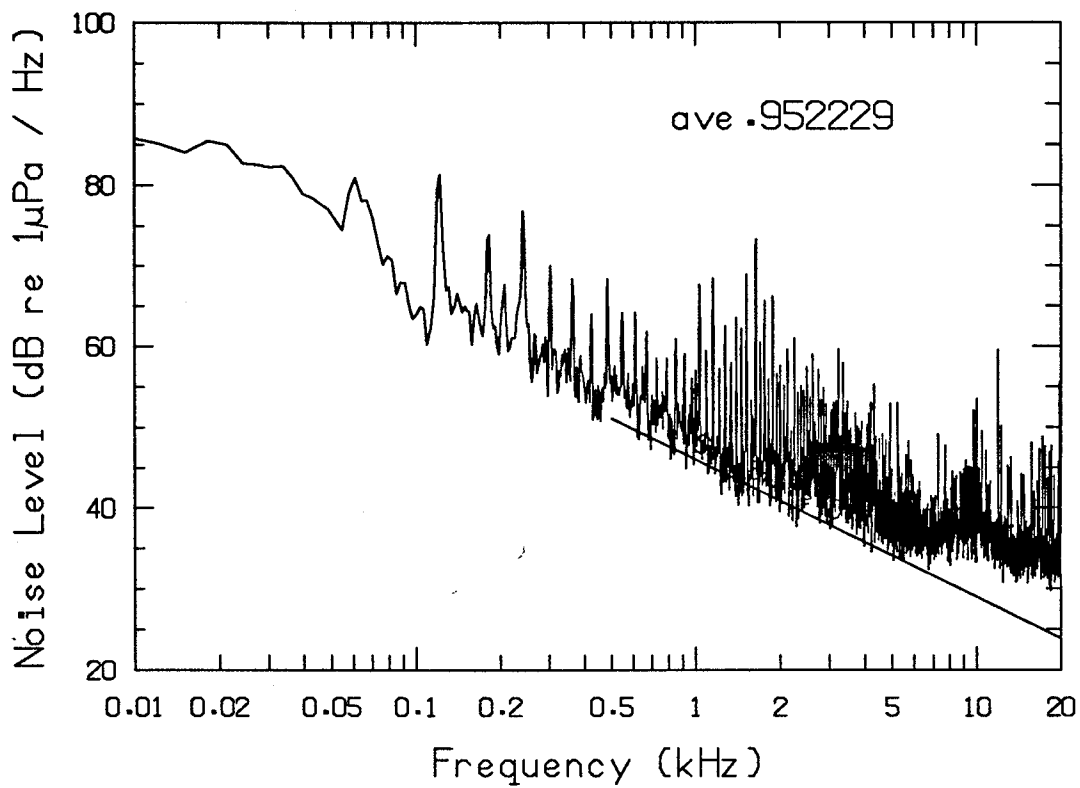
REPORT DOCUMENTATION PAGE		Form Approved OMB No. 0704-0188

1a. REPORT SECURITY CLASSIFICATION Unclassified	1b. RESTRICTIVE MARKINGS
2a. SECURITY CLASSIFICATION AUTHORITY	3. DISTRIBUTION / AVAILABILITY OF REPORT Approved for public release. Distribution is unlimited.
2b. DECLASSIFICATION / DOWNGRADING SCHEDULE	

4. PERFORMING ORGANIZATION REPORT NUMBER(S) APL-UW TR 9204	5. MONITORING ORGANIZATION REPORT NUMBER(S)

6a. NAME OF PERFORMING ORGANIZATION Applied Physics Laboratory University of Washington	6b. OFFICE SYMBOL (If applicable)	7a. NAME OF MONITORING ORGANIZATION Arctic Submarine Laboratory (Code 19) Naval Ocean Systems Center
6c. ADDRESS (City, State, and ZIP Code) 1013 N.E. 40th Street Seattle, Washington 98105-6698		7b. ADDRESS (City, State, and ZIP Code) San Diego, CA 92152-5000

8a. NAME OF FUNDING / SPONSORING ORGANIZATION Various	8b. OFFICE SYMBOL (If applicable)	9. PROCUREMENT INSTRUMENT IDENTIFICATION NUMBER SPAWARSYSCOM N00039-91-C-0072
8c. ADDRESS (City, State, and ZIP Code)		10. SOURCE OF FUNDING NUMBERS

10. SOURCE OF FUNDING NUMBERS			
PROGRAM ELEMENT NO.	PROJECT NO.	TASK NO.	WORK UNIT ACCESSION NO.

11. TITLE (Include Security Classification)

Environmental Measurements in the Beaufort Sea, Spring 1991

12. PERSONAL AUTHOR(S)
T. Wen, F. Karig, W. Felton (APL-UW), and P. Keller (NAVSURFWARCEN)

13a. TYPE OF REPORT Technical	13b. TIME COVERED FROM 3/91 TO 4/91	14. DATE OF REPORT (Year, Month, Day) January 1992	15. PAGE COUNT 124

16. SUPPLEMENTARY NOTATION

17. COSATI CODES			18. SUBJECT TERMS (Continue on reverse if necessary and identify by block number)
FIELD	GROUP	SUB-GROUP	Arctic Sea ice properties Weather
68	03		Beaufort Sea Floe drift Ambient noise
20	01		Currents STD profiles

19. ABSTRACT (Continue on reverse if necessary and identify by block number)

    This report presents environmental and ambient noise data obtained by the Applied Physics Laboratory of the University of Washington (APL-UW) and the Naval Surface Warfare Center (NSWC) at APLIS 91, an ice camp established in the Beaufort Sea in spring 1991 to support Navy-sponsored tests and research during ICEX-91.

    The purpose of this report is to provide field data to ice camp participants, so data analysis is limited here. The data were collected to document the meteorological and oceanographic conditions that existed during camp activities. The main data sets are weather, floe drift, STD profiles, current, ice properties, and ambient noise.

20. DISTRIBUTION / AVAILABILITY OF ABSTRACT ☐ UNCLASSIFIED/UNLIMITED ☒ SAME AS RPT. ☐ DTIC USERS	21. ABSTRACT SECURITY CLASSIFICATION Unclassified	
22a. NAME OF RESPONSIBLE INDIVIDUAL CDR B.B. Scott, USN	22b. TELEPHONE (Include Area Code) (619) 553-0190	22c. OFFICE SYMBOL NAVOCEANSYSCEN (19)

9086
Ser 96/061
4 Mar 92

From: Technical Director, Arctic Submarine Laboratory, Naval
        Undersea Warfare Center
To: Fred W. Karig, APL University of Washington

Subj: REVIEW OF APL/UW TECHNICAL REPORT 9204 FOR PUBLIC RELEASE

Ref: (a) APL/UW ltr Ser 5C1719 of 24 Feb 92

Encl: (1) "Environmental Measurements in the Beaufort Sea,
            Spring 1991" by T. Wen, et al., January 1992
        (2) Recommended Initial Distribution List for TR 9204

1.   Reference (a) requested review of Draft APL/UW Technical
Report 9204 for Public Release.

2.   Figure 4 on page 5 of TR 9204 shows a layout of Camp APLIS
91.   Several of the items shown in this figure related to
classified experiments and have no bearing on environmental
measurements.   This figure should be revised to delete all
locations of instruments not related to environmental data
collection.

3.   Enclosure (2) to reference (a) is the proposed distribution
list for TD 9204.   It is recommended that this distribution list
be updated to reflect the title/address changes resulting from
the recent Navy Laboratory reorganization.

4.   Subject document is approved for public release upon making
the changes specified in paragraph 2 above.

5.   Enclosures (1) and (2) are returned, as requested by
reference (a).

R. A. MCLENNAN

Commanding Officer
Naval Civil Engineering Laboratory
Port Hueneme, CA 93043-5003

       Library

Director
Naval Research Laboratory
Washington, DC 20375

       Library
       Code 5100
       Code 5550
       Code 5123
       Code 6090

Commanding Officer
Naval Coastal Systems Center
Panama City, FL 32407-5000

       Library

Commanding Officer
Naval Ocean Research and
  Development Activity
Stennis Space Center, MS 39529-5004

       Library   [2 cp]
       Code 113
       Code 200
       Code 240
       Code 242
       Code 252

Commanding Officer
Naval Oceanographic Office
Stennis Space Center, MS 39522-5001

       Code OA
       Code OAR
       Code OARU

Officer-in-Charge
New London Laboratory
Naval Underwater Systems Center
New London, CT 06320

>   Library
>   Code 01Y   [2 cp]
>   Code 341
>   Code 2111
>   Code 2113
>   Code 2122
>   Code 3422
>   Code 3423

Commander
Naval Weapons Center
China Lake, CA 93555

>   Library

Commander
Naval Surface Warfare Center
White Oak Laboratory
Silver Spring, MD 20903-5000

>   Library   [2 cp]
>   Code R-01
>   Code R-43   [2 cp]
>   Code U-04
>   Code U-06
>   Code U-13
>   Code U-42   [2 cp]

Commander
Naval Ocean Systems Center
San Diego, CA 92152-5000

>   Library
>   Code 00
>   Code 19   [3 cp]
>   Code 541
>   Code 542
>   Code 844   [3 cp]

Commander
Naval Sea Systems Command
Department of the Navy
Washington, DC 20362

       NSEA 05R
       NSEA 06
       NSEA 06U2
       NSEA 06UR
       NSEA 06UR-42
       NSEA 06URB
       NSEA 92R
       Code PMO-402
       Code PMO-406
       Code PMO-407

Commander
Naval Underwater Systems Center
Newport, RI 02840

       Library   [2 cp]
       Code 00
       Code 22201
       Code 382
       Code 3824
       Code 801
       Code 81
       Code 8211   [2 cp]
       Code 8212
       Code 8219
       Code 8231
       Code 82391   [2 cp]

Commanding Officer
Naval Maritime Intelligence Center
4301 Suitland Road
Washington, DC 20390

Commanding Officer
Naval Polar Oceanography Center
4301 Suitland Road
Washington, DC 20390-5140

      Library

Center for Naval Analyses
4401 Ford Avenue
P.O. Box 16268
Alexandria, VA 22302-0268

Attn: Technical Information Center

Commander
Naval Air Systems Command
Department of the Navy
Washington, DC 20361

      NAIR 340L

Commander
Space and Naval Warfare Systems Command
Department of the Navy
Washington, DC 20363-5100

      SPAWAR 09L
      PMW-180
      PMW-181
      PMW-182
      PMW-182-2

Office of the Chief of Naval Research
Department of the Navy
800 N. Quincy Street
Arlington, VA   22217-5000

OCNR 00
OCNR 000A
OCNR 112
OCNR 1125
OCNR 1125AR
OCNR 1125OA
OCNR 1222T
OCNR 124
OCNR 125   [2 cp]

Office of Naval Research Resident Representative,
  University of Washington (JD-16)
410 University District Bldg.
1107 N.E. 45th Street
Seattle, WA 98105-4631
(Cover Letter & Distribution List Only)

Office of Naval Technology
Department of the Navy
Ballston Center Tower #1
800 N. Quincy Street
Arlington, VA 22217-5000

Code 22
Code 23
Code 23D
Code 232
Code 234

Director
Defense Advanced Research Projects Agency
1400 Wilson Boulevard
Arlington, VA 22209

Assistant Secretary of the Navy
(Research, Engineering and Systems)
Department of the Navy.
Washington, DC 20350   [2 cp]

Chief of Naval Operations
Department of the Navy
Washington, DC 20350-2000

> OP 02
> OP 22
> OP 223
> OP 225
> OP 07
> OP 071
> OP 095
> OP 96T
> OP 0962E
> OP 0962X
> OP 098

Director of Defense Research
Office of Assistant Director (Ocean Control)
The Pentagon
Washington, DC 20301-5000

Defense Technical Information Center
Cameron Building #5
Alexandria, VA 22304-6145

25 February 1992
Serial 5C1719

To: Director
Arctic Submarine Laboratory
Naval Command Control and Ocean Surveillance Center,
RDT&E Division
Bldg. 371
San Diego, CA 92152-5000

Attn: Code 019 (R.A. McLennan, Deputy Director)

From: Fred W. Karig, Principal Mechanical Engineer

Subj: Review of APL-UW Technical Report 9204 for Public Release

Encl: (1) "Environmental Measurements in the Beaufort Sea, Spring 1991"
by T. Wen, et. al., January 1992

(2) Recommended Initial Distribution List for TR 9204

1. Enclosed for your review is a report on the environmental measurements taken during ICEX 1-91. Please certify your approval of public release of this report by signing in the space provided at the bottom of this letter, and return it (and the enclosed report) to APL-UW. If any changes are required to meet requirements for public release, please specify the modifications.

2. Enclosure (2) is a recommended initial distribution list. Please add, delete, or otherwise modify the list as needed and return the marked-up copy to APL-UW.

3. If you have any questions, please call me at (206)543-1354 or Al Brookes at (206)543-4216.

Fred W. Karig

APL-UW TR 9204 "Environmental Measurements in the Beaufort Sea, Spring 1991" is approved for public release.

R. A. McLennan
Deputy Director
Arctic Submarine Laboratory, NCCOSC RDT&E Div.

agb/KARIG/REPORTS/pub.rel.9204

Commander
Naval Air Development Center
Warminster, PA 18974

       Library
       Code 3031 (A. Horbach)

Commander
David Taylor Research Center
Bethesda, MD 20084

       Library
       Code 1720
       Code 1908
       Code 2751

Commanding Officer
Naval Submarine School
Box 70
Naval Submarine Base New London
Groton, CT 06340

Superintendent
Naval Postgraduate School
Monterey, CA 93943-5100

       Library   [2 cp]
       Code 68

Commander, SECOND Fleet
Fleet Post Office
New York, NY 09501

Commander, THIRD Fleet
Fleet Post Office
San Francisco, CA 96601

Commander Submarine Force
U.S. Atlantic Fleet
Norfolk, VA 23511

    Code 00
    Code 019
    Code 22
    Code N311

Commander Submarine Force
U.S. Pacific Fleet
Pearl Harbor, HI 96860

    Code 00
    Code N2
    Code N21

Commander
Submarine Squadron THREE
San Diego, CA 92132

Commander
Submarine Group FIVE
137 Sylvester Rd.
San Diego, CA 92106-3521

Commander
Submarine Development Squadron TWELVE
Box 70
Naval Submarine Base New London
Groton, CT 06340

    Code N20

Knut Aagaard
Pacific Marine Environmental Laboratory
NOAA
7600 Sand Point Way NE, Building 3
Bin C15700
Seattle, WA 98115-0070

Director
Applied Research Laboratories
The University of Texas at Austin
P.O. Box 8029
Austin, TX 78713-8029

Library
Dr. J. Huckaby

Director
Applied Research Laboratory
The Pennsylvania State University
State College, PA 16801

C. Ackerman
R. Ingram   [2 cp]
E. Liszka
S. McDaniel
F. Symons, Jr.
J. Kisenwether

CBNS
P.O. Box 4855
Washington, DC 20008
Attn: CAPT F. Hiscock, RN   [2 cp]

University of Washington
School of Oceanography   [2 cp]